EXPERT REPORT
U.S v. BP Exploration & Production, Inc., et al.

RATE PREDICTION FROM THE MACONDO WELL

Prepared on Behalf of the United States

Prepared by:
Mohan Kelkar
Kelkar and Associates, Inc.
528 East 104th Street
Tulsa, OK 74137

[redacted]

March 22, 2013

Mohan Kelkar

Mohan Kelkar

[redacted]

TABLE OF CONTENTS

LIST OF FIGURES

LIST OF TABLES

LIST OF ABBREVIATIONS AND ACRONYMS

B_{oi} - Initial oil formation volume factor

B_o - Oil formation volume factor

C – compressibility

EOS - Equation of state

GOR – Oil to gas ratio

h - Thickness (net pay)

k – Permeability

m – viscosity

MMSTB – million stock tank barrels

OOIP - original oil-in-place

P - pressure

P_i - Initial reservoir pressure

psia - pounds per square inch absolute

Pws - bottom-hole pressure

PI – Productivity Index

φ – porosity

PVT – pressure volume temperature

q_o - Oil rate

S_o – oil saturation

S_w – water saturation

STB - stock tank barrels

T - temperature

PERSONAL BACKGROUND

Dr. Mohan Kelkar. I currently serve as Department Chair and the Williams Endowed Chair Professor of the McDougall School of Petroleum Engineering at the University of Tulsa, with specializations including reservoir characterization, reservoir performance, production optimization, reservoir modeling, and risk analysis. For the past 30 years, I have taught undergraduate courses in petroleum engineering, reservoir characterization, production design and optimization, and petroleum economics.

I am also Director of the University of Tulsa Center for Reservoir Studies, which was created in 1999 to conduct research on reservoir description and optimization. I have authored or co-authored two books in the fields of petroleum and reservoir engineering, more than 50 refereed journal publications, technical reports, and have given more than two hundred technical presentations. I am currently serving a three year term on the Society of Petroleum Engineers (SPE) International Board of Directors. I became a distinguished member of SPE in 2010. I also served as distinguished speaker for SPE in 2007-2008 and received the SPE Distinguished Faculty Member Award in 2009.

I am currently President of Kelkar and Associates, a company I created in 1994 to apply state-of-the-art petroleum and reservoir engineering technologies to field applications. My specialization has been reservoir modeling, reservoir characterization, and production optimization. Our company has served clients from every walk of the oil industry. We have worked with small, independent, oil companies as well as large multi-nationals and national oil companies. During the Summer of 2010, I was a member of the reservoir modeling team for the United States' Flow Rate Technical Group.

My *curriculum vitae*, which lists my publications and other relevant professional experience and honors, is Appendix D to this report.

EXECUTIVE SUMMARY

The amount of oil that spilled from the Macondo Well can be accurately estimated using standard, industry-accepted petroleum engineering techniques. Using a variety of those techniques we conclude that the flow from the well on July 15, 2010 (the day the well was finally shut in) was 54,000 STB/day. We also conclude that our best estimate of the total amount of oil discharged from the Macondo reservoir over the approximately 86 days when oil flowed into the Gulf of Mexico is between 4.5 and 5.5 million STB.

Our analysis is in three parts. In Section I, we calculate the oil flow rate on the last day of the spill by evaluating the pressure loss through the capping stack used to permanently shut in the well. We use a loss coefficient factor, also known as K factor, to approximate the restrictions in the capping stack (pipes, bends, and a choke valve). We input the measured and calculated pressure data, as well as a PVT model that predicts the behavior of the Macondo reservoir fluid, to a commercial pipe flow software called PROSPER. Using this industry standard pipe flow software and methodology, we conclude that the flow from the Macondo Well on the last day of the spill was 54,000 barrels per day. Using our calculated flow rates as inputs, we also estimate the bottom hole pressure (BHP) in the well based on the pressure measurements from the capping stack, again using PROSPER and a PVT model for the Macondo fluid.

In Section II, we analyze the pressure buildup in the well after shut in. Using a pressure derivative curve, we confirm BP's pre-drill prediction that the reservoir has a channel shape (a long, generally rectangular shape), and that the Macondo well is located in a corner of that reservoir. We also estimate the average reservoir pressure on July 15, 2010 to be 10,396 psia, as compared with the initial reservoir pressure of 11,856 psia.

Finally, in Section III we analyze the cumulative amount of oil produced from the MC252 reservoir during the approximately 86 days of the spill using an industry standard material balance methodology. We evaluate the original volume of oil in place in the reservoir and, using calculated reservoir and fluid data, determine the amount of oil removed from the reservoir over 86 days. We conclude that our best estimate of the amount of oil produced is between 4.5 and 5.5 million STB (MMSTB).

We evaluate the validity of our assumptions and calculations by varying certain input parameters, assessing alternative methodologies, and comparing our data with that measured and calculated by BP before and after the Macondo blowout.

As noted above, this report employs standard, industry accepted principles and techniques to analyze the rate of oil from the Macondo Well on July 15, 2010, the day the well was finally shut in, as well as the total amount of oil produced from the reservoir between April 20 and July 15, 2010. These techniques are used by companies in their day to day operations and are used to make business decisions about how and whether to produce from certain reservoirs. We describe several of these techniques and methodologies, including their practical application, in Appendix A.

SECTION I. FLOW RATE AS A FUNCTION OF PRESSURE DROP THROUGH THE CAPPING STACK

We can calculate the flow rate through a piping system if we know the geometry of that piping system, the fluid density, and the change in pressure between the inlet and outlet to the system (i.e., the pressure drop). This is a basic fluid mechanics concept. We have the required information for the Macondo Well capping stack and estimate the flow rate using standard multi-phase flow equations and industry standard PROSPER software. PROSPER is one of the most popular software packages used in the oil industry to determine the rates from oil or gas wells using system analysis, a method of integrating various components in the production system to determine the potential rate at which the well can produce. For these calculations, we use PROSPER version 11.5 (2011).[1]

[1] PROSPER – System Analysis Program, Petroleum Experts, version 11.5 (2011).

On July 12, 2010, a capping stack was installed on the Macondo Well. On July 15, 2010, the well was permanently shut-in. During those three days, there were periods where the fluid flow was partially collected at the surface and was partially released into the ocean. There were also periods where all of the flow was released into the ocean. There were two avenues open to flow when all or some of the fluid was released into the ocean. The flow could be released through piping and valve systems on the sides of a capping stack - a "kill line" or a "choke line." Figure 1 below shows the geometry of the system and the location of the pressure gauges.[2] On July 15, the shut-in process was completed by a number of turns on a choke valve on the capping stack, in approximately 10 minute intervals. For approximately two hours prior to shut-in, all the oil from the well flowed through the choke line side of the capping stack, through a combination of pipes, bends, and a choke valve into the ocean. The upstream pressure of this combination was measured continuously using pressure gauge PT_3K_2. The pressure at the bottom of the ocean where the oil was coming out (i.e., the downstream pressure) was measured by BP on July 14.

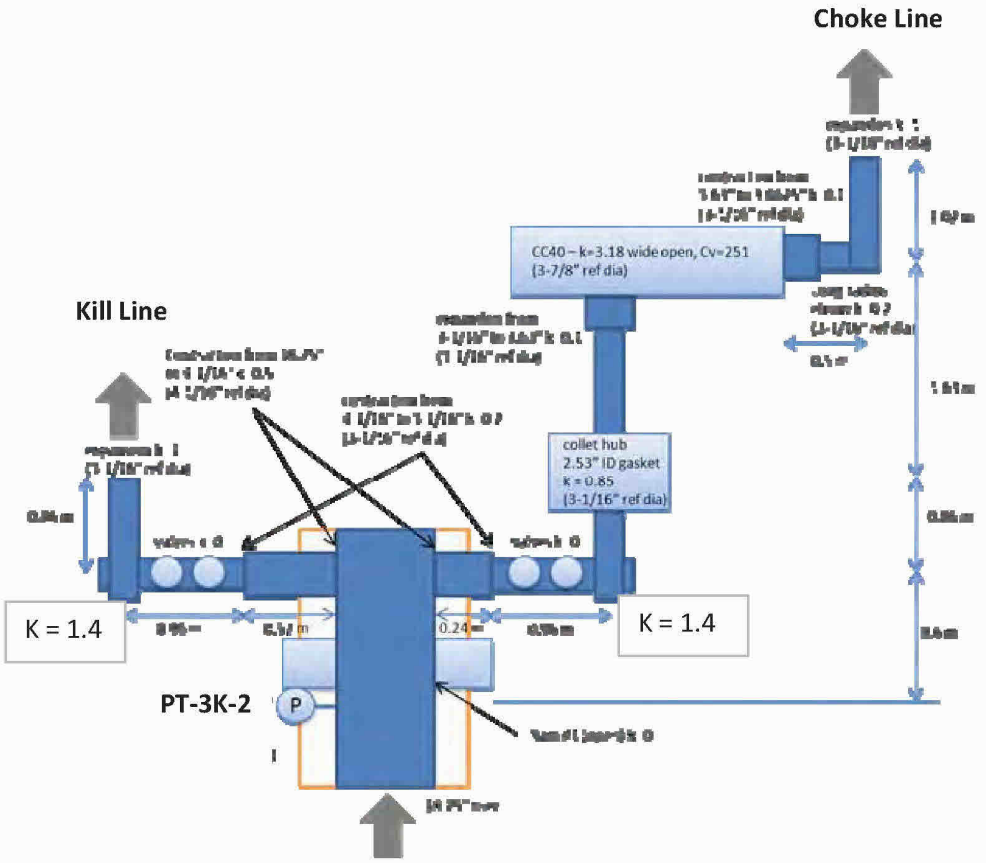

Figure 1: Geometry of capping stack and the release points - Choke and Kill Line

[2] Exhibit 9361, Ratzel, A.C.: "DOE-NNSA Flow Analysis Studies Associated with the Oil Release following the Deepwater Horizon Accident," SANDIA Labs (September 2011).

A. Inputs to Capping Stack Flow Rate Analysis

1. Upstream and Downstream Pressure Measurements

Our analysis of the flow rate through the capping stack mainly concentrates on a period of time on July 15 when all of the flow from the Macondo well was released through the choke line on the capping stack (Fig. 1).[3] The choke valve was gradually closed over a period of approximately two hours until the well was finally shut in. Figure 2shows the pressure data collected from pressure gauge PT_3K_2.[4]

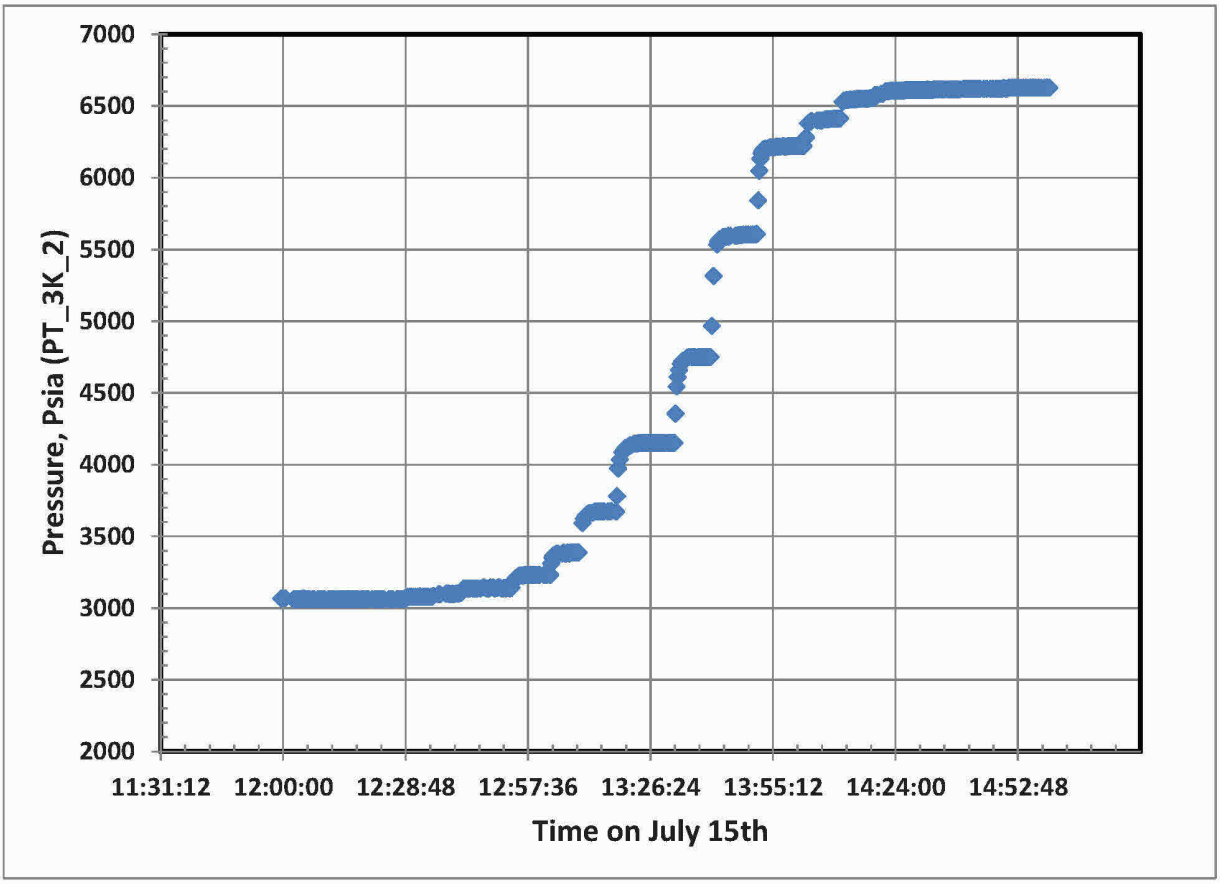

Figure 2: Pressure Data from Pressure Gauge PT_3K_2 before Well Shut in

The choke valve went through 8½ turns to completely close down. The first two turns were full turns followed by a series of half turns until the well was completely shut in. As can be seen

[3] In Section I of this report, we also calculate the flow rate through the kill line of the capping stack for a period of time on July 14 when all of the flow from the well was directed through the kill line.
[4] WIT Data 14July 9am – 3Aug 1pm, BP (BP-HZN-2179MDL07066615).

from Figure 2, as the choke valve dial was turned, the pressure in the gauge stabilized within a few minutes before the next turn was made. To calculate the flow rate, we use the stabilized pressure after each turn was made. That is, if 3½ turns are made, then the stabilized pressure was used just before turn 4 was made. Table 1 shows the stabilized pressure we use in our evaluation of the rate. The first column shows the number of turns, the second column shows the percent of the choke open to flow, the third column shows the time at which the turn was made, the fourth column shows the initial pressure after the turn is made, and the last column shows the stabilized pressure before the next turn. There is no stabilized pressure after the last turn since the flow reached a zero value.

Table 1: Initial and Stabilized Capping Stack Pressures as a function of Choke Opening

			Pressure, psig	
Turns	% open	Time	(initial)	(Stable)
0	100			
0.5	100			
1	99	12:29	3065	3074
1.5	93			
2	86	12:30	3075	3075
2.5	78	12:36	3083	3099
3	69	12:42	3103	3138
3.5	59	12:55	3185	3230
4	50	13:04	3310	3384
4.5	41	13:11	3592	3671
5	32	13:19	3778	4149
5.5	23	13:33	4353	4748
6	16	13:41	4906	5606
6.5	9	13:53	5840	6220
7	5	14:04	6280	6408
7.5	2	14:12	6543	6553
8	1	14:20	6575	6581
8.5	0	14:22	6600	

On July 14, BP measured the sea bottom pressure at ~2,190 psia.[5] We use this value as the downstream pressure in our model. We also assume the ambient sea bottom temperature to be 40 F.

[5] Exhibit 9361, Ratzel, A.C.: "DOE-NNSA Flow Analysis Studies Associated with the Oil Release following the Deepwater Horizon Accident," SANDIA Labs (September 2011).

2. Calculation of K Factors

We next use the capping stack geometry data from Figure 1 to determine potential obstructions to flow and the associated frictional loss. To account for the various restrictions in the system (bends, elbows, etc.), we define a resistance coefficient (also known as a "K factor") which in effect converts the restrictions into equivalent lengths of pipe which will generate the same pressure drop as a particular restriction. We define K factors for elbows, Ts, expansions and other restrictions in the system. For flow through the Cameron CC40 choke valve, we define an equivalent K factor by accounting for the choke valve geometry. We use the K factor values calculated in the DOE Tri-Lab Report as a baseline, and make some changes and simplifications based on an examination of the literature. These changes, in general, result in more conservative estimates of the flow rates. Figure 1 includes the K factor values for various restrictions within the capping stack. Specifically, we revise the K factor values for the cross used as an elbow in the capping stack choke and kill lines and the pipe connections to the Cameron CC40 choke valve (Fig. 1), and adjust those K factor values to account for choke valve closure and to correct for two phase flow. Our calculation of the K factor values is detailed in Appendix B. Table 2 shows the values we used for various restrictions excluding the choke.

Table 2: K Factor Values for Various Restrictions

Description	K Value
Expansion to Ocean	1.00
Long radius elbow	0.20
Collet Hub	0.85
Cross	1.40
Contraction (4 1/16" to 3 1/16")	0.20
Contraction (18 3/4" to 4.06")	0.50

Table 3 shows the K factor values we calculate for each of the restrictions in the capping stack, including the Cameron CC40 choke valve (in yellow). In the first column, we show the values of K factors for single phase flow for different restrictions. These values are the same as shown in Table 2. We then use a correction factor (C_f) to calculate K factor values for two phase flow. The first row in Table 3 represents the % of the choke valve open to flow. The last row represents the K factor value for the choke valve, which is a function of the % of the choke open to flow. The K factor values for two phase flow change for different choke openings because the value of C_f changes. As the percent of the choke valve open to flow decreases, the two phase K factor values increase. These calculations are detailed in Appendix B.

Table 3: K Factor Value Modifications due to Two Phase Flow

% Open											
1		5	9	23	32	41	50	59	78	86	99
1-Phase	2-Phase	2-Phase	2-Phase	2-Phase	2-Phase	2-Phase	2-Phase	2-Phase	2-Phase	2-Phase	2-Phase
1.000	1.000	1.000	1.000	1.044	1.068	1.077	1.082	1.086	1.095	1.095	1.095
0.200	0.200	0.200	0.200	0.209	0.214	0.215	0.216	0.217	0.219	0.219	0.219
0.850	0.850	0.850	0.850	0.887	0.908	0.915	0.919	0.923	0.931	0.931	0.931
1.400	1.400	1.400	1.400	1.462	1.495	1.508	1.514	1.521	1.534	1.534	1.534
0.200	0.200	0.200	0.200	0.209	0.214	0.215	0.216	0.217	0.219	0.219	0.219
0.500	0.500	0.500	0.500	0.522	0.534	0.539	0.541	0.543	0.548	0.548	0.548
52101.000	52101.000	1655.930	414.100	36.416	20.372	12.407	8.177	5.942	4.031	3.735	3.703

3. Macondo Fluid Properties, Fluid Temperature and Pipe Roughness

The Macondo reservoir fluid flowing through the system consisted of both oil and natural gas. We use a compositional PVT (pressure – volume – temperature) model developed by Zick[6] to best approximate the phase behavior of the fluid in the capping stack. We use an oil temperature in the capping stack of 180F,[7] and a pipe roughness of 0.0006 inches[8] (a common value for a new pipe).

B. Results of Capping Stack Flow Rate Calculations

We input our calculated two-phase K factors and the compositional PVT fluid model developed by Zick to the PROSPER commercial software, and calculate the flow rate through the choke line of the capping stack using an iterative procedure. We know the pressure upstream of the choke line and the downstream (ambient ocean) pressure. By assuming different flow rates, we determine the flow rate at which both the upstream and downstream pressures are matched. We conclude that the flow rate through the fully open choke line at the time of final shut in was 54,000 STB/day. Table 4 shows our calculation of the flow rate in tabular form, followed by the same data displayed pictorially in Figure 3.

[6] Macondo EOS Fluid Characterization, Aaron Zick, Zick Technologies (Sept. 4, 2012).
[7] BP did not collect a temperature measurement of the oil discharged from the well so we rely on the estimate BP provided to the DOE Tri-lab team, referenced in Exhibit 9361, Ratzel, A.C.: "DOE-NNSA Flow Analysis Studies Associated with the Oil Release following the Deepwater Horizon Accident," SANDIA Labs (September 2011).
[8] Kelkar, M.: Natural Gas Production Engineering, PennWell Publications, Chapter 5 (2008).

Table 4: Rate through Choke Line as function of Choke Opening

% open Choke	p(stable) (psig)	Rates (bbl/d)
100		
100		
99	3074	54000
93		54000
86	3075	54000
78	3099	54000
69	3138	54600
59	3230	54900
50	3384	55600
41	3671	57000
32	4149	57800
23	4748	55000
16	5606	46350
9	6220	24100
5	6408	12430
2	6553	10850
1	6581	2320
0	6600	0

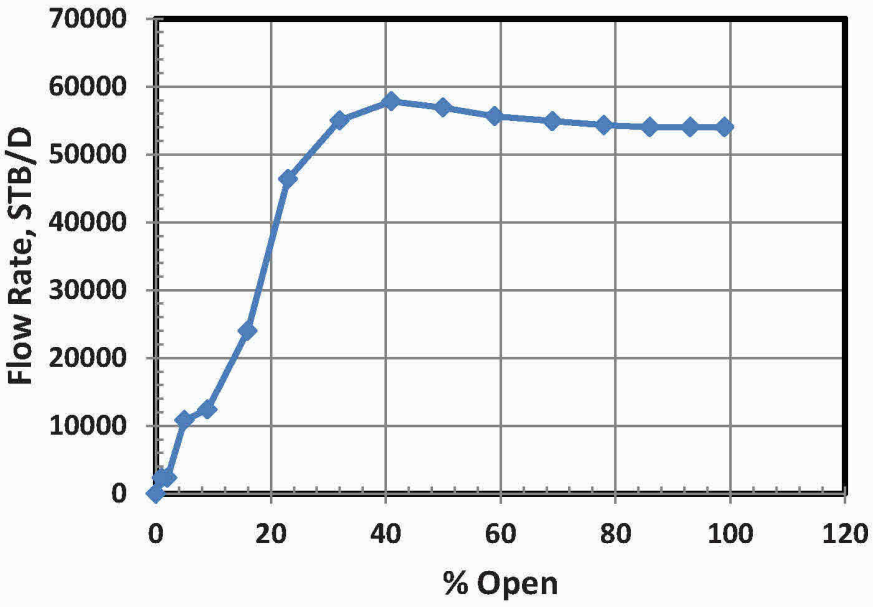

Figure 3: Rate through Choke Line as a Function of Choke Opening

Our calculations show an increase in flow as the choke valve is closed, however we do not believe that the flow rate did, in fact, increase. This observed phenomenon could be due to lack of equilibrium between gas and oil due to high flow rates, uncertainties in C_f values, or the choke valve size not being significantly smaller than the diameter of the piping on each side of the choke valve. It could also be due to hysteresis in choke closing. That is, the turns in the choke do not quite adjust the area as calculated. Data between 20 to 60% opening should be treated with caution since it is not consistent with what we would normally expect. However, multiple data points between 60% opening and 100% opening and consistent results obtained for many of these openings make us believe that the rate predictions above 60% opening are reliable. More importantly, we believe that the flow rate calculated with the choke 100% open (54,000 STB/day) is correct.

C. Parameter Variation/Sensitivity Analysis

We also consider the sensitivity of our analysis to potential variation or uncertainty in the upstream temperature, friction factor of the pipe, upstream pressure, and sensitivity to the PVT model on the rate calculations. The details of our sensitivity analysis and calculations are discussed in Appendix C. As noted above, our base value of upstream temperature is 180 F and our base value of pipe roughness is 0.0006 inches. We consider the upstream temperature to be in the range of 180 F to 200 F. The temperature uncertainty results in a rate variation of about 2% (higher temperature results in about 2% reduction in the rate). We also consider the relative roughness of pipe to vary between 0.0006" (new pipe) to 0.0015" (dirty pipe). This change in the relative roughness factor results in about 1% change in the flow rate values (higher roughness results in about 1% reduction in the rate). We also consider the uncertainty in pressure measurements. Based on information provided by BP, we assume that the uncertainty in the pressure measurement is as small as +/- 9 psi when the measured pressure is 2190 psig, and as large as +/- 68 psi when the measured pressure is 7,100 psig.[9] This variation in pressure results in a less than 2% variation in flow rate. Taken together, these potential parameter variations result in a flow rate that varies between -4% to +1% from the base value. Finally, we evaluate the sensitivity of our flow rate calculations to variations in the PVT model by using a black oil table provided by BP for the Macondo fluid in the PROSPER model.[10] Using the black oil model, we calculate a flow rate through the fully open choke of 53,750 STB/day, which represents a decrease in flow rate of approximately 0.5% when compared with the Zick compositional model.

[9] Exhibit 8687, Gochnour, M.: "MC252 Sensor Accuracy," BP Powerpoint Presentation (July 18, 2010).
[10] Exhibit 9732, E-mail from Ms. Baker to Dr. Ammerman, et al., dated 6/11/2010, Subject: FW: Black Oil Tables from EoS for All Temps 11June2010.xls (SDX009-0004236-0004237).

D. Calculation of Flow Through the Kill Line

In addition to calculating the flow through the capping stack choke line, we also calculate the flow rate through the kill line (depicted in Figure 1). After the capping stack was installed, from ~5:00 p.m. CDT on July 14 through ~10:00 a.m. CDT on July 15, 100% of the Macondo well flow was directed out of the kill line attached to the capping stack. The average upstream pressure was reported by BP to be 2,625 psig.[11] See Figure 4 below (period 1).

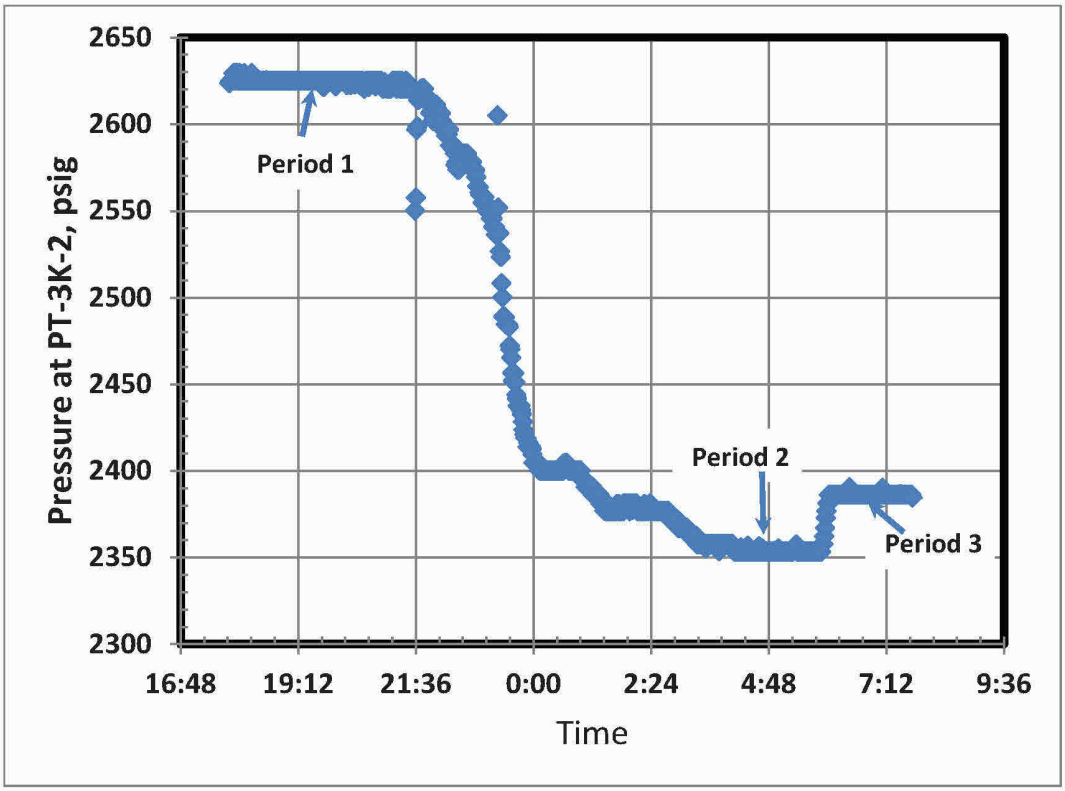

Figure 4: Upstream Pressure of Kill Line at PT-3K-2 Pressure Gauge

There were two additional steady state periods (Period 2 and Period 3 in Figure 4) where a portion of the oil was flowing through the kill line and a portion was being collected at the surface through a point upstream of the kill line. The upstream pressure reported by BP during Period 2 was 2,355 psig and the upstream pressure during Period 3 was 2,386 psig.[12] Using the kill line configuration show in Figure 1, we calculate the rates through the kill line for these three periods using the same methodology and inputs (temperature, roughness, K factors and Zick PVT model) as we use for the choke line. After adding any collection fluid during these periods,

[11] WIT Data 14July 9am – 3Aug 1pm, BP (BP-HZN-2179MDL07066615).
[12] WIT Data 14July 9am – 3Aug 1pm, BP (BP-HZN-2179MDL07066615).

we calculate the total rate of fluid flowing through the well.[13] Table 5 below shows the calculated flow rates during these three periods.

Table 5: Calculated Rates Through Kill Line

	Oil Rate (STB/D)		
Periods	**Kill Line**	**Collection**	**Total**
Period 1	52,000	0	52,000
Period 2	32,000	22,100	54,100
Period 3	34,500	18,900	53,400

With the same sensitivity parameters used in the choke line system flow rate calculation – the upstream temperature and pressure, friction factor of the pipe, and PVT model – the capping stack kill line flow rate estimate would have the same variation of -4% to +1% from the base value. The calculations performed with collection (Periods 2 and 3 in Table 5) give us further confidence in our calculations as we would expect the flow rate would be higher during times of collection because of the lower pressure upstream.

E. Bottom Hole Pressure Calculations (BHP)

We can use our predicted flow rates to calculate the bottom-hole pressure (BHP) in the well. These calculated BHPs provide the input pressure data after shut-in for the pressure buildup analysis (Section II below), and allow us to estimate a Productivity Index – an indicator of the production potential of a well – for the Macondo well (Section III below).

After the well was completely shut-in on July 15, the shut-in pressure was monitored for several more days. We use the stabilized rates and the stabilized pressures shown in Table 1 to calculate bottom-hole pressures. To do so, we need to assume a tubing configuration. Based on an analysis conducted by BP's contractor, we assume flow through the production casing.[14] The schematic of the well is shown below in Figure 5. As can be seen in Figure 5, if we assume the flow through the casing only, there are three paths the flow could take: flow through the drill pipe only before it enters the BOP; flow only in the annulus region (between the drill pipe and production casing); or flow through both the drill pipe and the annulus region between the drill pipe and production casing. In addition, we assume that sections of the BOP may provide some degree of restriction due to partially closed rams.

[13] Exhibit 9361, Ratzel, A.C.: "DOE-NNSA Flow Analysis Studies Associated with the Oil Release following the Deepwater Horizon Accident," SANDIA Labs (September 2011); Exhibit 9490, Vessel Collection Rates.

[14] Rygg, O.: "Macando 252 # 1 Blowout Static Kill Operation – Flow Path Analysis (August 2010) (AE-HZN-2179MDL00064585-64585).

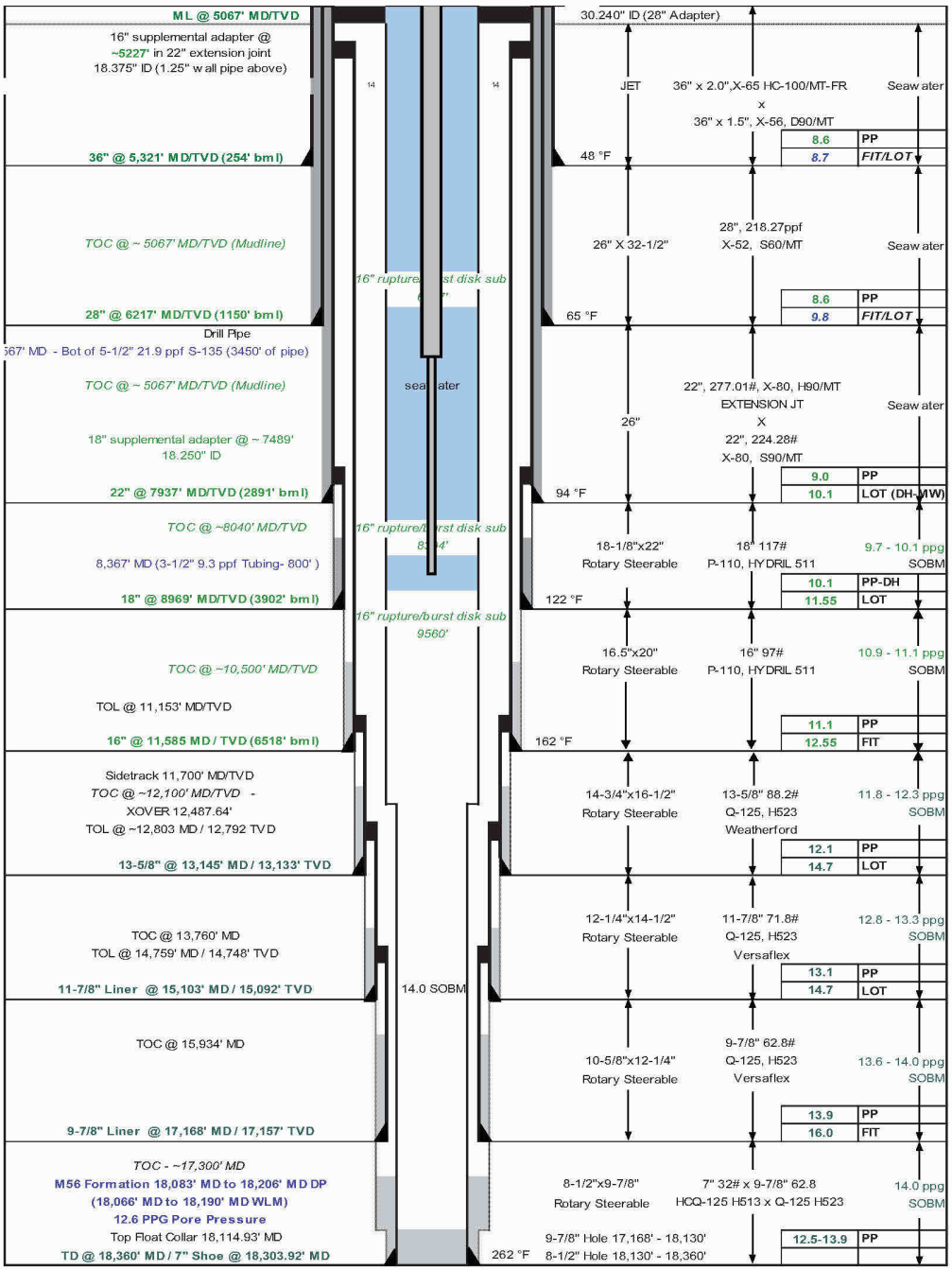

Figure 5: Macondo Well Bore Schematic[15]

[15] Excel sheet: MC252_well No 1 BP01 Schematic_Rev15_2_04 222010_with BOP, Provided by BP (April 2010)

To calculate the pressure drop created in the BOP, we examine the difference between pressure gauges in the BOP and PT-3K-2.[16] We calculate an offset of approximately -620 psi in the BOP pressure gauge on July 15 by comparing the BOP pressure and PT-3K-2 pressure during shut in. Except for the small hydrostatic head, those pressures should be equal during the shut-in period. We use this offset of -620 psi to recalculate the BOP pressure.

Using steady state pressure values for each choke turn at PT-3K-2 and then accounting for pressure drop across the BOP, we calculate the pressure value upstream of the BOP. We use the compositional model developed by Zick and the PROSPER program to calculate the BHP. In addition, we calculate the BHP under shut-in conditions (no flow) by using the hydrostatic head of oil, which we calculate using oil density calculated based on the Zick compositional model. The pressure drop due to the column of oil is 3,220 psi. Table 6 below shows the calculated BHP for different rates. The third column indicates the measured pressure at PT-3K-2.

Table 6: Oil Rate and BHP Values as a function of Choke Setting

Turns	% Open Choke	p(PT-3K-2) (psig)	Oil Rate (STB/d)	BHP (psig)
1.0	99	3074	54000	8104
2.0	86	3075	54000	8104
2.5	78	3099	54300	8133
3.0	69	3138	54300	8151
3.5	59	3230	55000	8232
4.0	50	3384	55500	8333
4.5	41	3671	57000	8577
5.0	32	4149	57900	8912
5.5	23	4748	55200	9237
6.0	16	5606	46400	9654
6.5	9	6220	24000	9624
7.0	5	6408	12500	9660
7.5	2	6553	10857	9783
8.0	1	6581	2350	9780
8.5	0	6600	0	9820

[16] WIT Data 14July 9am – 3Aug 1pm, BP (BP-HZN-2179MDL07066615).

Figure 6 below shows the plot of oil rate and BHP as a function of the choke opening.

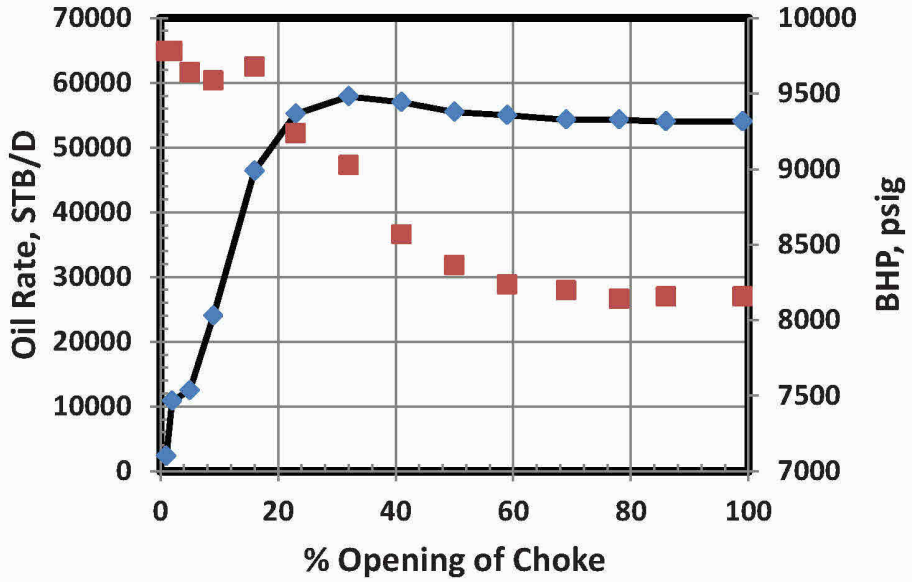

Figure 6: Plot of BHP and Oil Rate as a function of Choke Opening

Ideally, the oil rate should decrease as the BHP increases. As the BHP increases, there is less pressure drop across the reservoir, hence a lower flow rate. If we examine Figure 6, we can see that for the % opening between 60 and 100, the rate is approximately constant and so is the BHP. For a choke opening less than 20%, as the rate declines, BHP increases. This is also consistent. However, between the choke opening of 20% and 60%, the rate shows a slight increase as the BHP increases. This is inconsistent with typical well behavior. The rate calculations for 20% to 60% opening should be used with caution. However, for valve openings above 60%, repeated measurements and consistent results give us confidence that these rates are reliable.

SECTION II. PRESSURE BUILDUP ANALYSIS

We provide a summary of our evaluation of the pressure buildup test following the 86-day blowout of the Macondo well after shut in on July 15, 2010.[17] We use the data gathered during the shut-in to assess certain characteristics of the reservoir, including the shape and well location. As discussed in Section I, the shut-in process consisted of a number of valve turns at the capping stack, with 10-minute rest periods between valve turns; that is, oil discharge was reduced in a step-wise fashion. This sequence of steps was apparently for safety considerations and for avoiding further failure. At the time of shut in, the evaluation of shut-in pressure responses to determine formation properties did not appear to be a primary consideration.[18]

A pressure buildup test is a standard petroleum engineering technique for evaluating well conditions and reservoir characteristics. It involves shutting in the well and observing the pressure response for the well. Although the pressure buildup data for the Macondo well is not ideal due to the manner in which BP shut in the well, it is sufficient to inform us on the shape of the reservoir, the location of the well in the reservoir, and our estimation of average reservoir pressure in Section III below.

Our initial preprocessing of the shut-in pressure data[19] and examination of the derivative curve including the un-convolved derivative (derivative without incorporation of a flow rate schedule)[20] suggests the existence of one or more sealing boundaries (i.e., the "outside walls") in the reservoir and the existence of a channel-type system, as shown in Figure 7 below. The top curve shows the changes in pressure that were measured during the test. The bottom curve is the pressure derivative curve (un-convolved) that we calculate from the measured pressures.[21] This curve reflects the local slope of the pressure curve (the top curve) with respect to the logarithm of time.[22] Typical values for slopes that are encountered in pressure buildup analysis are -1/2, 0,

---

[17] We understand that the principal reason for shutting in the well on July 15 was to determine its mechanical integrity so that one may then determine whether the well could remain shut in to avoid additional spillage, and determine if the well needed to be reopened if it appeared that the sea floor would be breached.

[18] Before considering details pertaining to this pressure buildup test, we note that quality control checks suggest that the resolution of the PT-3K-2 gauge was not optimal, however these resolution issues have a minimal effect on the conclusions presented here.

[19] WIT Data 14July 9am – 3Aug 1pm, BP (BP-HZN-2179MDL07066615).

[20] A derivative curve that incorporates a rate schedule goes by the name of convolved derivative.

[21] In pressure analysis parlance the term "derivative" is often used. This term may be used in a global sense or in a local sense. Many forms of the pressure derivative are used in pressure analysis. Unless specifically noted, the term usually means the slope of the curve with respect to the logarithm (log) of time, and usually the local form is implied. The word slope, in an engineering context, represents the grade or pitch of a line.

[22] Logarithms are handy functions that engineers and scientists use, principally, so that information can be compressed in a manageable and systematic way. A well test analyst often has to deal with time scales from a few seconds to several days. As numbers progress multiplicatively, their corresponding logarithms

1/4, 1/2 and 1. Each of these values suggests to an analyst certain characteristic features of the reservoir or well. Here, we found a one-half slope line corresponding to the derivative curve, which is a signature that suggests the existence of a channel-type reservoir (i.e., a long generally rectangular shape). This one-half slope line is also shown in Figure 7. Our analysis of the data also suggests that the Macondo well is in the corner of a reservoir with a rectangular shape. Both of these observations are consistent with the BP pre-drill report, which suggests that the well is indeed located at the corner of a reservoir with a rectangle shape, as show in Figure 8.[23]

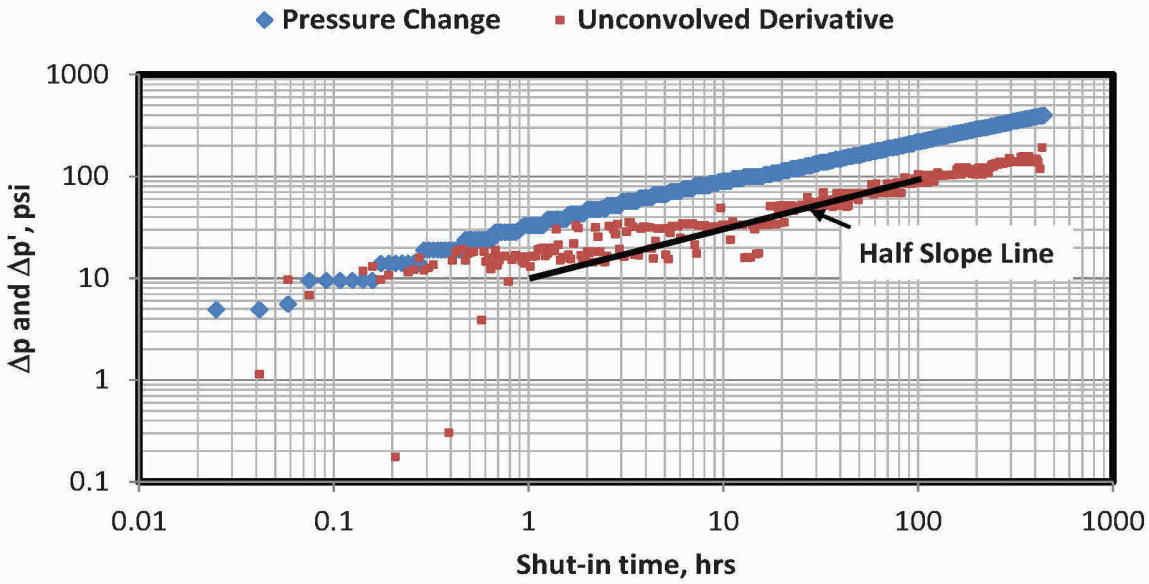

Figure 7: Shut-in Pressure and Pressure Derivative Changes

increase additively; for example, the logarithms of 1, 10, 100 and 1,000 are, respectively, 0, 1, 2 and 3. The Richter scale is a good example of a measurement expressed on a logarithmic scale – an earthquake of 2.0 is 10 times as strong, and earthquake of 3.0 is 100 times as strong, and so on.

[23] Exhibit 3533, Technical Memorandum: Post-Well Subsurface Description of Macondo Well, BP (July 26, 2010).

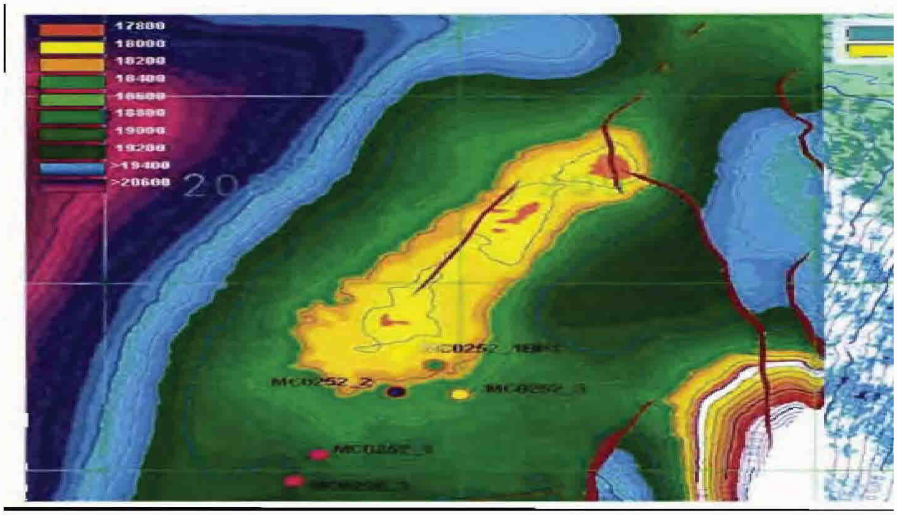

Figure 8: Seismic Map and Relative Well Location - BP Pre-drill Report

SECTION III. ESTIMATE OF TOTAL VOLUME DISCHARGED FROM MACONDO RESERVOIR USING MATERIAL BALANCE ANALYSIS

In this section of our report, we further analyze all of the data collected and calculated for the Macondo reservoir to determine the cumulative volume of oil released between April 20 and July 15, 2010. We use a material balance analysis, a standard petroleum engineering calculation based on the basic principle of conservation of mass. In simple terms, a material balance calculation takes the initial estimate of oil volume in the reservoir, known as original oil in place (OOIP) or stock tank oil initially in place (STOIIP), and subtracts the oil volume at a given point in time to obtain an estimate of the oil that was produced. The average reservoir pressure is a measure of the amount of fluid that exists in the reservoir at any given time and represents the equilibrium pressure the well will attain ultimately. The difference between the Macondo initial reservoir pressure (11,856 psia) and the final average reservoir pressure calculated below (between 10,235 and 10,396 psia) represents the lost volume of oil from the Macondo reservoir during the blowout.

A. Estimation of Average Reservoir Pressure

A few methods are available to calculate average reservoir pressure based on pressure buildup after shut in. One of them is the method proposed by Mead.[24] Originally the method was introduced on an empirical basis; however, it has been provided a theoretical basis.[25] Mead's

[24] Mead, H.N., A Practical Approach to Transient Pressure Behavior paper SPE 9901-MS presented at the SPE California Regional Meeting, March 25-27, Bakersfield, California (1981).
[25] Haugland, T., Larsen, L., and Skjæveland, S.M., Analyzing Pressure Buildup Data by the Rectangular Hyperbola Approach," paper SPE 13079-MS presented at the SPE Annual Technical Conference and Exhibition, September 16-19, Houston, Texas, (1984). Using the rectangular hyperbola as the basis,

method consists of fitting a curve known as a rectangular hyperbola to measured responses. Mead shows that the asymptote[26] of the hyperbola yields the average reservoir pressure at shut in.

We therefore calculate the average pressure of the Macondo reservoir on July 15 by fitting parameters to the pressure buildup response during the well integrity test. Using this method, we calculate an average reservoir pressure of 10,396 psia, as show in Figure 9. This pressure represents the final average reservoir pressure after the well was shut in and allowed to reach equilibrium. This pressure also represents the Macondo reservoir pressure today.[27]

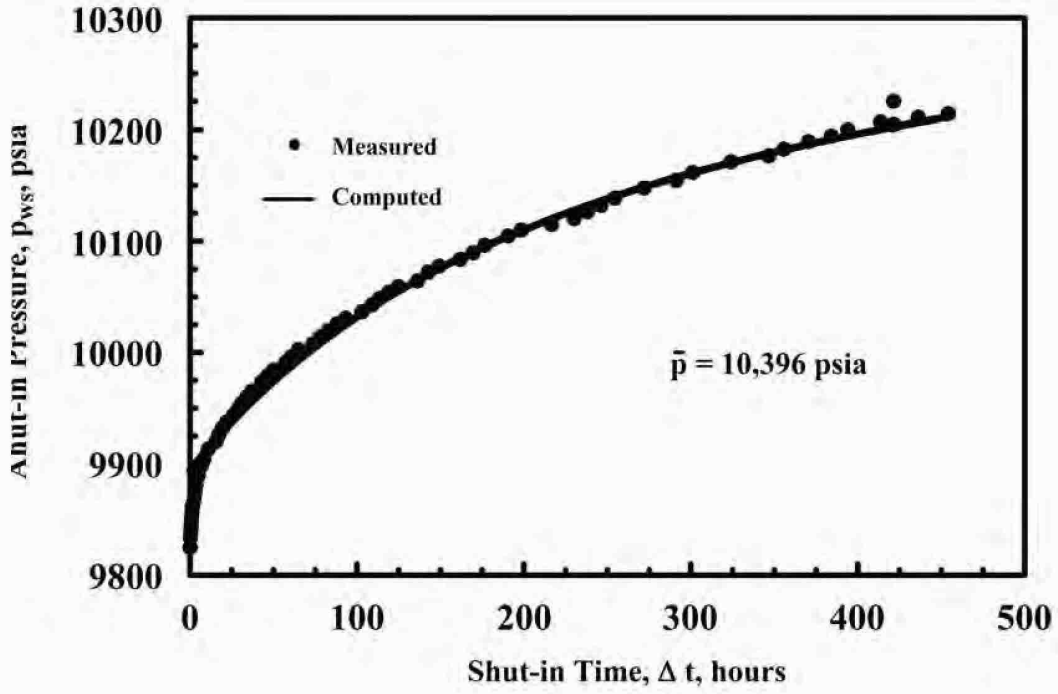

Figure 9: Evaluation of Pressure Responses by Mead's Method

Haugland *et al.* provide quantitative justification for the calculation of average reservoir pressure by Mead's method.

[26] The asymptote of a curve is a line such that the distance between the curve and the line approaches zero as they tend to infinity.

[27] The initial reservoir pressure when the Macondo well was drilled was 11,856 psia.

[redacted]

B. Calculation of OOIP

One of the most important reservoir parameters in the oil industry is the original oil in place. OOIP is a volumetric estimate of oil in place in a reservoir before production begins, and is based on integration of seismic, geological, petrophysical and reservoir engineering data. Larger OOIP means more oil is available to produce from the reservoir. In most off-shore reservoirs, a critical, threshold value of OOIP is needed before a company will make the decision to develop of the oil field. Below, we examine various documents published by BP and calculate OOIP using BP's pre- and post-drill data for the Macondo well.

1. BP's Pre-drill/Post-drill Analysis

In the pre-drill Technical Assurance Memorandum published by BP,[31] several reservoir data points are listed. Table 7 summarizes BP's analysis of the possible range of reservoir parameters. The figures 10, 50 and 90 in the top row of the Table 7 represent the probability that the actual reservoir parameter will exceed the listed value.[32] For example, this table predicts that there is a 90% probability that STOIIP for the Macondo reservoir is at least 138 MMSTB.

[redacted]

[31] Exhibit 5246, BP Technical Assurance Memorandum, Section 1, Subsurface (April 2009).

[32] Although BP's pre-drill Technical Assurance Memorandum predicted that the total reservoir has a 50% probability of having an average thickness of 42 feet, it also predicted that the thickness at the proposed well location had a 50% probability of 95 feet. Exhibit 5246, BP Technical Assurance Memorandum, Section 1, Subsurface (April 2009). The actual thickness of the formation at the well location turns out to be very close (~90 feet) to the predicted value, further validating the initial estimates in the pre-drill model.

Table 7: BP's Pre-Drill Analysis of Reservoir Properties

	90	50	10
Reservoir Size (acres)	3639	4498	8697
NTG	100%	100%	100%
Porosity (%)	17%	23%	28%
Permeability, md	20	500	1,000
Oil saturation (%)	60%	75%	80%
Formation Vol Factor (bbl/STB)	1.31	1.46	1.61
Recovery Factor	15%	30%	45%
thickness (ft)	25	42	44
STOIIP (MMSTB)	138.00	181.00	239.00
Reserves (MMSTB)	44.00	64.00	86.00

The relationship between STOIIP and pore volume is:

$$STOIIP = PV \times S_o/B_{oi}$$

This equation indicates that STOIIP increases with increases in pore volume and oil saturation, and decreases as initial formation volume factor (FVF or B_{oi}) increases. As the probability becomes smaller (i.e., < 90%), the STOIIP increases. Pore volume of the reservoir is the total void space in the reservoir rock where the oil resides. FVF or B_{oi} is the ratio of liquid oil in the reservoir to liquid oil at surface, also known as "stock tank" conditions (because some amount of gas will evolve from the oil as it moves to the lower temperatures and pressures). Oil saturation (S_o) is simply the percentage of the pore volume occupied by oil (as opposed to water).

When the Macondo well was drilled, BP collected core samples from the reservoir and hired Weatherford Laboratories to characterize the reservoir.[33] We considered the three main hydrocarbon bearing reservoirs analyzed by Weatherford: M56D, M56E and M56F. Table 8 below summarizes some of the data collected from the well.

Table 8: Observed Data at Macondo Well 252

	Net sand, ft	S_o (%)	Porosity (%)
M56D	22	83	20.7
M56E	69.5	90.3	22.1
M56F	6.5	78	21.1

From Table 8, we can calculate the thickness-weighted porosity and oil saturation. Porosity is the percentage of void space in the reservoir rock – the space that is filled with oil. The average porosity is 21.72% and the average oil saturation is 88%. The oil saturation at the well location is higher than what was predicted in BP's pre-drill technical report. The porosity

[33] Macondo Data Summary, Nov 2010, BP (BP-HZN-2179MDL05368315).

value is slightly lower than what is predicted in BP's most likely model. More importantly, the FVF or B_{oi} in the laboratory observed oil sample[34] is significantly greater than the value indicated in Table 7 (2.14 bbl/STB is the observed value versus 1.46 bbl/STB in Table 7). If we concentrate on the 50% probability value of STOIIP from BP's pre-drill estimates (in Table 7) and correct for the variation in porosity, saturation and formation volume factor, we calculate the modified STOIIP as:

$$STOIIP = 181 \times \frac{0.2172 \times 0.88 \times 1.46}{0.23 \times 0.75 \times 2.14} = 137 \text{ MMSTB}$$

3. Cumulative Volume of Oil Removed from the Reservoir

As noted above, material balance is a standard industry technique used to determine the amount of oil and gas produced given the pressure changes in the reservoir, and requires the knowledge of initial oil in place, fluid properties as a function of pressure and temperature, and changes in the reservoir pressure.

BP measured the initial reservoir pressure (p_i) as 11,856 psia.[35] Our well test analysis applying the Mead method provides us with an average pressure ($\bar{p}$) value of 10,396 psia. We calculate the total compressibility (c_t) of the reservoir by combining the compressibilities of oil, water and reservoir formation:

$$c_t = c_o S_o + c_w S_w + c_f$$

The average of the oil compressibility of the last BHP and the initial pressure is 14.3×10^{-6} psi^{-1},[36] water compressibility is 3×10^{-6} psi^{-1} and formation compressibility is 12×10^{-6} psi^{-1}.[37] Oil saturation is 0.88 and water saturation is 0.12.[38] Using those values, we calculate the total compressibility (c_t) of the reservoir as 2.494×10^{-5} psi^{-1}. We can then use our calculated values for STOIIP, total compressibility, average reservoir pressure, and oil formation volume factor to calculate the amount of oil removed from the reservoir using a simple material balance equation:[39]

---

[34] Exhibit 9732 (E-mail from Ms. Baker to Dr. Ammerman, et al., dated 6/11/2010, Subject: FW: Black Oil Tables from EoS for All Temps 11June2010.xls, SDX009-0004236-0004237).
[35] Macondo Data Summary, Nov 2010, BP (BP-HZN-2179MDL05368315).
[36] Exhibit 9732 (E-mail from Ms. Baker to Dr. Ammerman, et al., dated 6/11/2010, Subject: FW: Black Oil Tables from EoS for All Temps 11June2010.xls, SDX009-0004236-0004237).
[37] Merrill, R.: Powerpoint Presentation, Reservoir Response, 8_july-2010 (BP-HZN-2179MDL07033641).
[38] Exhibit 5246, BP Technical Assurance Memorandum, Section 1, Subsurface (April 2009).
[39] Dake, L.P.: Fundamentals of Reservoir Engineering, El Sevier (1978) chapter 3.

$$Oil\ Removed = \frac{STOIIP \times c_t \times (p_i - \bar{p})}{(1 - S_{wi})} \frac{B_{oi}}{B_o}$$

In the above equation, S_{wi} represents initial water saturation (12%), B_{oi} represents the initial formation volume factor (2.14 bbl/STB) and B_o represents the formation volume factor at the average reservoir pressure (2.1858 bbl/STB). In addition to using the STOIIP value derived based on BP's pre- and post-drill estimates, we also use the STOIIP of 110 million STB as reported by BP.[40] Using these STOIIP values, we compute the oil removed from the reservoir as shown in Table 9, below:

Table 9: Oil Removed from the MC252 Reservoir

		STOIIP (MMSTB)	Oil Removed (MMSTB)
	Pre-drill/Post-Drill	136.7	5.5
	BP Estimate	110	4.5

Based on our STOIIP and material balance calculations, we conclude that the amount of oil released from the Macondo reservoir over the 86 days of the spill was between 4.5 and 5.5 MMSTB.

Our calculation uses a formation compressibility is 12×10^{-6} psi^{-1}. According to BP, this is the most likely value of formation compressibility and is consistent with BP's presentations to the U.S. Government.[41] We do not include the influence of water influx since only limited knowledge regarding the size and the strength of aquifer support in the Macondo reservoir is available. As a result, our estimates are conservative in that they are low. [redacted]

Table 10: Oil Removed from the Reservoir

			Mead	[redacted]
Average Pressure (psia)			10,396	[redacted]
		STOIIP (MMSTB)	Oil Removed (MMSTB)	
Pre-drill/Post-Drill		136.7	5.5	[redacted]
BP Estimate		110	4.5	[redacted]

[40] This value has been reported by BP and others in various reports, e.g., Merrill, R.: Powerpoint Presentation, Reservoir Response, 8_july-2010 (BP-HZN-2179MDL07033641).
[41] Merrill, R.: Powerpoint Presentation, Reservoir Response, 8_july-2010 (BP-HZN-2179MDL07033641).

D. Productivity Index Calculations

Productivity index (PI) calculations are a measure of the rate at which the well can produced per unit change in the pressure drop. PI can be calculated from the reservoir properties or it can be calculated from the actual flow data (production data). If we are able to match PI values calculated from reservoir parameters with actual PI values based on production data (or estimated production rates), that will increase our confidence in our reservoir model. We therefore calculate PI values from our estimated rates and compare the PI value to the one obtained from the reservoir parameters to see consistency between the two numbers.

In addition to calculating the oil produced from the Macondo reservoir, we also use the average reservoir pressure estimate to calculate a productivity index for the reservoir. The productivity index (PI) is calculated as:

$$PI = \frac{(q)}{(\bar{p} - p_{wf})}$$

In the above equation q represents the oil rate, $\bar{p}$ represents the average pressure and p_{wf} represents BHP. Using the data in Table 6, and the average reservoir pressure of 10,396 psia from the Mead method, we can calculate a PI of 45 STB/D/psi. We can also determine the PI value using reservoir data. BP's post-drill summary report indicates a permeability of 300 millidarcies and a reservoir thickness of 90 feet.[42] As an approximation, we determine the PI value as (where k is in darcies):[43]

$$PI \approx \frac{kh}{\mu B} = \frac{0.3 \times 90}{0.199 \times 2.166} = 62$$

The viscosity and formation volume factor (B) are obtained from BP's black oil tables.[44] In the above equation, we used the thickness at the well location. However BP estimated the average thickness in the reservoir to be 42 feet. If we substitute 42 feet instead of 90 feet, we obtain a PI of 21. Our PI value of 45 falls between the two limits we obtain from the thickness variation (21-62). This further validates our flow rate calculations and our calculated PI value. The PI values are almost identical to PIs used by BP and its contractors during the blowout and indicate a very productive reservoir.[45]

---

[42] Macondo Data Summary, Nov 2010, BP (BP-HZN-2179MDL05368315)
[43] Brown, K.E.: Artificial Lift Methods – Volume 4, PennWell Publications (1983)
[44] Exhibit 9732 (E-mail from Ms. Baker to Dr. Ammerman, et al., dated 6/11/2010, Subject: FW: Black Oil Tables from EoS for All Temps 11June2010.xls, SDX009-0004236-0004237).
[45] TREX 1, Appendix W to Bly Report; Exhibit 9254 ("Relief well kill for Macondo MC 252 #1, Well Kill Modeling and Evaluations, July 2010); Exhibit 11163 (E-mail from Tony Liao, BP, to Maria Nass, BP, dated June 28, 2010, Subject: FW: Information on MC-252 well) (citing a PI of 45).

INFORMATION REQUIRED BY THE FEDERAL RULES OF CIVIL PROCEDURE

1. This report contains our opinions, conclusions and reasons therefore.
2. A general statement of our qualifications is contained in the Personal Background section of this report. A more detailed statement of Dr. Kelkar's qualifications, including publications authored in the last 10 years, is included in Appendix D. [redacted]
3. Our compensation for the preparation of this report and any testimony as an expert witness at trial or deposition is $300 per hour.
4. Neither Dr. Kelkar [redacted] has testified as an expert witness in the last four years.
5. The facts and data we considered in forming our opinions are listed in Appendix F.

The opinions expressed in this report are our own and are based on the data and facts available to us at the time of writing. Should additional relevant or pertinent information become available, we reserve the right to supplement the discussion and findings in this report.

APPENDIX A. BASIC PETROLEUM ENGINEERING CONCEPTS

Reservoir Engineering

Our report is based on our experience in petroleum and reservoir engineering. Reservoir engineering is a study of oil and gas reservoirs. The primary job of a reservoir engineer is to obtain a production forecast, and he or she does so after addressing three primary questions: (1) what is the volume of the hydrocarbons in the reservoir; (2) how rapidly may the fluid be extracted and recovered at the surface, and (3) how much of the available quantity of fluid may be produced. These answers establish the commercial viability of the oil or gas field. The typical reservoir engineer's responsibilities include: a) determining the reservoir characteristics or properties which can help predict the performance, including permeability, porosity, and pressure applied against the reservoir, b) determining the amount of oil or gas that can be eventually produced from the reservoir before the reservoir reaches an abandonment pressure, and c) optimizing the number of wells in the field so that the reservoir can be depleted at the lowest cost.

Techniques for Characterizing the Reservoir

Material Balance Analysis: a technique that can be used to determine how much oil and/or gas has been produced from a reservoir based on the depletion of the reservoir (the difference between the initial reservoir pressure and the current reservoir pressure) and the volume of oil and/or gas originally present in the reservoir. It can also be used to determine the initial volume of oil and/or gas originally present in the reservoir, based on the initial reservoir pressure, the current reservoir pressure, and the amount of oil and/or gas produced from the reservoir.

Reservoir Simulation: development of a model that allows the simulation of reservoir performance, by incorporating the reservoir characteristics; the process begins by collecting and integrating data and assumptions about the reservoir to create an "image" of the reservoir (alternate images of the reservoir may be created to account for uncertainties); a grid is then imposed on the image of the reservoir, which divides it into small grid blocks; properties are then assigned to each grid block; there may be tens of millions of grid blocks in a first-generation model; due to computational demands, such models are often "upscaled" by combining multiple grid blocks into one grid block; dynamic data is then added to the model so that a simulation of the actual flow process in the reservoir can be conducted.

History Matching: a technique used to adjust a reservoir model when production data is known, so that the simulated data matches the known production data; the history-matched model can then be used to predict future performance of the reservoir with greater confidence.

Pressure Analysis: a field-scale experiment that can be conducted to ascertain the permeability of a reservoir, determine if there are any impediments to the flow of hydrocarbons right around

the wellbore (skin factor), the degree of connection to other wells (connectivity), and the location of boundaries or barriers (faults); a pressure buildup test can also provide a measure of the volume of hydrocarbons that may be produced (reserves) and may also be used to achieve many other goals; for example, the primary purpose of the pressure buildup test at the Macondo well was to ascertain the mechanical integrity of the wellbore.

Key Reservoir Engineering Terms

Reservoir: a porous, permeable underground formation containing an accumulation of hydrocarbons.

Porosity: the percentage of void space in the reservoir – the space that is filled with oil.

Pore volume: the total void space in the reservoir where the oil resides along with gas and water.

Permeability: a measure of the conductivity of the rock to flow, an indicator of how fast the liquid or gas can flow through the porous material in the reservoir. The usual unit used to describe permeability is the *millidarcy* (mD).

Saturation (of various phases): the percentage of pore space that is occupied by oil, gas and water phases (S_o = oil saturation, S_w = water saturation, S_g = gas saturation)

Formation Volume Factor (FVF or B_{oi}): the ratio of liquid oil in the reservoir to liquid oil at surface, also known as "stock tank" conditions (because some amount of gas will evolve from the oil as it moves to lower temperatures and pressures).

Aquifer drive: Ground water located below the hydrocarbons in a reservoir may exert pressure in the reservoir "driving" the oil or gas out.

Skin: a numerical value used to describe formation damage that can impede flow from a reservoir into a well.

Pressure applied against the reservoir: the pressure that is applied due to: (i) the oil, gas or both are expanding; (ii) the aquifer (water volume underneath the reservoir) is expanding and encroaching in the reservoir; (ii) the formation is getting compacted because of overburden pressure; and/or (iv) additional water or other chemicals are injected in the reservoir through injection well to force the oil from the reservoir.

Original oil in place (OOIP): OOIP is a volumetric estimate of oil in place in a reservoir before production begins, and is based on integration of seismic, geological, petrophysical and reservoir engineering data.

Productivity Index: a measure of the rate at which the well can produce per unit change in the pressure drop, usually expressed in stock tank barrel per psi per day (STB/psi/day).

Average reservoir pressure: represents the amount of driving force available to drive the remaining fluid out of the reservoir during a production sequence. The average reservoir pressure in a reservoir at a given time is one of the factors which determine an indication of how much fluid (gas, oil, or water) remains in the reservoir.

Pipe Flow Calculations

In the oil industry, understanding the behavior of multi-phase flow in pipes and restrictions is critical to understanding how a well will perform and how the performance of a well can be optimized. The most important part of this understanding is the calculation of pressure drop between the reservoir and the surface under multi-phase flow conditions. The pressure drop calculation under multi-phase flow conditions is a function of (i) angle of inclination of the pipe; (ii) the relative magnitude of gas and liquid fractions; (iii) physical properties of the fluids; and (iv) flow regimes which are present in the pipes.

In addition to calculating the pressure drop in pipes, different correlations are available to calculate the pressure drop for flow through chokes. Similar to flow through pipes, they consider the importance of multi-phase flow on pressure drop across chokes. In most of the choke calculations, we make an assumption that the pressure drop across the choke is related to the flow rate. This relationship is a function of the fluid properties, the relative amounts of gas and liquid flowing through the choke and the relative cross sectional area of choke compared to the pipe. It can also be a function of choke geometry. Knowing the pressure changes in the pipe or choke allows one to make estimates of the rate of flow through the pipe or choke.

Pressure drop calculation: a technique for calculating pressure drop across a section of pipe based on fluid rates in the pipe. This procedure can also be used for calculating pressure drop across a choke valve. If a pressure drop is known, a slightly different procedure can be used to estimate the flow rates for a given pressure drop.

Multi-phase flow: flow fluids that includes more than one phase; phases include oil, gas and water.

APPENDIX B. CALCULATION OF K FACTORS

Based on an examination of the literature, we made several modifications to the K factor values used in the DOE Tri-Lab Report.[46] Each of the modifications is explained below.

Cross on Choke and Kill Lines

The K factor value for the elbow cross in the DOE Tri-Lab calculations was assumed to be 1.0. Other references indicate that the value potentially could be as high as 1.4.[47] For these calculations, we used 1.4 as the most conservative value.

Pipe Connection to Choke Valve

On both the downstream and the upstream sides of the choke valve, the pipe diameter expands from 3 1/16" to 3.63", as shown in Figure 1 in the main body of our report. This expansion results in additional K factor. We simplify this part of the flow as demonstrated in Figure B.1, below. Instead of a small expansion section, where the diameter changes from 3 1/16" to 3.63", we assumed that the diameter of pipe connecting to the choke valve (upstream and downstream) is 3.63". We incorporate the expansion K factor values as part of the choke valve K factor by increasing the K factor value for the fully open choke by 0.2, from 3.18 to 3.38. The value 0.2 represents a 0.1 expansion value both upstream and downstream of the choke.[48] Because of our simplification, the diameter of the small segment connected to the choke valve both upstream and downstream is slightly larger in our model than the actual value (3.63" vs. 3 1/16"). This modification has a negligible impact on our pressure drop calculations since the majority of the pressure drop is across the restrictions and not in the pipe segments.

[46] Exhibit 9361, Ratzel, A.C.: "DOE-NNSA Flow Analysis Studies Associated with the Oil Release following the Deepwater Horizon Accident," SANDIA Labs (September 2011).
[47] Fiber Glass Pipe Design, American Water Works Association (2005); Sarplast Iniziative Industriali Engineering Guide (2008) (value of head loss provided for 90 degree elbow dingle miter is 1.4).
[48] Exhibit 9361, Ratzel, A.C.: "DOE-NNSA Flow Analysis Studies Associated with the Oil Release following the Deepwater Horizon Accident," SANDIA Labs (September 2011).

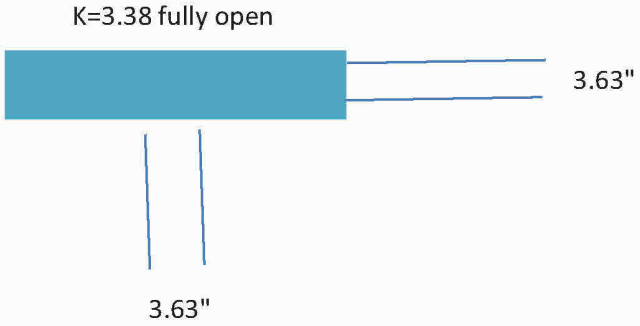

Figure B.1: Simplification of Upstream and Downstream of the Choke

K Factor for the Partially Open Choke Valve

The choke valve in the capping stack (CC40) is manufactured by Cameron. We use an equation provided by Cameron[49] to calculate the flow rate across the choke:

$$q = C_V\sqrt{\frac{\Delta p}{\gamma}} \quad (1)$$

where q is the rate in gal/min, C_v is the constant provided by Cameron for different choke openings, Δp is the pressure drop across the restriction (choke) in psi, and γ is the specific gravity of the liquid. Cameron has also published the value of C_v for different choke openings, and we used those published values in our calculations.[50] The maximum value of C_v is 251 for a fully open choke and the value declines all the way to zero.

Based on pressure drop calculations, we write the relationship between K and C_v:

$$K \propto \frac{1}{C_V^2} \quad (2)$$

Using this equation and the published values for C_v, we calculate the value of K, as shown in Table B.1. These values include the addition of 0.2 to account for expansion before and after the choke.

[49] www.c-a-m.com: Control Choke Catalog (2009).
[50] Cameron Willis: Flow Curve for CC40 Plug and Cage Choke, Cameron Willis, Longford, Ireland.

Table 1		
Cv	% open	K
0	0	
2	1	50086.00
5	2	8013.93
11	5	1655.93
22	9	414.13
49	16	83.64
76	23	34.89
103	32	19.08
133	41	11.53
165	50	7.56
195	59	5.47
220	69	4.34
240	78	3.68
250	86	3.41
251	93	3.38
251	99	3.38
251	100	3.38

Table B.1: K Factors for Choke Valve Openings (Single Phase)

According to Cameron, its equation for flow rate across the choke is strictly for single phase liquid flow. The Table B.1 K factor values are therefore applicable for single phase flow. However, we can infer the impact of two phase flow using prior literature. The following Figure B.2, provided by Willis Cameron Choke is reproduced from Surbey[51] and shows C_f as a function

[51] Surbey, D.W.: "An Investigation of Two Phase Flow through Willis MOV Wellhead Chokes," MS Thesis, The University of Tulsa (1985).

of gas-liquid ratio (GLR) for a range of pressures.

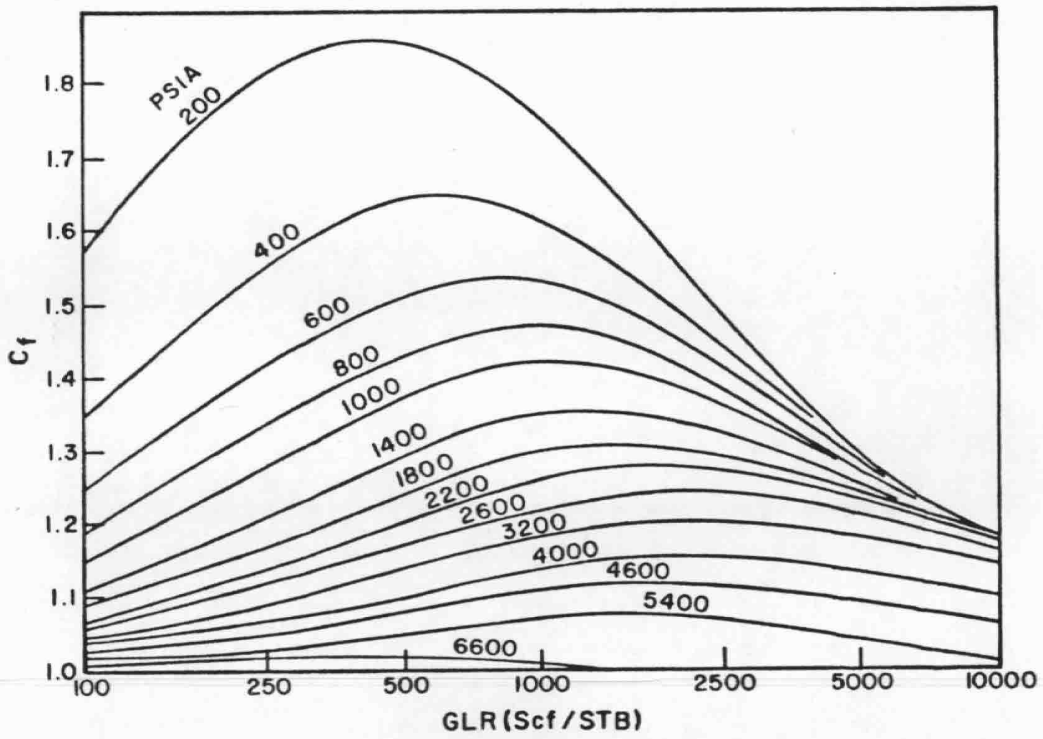

Figure B.2: Correction for Two Phase Flow for the Value C_v

The correction factor represents the correction needed to account for two phase flow. We calculate the value of C_v under two phase flow by dividing C_v under single phase flow by C_f. Note that the correction factor approaches one as the pressure increases. The sensitivity of GLR (which represents free gas present in the two phase flow stream) on C_f values at low pressures is significant as evidenced by large changes in C_f values, but as the pressure increases, the correction factor becomes less sensitive to GLR. At high pressures, C_f values become relatively insensitive to changes in GLR. This observation is consistent with the notion that at higher pressures, the gas will flow more like a liquid and the difference between the two phases becomes less significant. At high GLRs, gas will dominate the flow and hence the effect of two phase flow will be minimal.

Most of the reported pressures upstream of the choke valve in the capping stack on the Macondo well exceeded 3,000 psig; therefore, we conclude C_f would not be very sensitive to GLR. We calculate the GLR by subtracting the solution gas oil ratio at upstream conditions

from intitial gas oil ratio at the bubble point, using black oil tables provided by BP.[52] We then take the values of C_f based on upstream pressure and correct the C_v value for two phase flow by dividing the single phase C_v value by the appropriate C_f .

The value of C_f is different for each turn since the upstream pressure changes as the choke is progressively closed. We show the values of C_f for each choke closure step in the following Table B.2. As shown in Table B.2, the value of C_f, is equal to one at high pressures.

Table 2
C_f Factor as a Function of Choke Opening

% Open	Turns	p(stable)	C_f
1	8	6581	1.00
5	7	6408	1.00
9	6.5	6220	1.00
23	5.5	4748	1.09
32	5	4149	1.14
41	4.5	3671	1.16
50	4	3384	1.17
59	3.5	3230	1.18
78	2.5	3099	1.20
86	2	3075	1.20
99	1	3074	1.20

Table B.2: C_f Factor as a Function of Choke Opening

We use the values provided in Table B.2 to correct for K factors. We write the relationship as:

$$K_{Two-phase} = K_{single-phase} \times \sqrt{C_f} \qquad (3)$$

Using the C_f values shown in Table B.3, we convert the single phase K factor values to two phase K factor values.

[52] Exhibit 9732 (E-mail from Ms. Baker to Dr. Ammerman, et al., dated 6/11/2010, Subject: FW: Black Oil Tables from EoS for All Temps 11June2010.xls, SDX009-0004236-0004237).

Description	K Value
Expansion to Ocean	1.00
Long radius elbow	0.20
Collet Hub	0.85
Cross	1.40
Contraction (4 1/16" to 3 1/16")	0.20
Contraction (18 3/4" to 4.06")	0.50

Table B.3: Single Phase K Factor Values for Different Restrictions

The same value of C_f is used to convert the single phase K factor to the two phase K factor for all restrictions. These values are shown in Table B.4 below.

Table 4
% Open

1		5	9	23	32	41	50	59	78	86	99
1-Phase	2-Phase	2-Phase	2-Phase	2-Phase	2-Phase	2-Phase	2-Phase	2-Phase	2-Phase	2-Phase	2-Phase
1.000	1.000	1.000	1.000	1.044	1.068	1.077	1.082	1.086	1.095	1.095	1.095
0.200	0.200	0.200	0.200	0.209	0.214	0.215	0.216	0.217	0.219	0.219	0.219
0.850	0.850	0.850	0.850	0.887	0.908	0.915	0.919	0.923	0.931	0.931	0.931
1.000	1.000	1.000	1.000	1.044	1.068	1.077	1.082	1.086	1.095	1.095	1.095
0.200	0.200	0.200	0.200	0.209	0.214	0.215	0.216	0.217	0.219	0.219	0.219
0.500	0.500	0.500	0.500	0.522	0.534	0.539	0.541	0.543	0.548	0.548	0.548
52101.000	52101.000	1655.930	414.100	36.416	20.372	12.407	8.177	5.942	4.031	3.735	3.703

Table B.4: The K Factor Values for Different Restrictions Under Two Phase Flow

Table B.4 requires some additional explanation. In the first column, values of K factors for single phase flow are given for all restrictions (including the choke, which is given in the last row). The values of K factor for all the other restrictions for single phase flow do not change for different choke openings. However, the values of the K factors for two phase flow for all of the restrictions do change for some of the choke openings because the value of C_f changes, as shown in Table B.2. As the percent of the choke open to flow decreases, the values of K factor increase.

Potential Interference Between Restrictions

As shown in the capping stack diagram (Figure 1 of main report), oil flows through many restrictions (elbows and bends) before it is released to the ocean. We therefore consider whether there is interference between the successive restrictions that may cause additional pressure drops, and conclude that any such impact is negligible. For flow through the choke, the straight pipe section length (as number of times the pipe diameter size) required for a turbulent flow of oil to be fully developed is (White):[15]

$$\frac{L_E}{d} = 4.4\,\mathrm{Re}^{1/6} \qquad (4)$$

where L_E is the entrance pipe length, d is the pipe inner diameter, and Re is the Reynolds number.[53] Based on an assumed oil flow rate of 50,000 STB/D, the estimated Reynolds number is about 4,800,000. The entrance section required for the turbulent flow to be fully developed is about 57d. The straight section before the choke valve in the choke line of the capping stack is about 33d. This is large enough so that the entrance effect can be assumed to be very small compared with the effect of two phase flow.[54]

[53] Reynolds number is a dimensionless number which is used to determine if the flow in pipe is laminar or turbulent.

[54] Sookprasong studied the interference between different valves in 1980. He noted that if two valves are located too close (within 1.5" to 60") to each other, the value of K factor would be about 20% greater than the value without interference. The values reported in his thesis are specific to the distances between the valves and the diameter of the pipe. His work is not directly applicable here because we do not have successive valves in the system. Sookprasong, P.: "Two Phase Flow in Piping Components," MS Thesis, The University of Tulsa (1980).

APPENDIX C. PARAMETER VARIATION AND SENSITIVITY ANALYSIS

In this Appendix, we examine the sensitivity of the Capping Stack rate calculations to a variety of model parameters: temperature, pipe roughness, pressure, and fluid properties. We also examine the sensitivity of the reservoir material balance calculations to variations in final average reservoir pressure, formation compressibility, and aquifer support.

A. Capping Stack Calculations

Temperature Variation

In our Capping Stack rate calculation, we assume that the upstream temperature of the oil (temperature at the pressure gauge) is 180 F. To evaluate the sensitivity of our analysis to temperature variation, we consider the possibility that the temperature could be as high as 200 F. Using 200 F, we recalculate the rate through the choke valve at certain choke settings. In Table C.1 below we show the comparison between the rates calculated at 180 F versus the rates calculated at 200 F at certain choke valve steps. The higher temperature results in an average 2% reduction in flow rate.

Table C.1: Effect of Temperature on Rate Calculation (K Factor Calculations under Multi-Phase)

	Predicted Rate (STB/D)		
% Open	T = 200 F	T = 180 F	% Difference
5	12,310	12,430	0.97%
23	54,250	55,000	1.36%
59	53,750	54,900	2.09%
99	52,200	54,000	3.33%

Pipe Roughness Variation

We also consider sensitivity with respect to roughness. For a new pipe, a typical roughness value is 0.0006 inches. However, we also consider the possibility of a pipe which is dirty or damaged, which may have a higher value of roughness. To account for additional roughness, we consider a value of 0.0015 inches (a 250% increase). The larger roughness results in 1% reduction in the rate. See Table C.2 below.

Table C.2: Effect of Roughness on Rate Calculation (K Factor Calculations under Multi-Phase)

	Predicted Rate (STB/D)		
% Open	ε = 0.0015"	ε = 0.0006"	% Difference
5	12,420	12,430	0.08%
23	54,780	55,000	0.40%
59	54,000	54,900	1.64%
99	53,000	54,000	1.85%

Pressure Measurement Variation

We also considered variation in the pressure measurements, and the sensitivity of our analysis to that pressure variation. According to a BP report on the precision of the pressure gauges,[55] the error in the pressure gauge is about 9 psi at 2190 psi measurement and may be as much as 68 psi when the pressure measurement is 7,100 psi. In a subsequent BP report,[56] the pressure measurement error was found to be smaller than what was earlier reported; however we used the larger uncertainty range for our analysis. Using the two errors as lower and upper measurements, we assume that the error would increase linearly with the pressure measurement. That is, as the measured pressure increases the absolute error in pressure measurement would increase linearly. Making this assumption, we calculate the possible range of pressure for each choke valve step as shown in Table C.3. P(+) represents maximum pressure value possible and P(-) represents minimum pressure possible at the pressure gauge for a given choke setting.

Table C.3: Pressure Variation for Different Choke Settings Under Multiphase Flow

Turns	% open	P(stable)	Δp	P(+)	P(-)
1	99	3074	19.622	3094	3054
2.5	78	3099	19.923	3119	3079
3.5	59	3230	21.497	3251	3209
4.5	41	3671	26.796	3698	3644
5.5	23	4748	39.738	4788	4708
6.5	9	6220	57.426	6277	6163
7	5	6408	59.685	6468	6348
8	1	6581	61.764	6643	6519

Using these pressure values, we calculate the rates as shown in Table C.4, below. As before, we did not calculate the rate at every choke setting. We conclude that the pressure variation results in a change in flow rate of approximately +/-1%.

[55] Exhibit 8687, Gochnour, M.: "MC252 Sensor Accuracy," BP Powerpoint Presentation (July 18, 2010).
[56] Exhibit 8680, Gochnour, M.: "BP MC252 Pressure Measurement Reconciliation" (2011).

Table C.4: Impact of Pressure Uncertainty on Rate Calculation (K Factor)

	Predicted Rate (STB/D)			% Difference from base	
% Open	p(+)	p(-)	Base	(+)	(-)
5	12,535	12,325	12,430	0.84%	-0.84%
23	55,600	54,600	55,000	1.09%	-0.73%
59	55,200	54,200	54,900	0.55%	-1.28%
99	54,600	53,200	54,000	1.11%	-1.48%

In addition to considering these uncertainties, we also consider the possibility that the fluid temperature at the exit does not reach the ocean temperature instantaneously. Instead, the temperature of the fluid at the exit is 170 F. Using this assumption, we observe a 1-2% reduction in rate.

Upper and Lower Bounds of Parameter Variation

The percent variations we calculate above are not cumulative. That is, some of the parameter variations offset one another to a degree. Therefore, we also consider the maximum variation possible by considering both lower and upper bounds of different variables. In the lower bound case, we consider maximum roughness, higher temperature and lower upstream pressure. In the upper bound case, we consider lower roughness, lower temperature and higher upstream pressure. Table C.5 below shows the results. The overall bounds provide between -5% to +1% variation in the rates.

Table C.5: Upper and Lower Bounds of Rate Calculation (K Factor)

	Predicted Rate (STB/D)			% Difference from base	
% Open	Lower	Upper	Base	Lower	Upper
5	12,200	12,535	12,430	-1.85%	0.84%
23	54,000	55,600	55,000	-1.82%	1.09%
59	52,400	55,200	54,900	-4.55%	0.55%
99	51,250	54,600	54,000	-5.09%	1.11%

In addition to the uncertainties considered here, there are also uncertainties with respect to the C_f value which accounts for the two phase flow effect. While it is difficult to quantify the uncertainty with respect to C_f, we can state that this effect should be small because our pressure values are more than 3000 psia in most situations (Fig. B.2). At high pressures, the gas behaves more like a liquid and the two phases behave more like a pseudo-homogeneous single phase fluid.

Use of BP's Black Oil PVT Model

Finally, we evaluate the sensitivity of our flow rate calculations to variations in the PVT model by using a black oil table provided by BP for the Macondo fluid.[57] Using the black oil model while keeping all other inputs constant at our base case values, we calculate a flow rate through the fully open choke of 53,750 STB/day, which represents a decrease in flow rate of approximately 0.5% when compared with the compositional model. Table C.6 shows the calculations for the black oil model in tabular form followed by the same data displayed pictorially in Figure C.1. The figure also includes the rates calculated using compositional model. The difference between the two rates is negligible.

Table C.6: Calculated Rates Using Black Oil Model

% open Choke	p(stable) (psig)	Rates (K factor) (bbl/d)
100		
100		
99	3074	53750
93		53750
86	3075	54000
78	3099	53756
69	3138	54600
59	3230	55300
50	3384	56400
41	3671	57350
32	4149	54500
23	4748	46100
16	5606	24100
9	6220	12400
5	6408	10857
2	6553	2330
1	6581	2330
0	6600	0

[57] Exhibit 9732 (E-mail from Ms. Baker to Dr. Ammerman, et al., dated 6/11/2010, Subject: FW: Black Oil Tables from EoS for All Temps 11June2010.xls, SDX009-0004236-SDX009-0004237)

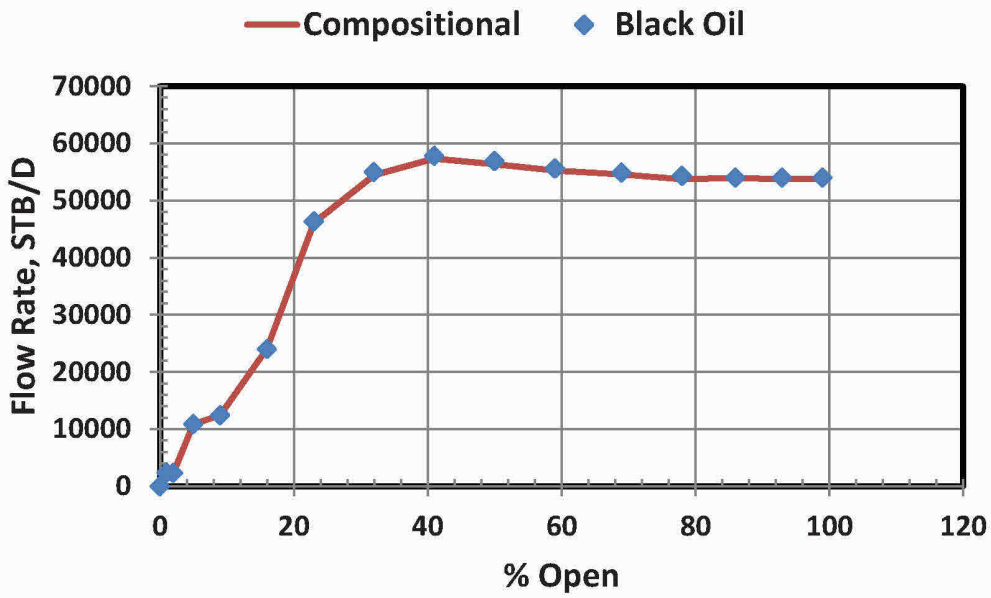

Figure C.1: Flow Rate versus Choke Valve Opening - Black Oil vs. Compositional Model

B. Reservoir Material Balance Calculations

There are a number of variables relevant to a material balance calculation. We have considered the sensitivities here. Our best estimate of the total amount of oil discharged from the Macondo reservoir from April 20 through July 15 is 4.5 to 5.5 MMSTB. If we consider a possible range of formation compressibility to be between 6×10^{-6} psi^{-1} to 18×10^{-6} psi^{-1},[58] the amount of oil spilled could vary between 3.4 MMSTB to 6.9 MMSTB. In our analysis, we did not quantify the influence of water influx since only limited knowledge regarding the size and the strength of aquifer is available. As a result, our estimates are conservative. If we include the influence of aquifer, the amount of oil spilled would increase as the strength of the aquifer increases. In the BP presentation by Merrill, there is some consideration of aquifer support with some reduction in the permeability value indicating that there is a possibility of aquifer support in this reservoir. In that presentation, BP identified the Macondo reservoir as having aquifer support and considered aquifer sizes ranging from 1.5x to 3.7x the size of the oil reservoir. If the aquifer properties are similar to the reservoir properties, this sized aquifer can result in a significant increase in the oil released from the reservoir.

In addition, we use the average reservoir pressure data generated by Mead's method. [redacted]

[58] Merrill, R.: Powerpoint Presentation, Reservoir Response, 8_july-2010 (BP-HZN-2179MDL07033641).

[redacted]

Table C.7: Oil Removed from the Reservoir

			Mead	[redacted]	[redacted]	[redacted]
Average Pressure (psia)			10,396	[redacted]	[redacted]	[redacted]
		STOIIP	Oil Removed			
		(MMSTB)	(MMSTB)			
Pre-drill/Post-Drill		136.7	5.5	[redacted]	[redacted]	[redacted]
BP Estimate		110	4.5	[redacted]	[redacted]	[redacted]

APPENDIX D. CURRICULUM VITAE AND SELECT PUBLICATIONS FOR DR. MOHAN KELKAR

DEGREES EARNED

B.S., Chemical Engineering, 1979, University of Bombay, INDIA

M.S., Petroleum Engineering, 1981, University of Pittsburgh, PA

Ph.D., Chemical Engineering, 1982, University of Pittsburgh, PA

J.D., 1989, The University of Tulsa, OK

AREA OF SPECIALIZATION

Reservoir Characterization

Production Optimization

Risk Analysis

Scale-up and Design of Multiphase Reactors

PROFESSIONAL EXPERIENCE

Research Assistant, University of Pittsburgh, 1979-82

Worked on scale-up and design of multiphase coal liquefaction reactors. Collected experimental data on hydrodynamics and backmixing characteristics of multiphase reactor.

Visiting Assistant Professor, Drexel University, 1982-83

Taught undergraduate courses in fluid dynamics, mass and energy balance, heat transfer and chemical engineering lab. Was involved in research areas of biochemical engineering and multiphase reactor modeling.

Assistant Professor, The University of Tulsa, 1983-1987

Associate Professor, The University of Tulsa, 1987-1996

Professor, The University of Tulsa, 1996-Present

Chairman, Petroleum Engineering, The University of Tulsa, 2002-Present

Williams Endowed Chair Professor, The University of Tulsa, 2005-Present

Teaching undergraduate courses in secondary recovery techniques, petroleum economics, natural gas engineering, petroleum engineering laboratory, production design, reservoir characterization and production optimization. Involved in research areas of two-phase flow in pipes, risk analysis, and reservoir characterization.

Research Engineer, Amoco Production Company, Summers 1986, 1987, 1988

Studied the applications of dispersion in CO_2 flooding process. Investigated the effects of heterogeneities in porous media on the effective dispersion coefficient. Studied the application of fractals to reservoir characterization.

President, Kelkar and Associates, Inc, 1994 - Present

Been involved in various reservoir integration studies incorporating geological, geophysical and engineering data.

PROFESSIONAL MEMBERSHIPS

Member, American Institute of Chemical Engineers

Member, Society of Petroleum Engineers

Member, Society of Exploration Geophysicists

HONORS/AWARDS

Tau Beta Pi 2001 Teaching Excellence Award, The University of Tulsa

SPE International, 2006 Mid-Continent North America Region, Regional Service Award

SPE, 2007 "A Peer Apart" Reviewer Award

SPE International, 2007-08, Distinguished Speaker

SPE International, 2009, Distinguished Faculty Award

SPE International, 2010, Distinguished Member Award

PUBLICATIONS IN REFEREED JOURNALS

Kara, S., Kelkar, B.G., Shah, Y.T. and Carr, N.L.: "Hydrodynamics and Axial Mixing in Three Phase Bubble Column," *Ind. Eng. Chem. Process Des. Dev.*, Vol. 21 (1982) pp 580.

Shah, Y.T., Kelkar, B.G., Godbole, S.P. and Deckwer, W.D.: "Design Parameter Estimations for Bubble Column Reactors," Journal Review, *AIChE Journal*, Vol. 28 (1982) pp 353.

Kelkar, B.G., *et al.*: "Effect of Addition of Alcohols on the Gas Holdup and Backmixing in Bubble Columns," *AIChE Journal*, Vol. 29 (1983) pp 361.

Deckwer, W.D., Nguyen-Tien, K., Kelkar, B.G. and Shah, Y.T.: "On the Applicability of Axial Dispersion Model to Analyze Mass Transfer Measurements in Bubble Columns," *AIChE Journal*, Vol. 29 (1983) pp 915.

Phulgaonkar, S.P., Kelkar, B.G. and Shah, Y.T.: "Effect of Electrolyte Solutions on Hydrodynamics and Backmixing in Bubble Columns," *Chemical Engineering Journal*, Vol. 27 (1983) pp 125.

Kelkar, B.G., Shah, Y.T. and Carr, N.L.: "Hydrodynamics and Backmixing in Three Phase Bubble Column - Effect of Slurry Properties," *Ind. Eng. Chem. Process Des. Dev.*, Vol. 23 (1984) pp 308.

Kelkar, B.G. and Shah, Y.T.: "Effect of Polymer Solutions on Hydrodynamics and Backmixing in Bubble Column Reactors," *AIChE Journal*, Vol. 31 (1985) pp 700.

Lee, Y.H., Kim, Y.J., Kelkar, B.G. and Weinberger, C.B.: "A Simple Digital Sensor for Dynamic Gas Holdup Measurement in Bubble Column," *Ind. Eng. Chem. Fundamentals*, Vol. 24 (1985) pp 105.

Joseph, S., Shah, Y.T. and Kelkar, B.G.: "A Simple Experimental Technique to Measure Gas Phase Backmixing in Bubble Columns," *Chemical Engineering Communications*, Vol. 28 (1984) pp 223.

Kelkar, B.G.: "Flow Regime Characteristics in Concurrent Bubble Column Reactors," *Chemical Engineering Communications*, Vol. 41 (1986) pp 237.

Surbey, D.W., Kelkar, B.G. and Brill, J.P.: "Study of Multiphase Critical Flow Through Wellhead Chokes," paper SPE 15140, *SPE Production Engineering* (May, 1989) pp 142.

Surbey, D.W., Kelkar, B.G. and Brill, J.P.: "Study of Subcritical Flow Through Multiphase Orifice Valves," paper SPE 14285, *SPE Production Engineering* (February, 1988) pp 103.

Kulkarni, A., Shah, Y.T. and Kelkar, B.G.: "Gas Holdup in Bubble Column with Surface Active Agents," *AIChE Journal*, Vol. 33 (1987) pp 690.

Hornbrook, J. and Kelkar, B.G.: "New Method Simplifies Waterflood Predictions," *Oil and Gas Journal* (May 25, 1987) pp 65.

Kelkar, B.G.: "The Effect of Cessation of Production Clause During the Secondary Term of an Oil and Gas Lease," *Tulsa Law Journal*, Vol. 22, No. 4 (1987) 531.

Kelkar, B.G.: "Forced Pooling by Wellbore: Just and Reasonable?" *Tulsa Law Journal*, Vol. 23, No. 4 (1988) pp 681.

Kelkar, B.G. and Perez, G.: "Discussion of a New Approach to thy Hyperbolic Curve," paper SPE 18728, *Journal of Petroleum Technology* (December, 1988) pp 1617-19.

McCoy, T.F. and Kelkar, B.G.: "Investigation of Radial Dispersion - Capacitance System in Porous Media," Vol. 26, *Journal of Water Resources Research* (January, 1990) pp 87.

Perez, G. and Kelkar, B.G.: "A Simplified Method to Predict Overall Production Performance," Vol. 29, *Canadian Journal of Petroleum Technology* (January-February, 1990) pp 78.

Perez, G. and Kelkar, B.G.: "PRAP - Computer Program for Production Performance Analysis," *SPE Microcomputer News (*July-August, 1989) pp 13.

Kelkar, B.G. and Gupta, S.P.: "A Numerical Study of Viscous Instabilities: Effect of Controlling Parameters and Scaling Consideration," *SPE Reservoir Engineering (*February, 1991) pp 121.

Perez, G. and Kelkar, B.G.: "A New Method to Predict Two Phase Pressure Drop Across Perforations," *SPE Production Engineering (*February, 1991) pp 93.

Aasum, Y., Kelkar, B.G. and Gupta, S.P.: "An Application of Geostatistics and Fractal Geometry for Reservoir Characterization," *SPE Formation Evaluation (*March, 1991) pp 11.

Kantak, M.V., Shetty, S.A., and Kelkar, B.G.: "Liquid Phase Backmixing in Bubble Column Reactors," *Chemical Engineering Communications,* Vol. 127 (1994) pp 23.

Shetty, S.A., Kantak, M.V. and Kelkar, B.G.: "Gas Phase Backmixing in Bubble Column Reactors" *AIChE Journal,* Vol. 38 (1992) pp 1013.

Perez, G. and Kelkar, B.G.: "Assessing Distribution of Reservoir Properties using Horizontal Well Data," *Reservoir Characterization - III,* PennWell Publishing Company, Tulsa, OK (1993) pp 399.

Kantak, M. and Kelkar, B.G.: "Effect of Individual Phase Properties on Gas Phase Backmixing in Bubble Columns," *Chemical Engineering Journal (*1995) pp 91.

Aasum, Y., Kasap, E. and Kelkar, B.G.: "Analytical Upscaling of Small Scale Permeability Using a Full Tensor," *Journal of Petroleum Geoscience (*1995) pp 365.

Kelkar, B.G. and Paz, R.: "Using Nodal Analysis for Determining Gas Well Compression Needs," *The American Oil and Gas Reporter (*May, 1993) pp 21.

Kelkar, B.G. and Shibli, S.: "Description of Reservoir Properties Using Fractals," in *Stochastic Modeling and Geostatistics: Practical Applications and Case Histories (*ed. J.M. Yarus and R.L. Chambers) AAPG Publishing Company, Tulsa, OK (1995) Chapter 20.

Hird, K.B. and Kelkar, B.G.: "Conditional Simulation Method for Reservoir Description Using Spatial and Well Performance Constraints," *SPE Reservoir Engineering (*May, 1994) pp 145.

Perez, G. and Kelkar, B.G.: "Three Dimensional Reservoir Description Using Conditional Simulation," *Oklahoma Geological Survey Circular 95* (ed. Johnson, K.S. and Campbell J.A.) (1993) pp 182.

Poquioma, W. and Kelkar, B.G.: "Application of Geostatistics to Forecast Performance for Waterflooding on Oil Field," *SPE Advanced Technology Series,* Vol. 2, No. 1 (1994) pp 142.

Lee, J., Kasap, E. and Kelkar, B.G.: "Analytical Upscaling of Permeability for 3D Grid Blocks," paper SPE 27875, accepted as a peer reviewed paper by Society of Petroleum Engineers, Richardson, TX (1995), *SPE Journal* (March, 1996) pp 59.

Sagar, R., Kelkar, B.G. and Thompson, L.G.: "Reservoir Description by Integrating Well Test Data and Spatial Statistics," paper SPE 26462, accepted as a peer reviewed paper by Society of Petroleum Engineers, Richardson, TX (1995); *SPE Formation Evaluation* (December, 1995) pp 267.

Kelkar, B.G. and Richmond, D.: "Reservoir Management Plan Implemented in Glenn Pool Field," *Petroleum Engineer International (*July, 1996) pp 45.

Gajraj, A. and Kelkar, B.G.: "Simulteneous Fine and Coarse Scale Reservoir Description Using Static and Dynamic Data," *In Situ* Vol. 20(1996) pp 395.

Soeriawinata, T., Kasap, E. and Kelkar, B.G.: "Permeability Upscaling for Near-Wellbore Heterogeneties," *SPE Formation Evaluation* (December, 1997) pp 255.

Huang, X., Gajraj, A. and Kelkar, M.: "The Impact of Integrating Static and Dynamic Data in Quantifying Uncertainties in the Future Prediction of Multiphase Systems," *SPE Formation Evaluation* (December, 1997) pp 263.

Ates, H. and Kelkar, M.: "Two-Phase Pressure-Drop Predictions Across Gravel Pack," *SPE Production & Facilities* (May, 1998) pp 104.

Kerr, D., Ye, S., Bahar, A. and Kelkar, M.: "Glenn Pool Field, Oklahoma: A Case of Improved Production for a Mature Reservoir," *American Association of Petroleum Geologiss Bulletin* V. 83, No. 1 (January, 1999) pp 1.

Bahar, A. and Kelkar, M.: "Journey from Well Logs/Cores to Integrated Geological and Petrophysical Properties Simulation: A Methodology and Application," *SPE Reservoir Evaluation and Engineering* (October 2000) pp 444.

Kelkar, M.: "Estimation of Turbulence Coefficient Based on Field Observations," *SPE Reservoir Evaluation and Engineering* (April 2000) pp 160.

Kelkar, M.: "Application of Geostatistics for Reservoir Characterization – Accomplishments and Challenges," Distinguished Authors Series, *Journal of Canadian Petroleum Technology,* Vol. 39, No. 7 (July 2000).

Jiang, W., Sarica, C., Ozkan, E., and Kelkar, M.: "Effects of Completion Geometry on Single-Phase Liquid Flow Behavior in Horizontal Wells," *Journal of Energy Resources Technology, ASME* (June, 2001).

Kelkar, M.: "New Developments in the Upstream Oil Industry," Chapter 7, *The Future of Oil as a Source of Energy*, ECSSR Publications, Abu Dhabi, UAE (2002).

Tang, Y., Yildiz, T., Kelkar, M.: "Effects of Formation Damage and High-Velocity Flow on the Productivity of Perforated Horizontal Wells," SPE 77534, published in *SPE Reservoir Evaluation & Engineering* (2004).

Ates, H., Bahar, A., El-Abd, S., Charfeddine, M., Kelkar, M., and Datta-Gupta, A.: "Ranking and Upscaling of Geostatistical Reservoir Models by Use of Streamline Simulation: A Field Case Study," SPE 81497 published in *SPE Reservoir Evaluation & Engineering* (February, 2005) Vol. 8, No. 1.

Tang, Y., Yildiz, T., Ozkan, E., and Kelkar, M.: "Effects of Formation Damage and High-Velocity Flow on the Productivity of Perforated Horizontal Wells," SPE Reservoir Evaluation & Engineering (August 2005) Vol. 8, No. 4.

Bahar, A., Ates, H., Al-Deeb, M.H., Salem, S.E., Badaam, H., Linthorst, S., and Kelkar, M.: "An Innovative Approach to Integrate Fracture, Well-Test, and Production Data into Reservoir Models," SPE Reservoir Evaluation & Engineering (August 2005) Vol. 8, No. 4.

Salem, S.E., Al-Deeb, M., Abdou, M., Linthorst, S., Bahar, A., and Kelkar, M.: "Practical Flow-Simulation Method for a Naturally Fractured Reservoir: A Field Study," SPE Reservoir Evaluation and Engineering (April 2006) Vol. 9, No. 2.

Gang, T. and Kelkar, M.: "History Matching for Determination of Fracture Permeability and Capillary Pressure," SPE 101052, paper published in SPE Reservoir Evaluation and Engineering (November 2008).

Al-Safran, E.M. and Kelkar, M.: "Prediction of Two Phase Critical Flow Boundary and Mass Flow Rate across Chokes," SPE 109243, SPE Production and operations (May 2009) p. 249.

Hosseini, S. and Kelkar, M.: "Analytical Upgridding Method to Preserve Dynamic Flow Behavior," SPEREE (June 2010), p. 473

Rittirong, A. and Kelkar, M.: "Upgridding of Geocellular Models in the Presence of Gravity Dominated Displacement," SPE 129774, presented at the SPE IOR Meeting, Tulsa, OK (April 2010), SPE Journal, Vol. 4 (December 2012).

Sharifi, M. and Kelkar, M.: "New Upgridding Method to Capture Dynamic Performance of the Fine Scale Heterogeneous Reservoir," J. Pet. Science and Engineering, V.86-87 (2012), pp. 225-236.

Luo, S. and Kelkar, M.: "Infill Drilling Potential in Tight Gas Reservoirs," J. of Energy Resources Technology, (March 2013).

Sharifi, M. and Kelkar, M.: "New Dynamic Permeability Upscaling Method for Depletion Drive Under No-Crossflow," J. Pet. Science, Accepted for publication (2013).

PROFESSIONAL PRESENTATIONS

Kelkar, B.G.: "Design and Characteristics of Multiphase Bubble Column Reactors," talk presented to Dow Chemicals, R & D Division, Midland, TX (July, 1985).

Surbey, O.W., Kelkar, B.G. and Brill, J.P.: "Study of Subcritical Flow Through Multiphase Orifice Valves," presented at the 60th SPE Annual Meeting, Las Vegas, NV (September 22-25, 1985).

Tompang, R. and Kelkar, B.G.: "Prediction of Waterflood Performance in Stratified Reservoirs," paper SPE 17289, presented at the SPE Permian Basin Oil and Gas Recovery Conference, Midland, TX (March 10-11, 1988).

Kelkar, B.G. and Gupta, S.P.: "The Effects of Small Scale Heterogeneities on the Effective Dispersivity of Porous Medium," paper SPE 17339, presented at the SPE/DOE EOR Symposium, Tulsa, OK (April 17-20, 1988).

Perez, G. and Kelkar, B.G.: "A Simplified Method to Predict Overall Production Performance," Paper No. 88-39-63, presented at the 39th Annual CIM Meeting, Calgary (June 12-16, 1988).

Kelkar, B.G. and Perez, G.: "A New Method to Predict Two-Phase Pressure Drop Across Perforations," paper SPE 18248, presented at the SPE Annual Technical Conference and Exhibition, Houston, TX (October 2-5, 1988).

Aasum, Y., Kelkar, B.G. and Gupta, S.P.: "Application of Geostatistics and Fractal Geometry for Reservoir Characterization," paper SPE 20257, presented at the EOR Symposium, Tulsa, OK (April 23-25, 1990).

Perez, G. and Kelkar, B.G.: "Three Dimensional Reservoir Description Using Conditional Simulation," presented at the Workshop on Petroleum-Reservoir Geology in the Southern Midcontinent, Norman, OK (March 26-27, 1991).

Aasum, Y., Kelkar, B.G. and Gupta, S.P.: "Effect of Scaling Parameters on Miscible Displacement," presented at the ASME Winter Annual Meeting, Atlanta, GA (December 1-6, 1991).

Shetty, S.A., Kantak, M.V. and Kelkar, B.G.: "Measurement of Gas Phase Mixing in Bubble Column Reactors," Paper 34A, presented at the Spring AIChE National Meeting, Houston, TX (April 7-11, 1991).

Perez, G. and Kelkar, B.G.: "Assessing Distributions of Reservoir Properties Using Horizontal Well Data," presented at the Third International Reservoir Characterization Conference, Tulsa, OK (November 3-5, 1991); also presented at the Joint TGS/GST/SPE/SPWLA Workshop, Tulsa, OK (May 10-11, 1993)

Aasum, Y., Kasap, E. and Kelkar, B.G.: "Effective Permeability of Grid Block in the Presence of Heterogeneities," presented as a poster session in SPE Forum Series on Reservoir Characterization, Creste Butte, CO (July 29-August 2, 1991); and presented as a poster session at the Third International Reservoir Characterization Conference, Tulsa, OK (November 3-5, 1991).

Lotfi, B. and Kelkar, B.G.: "Application of Geostatistical Technique for Reservoir Performance Prediction," presented at the SPE Forum Series on Reservoir Characterization, Creste Butte, CO (July 29-August 2, 1991).

Poquioma, W. and Kelkar, B.G.: "Application of Geostatistics to Forecast Performance for Waterflooding on Oil Field," paper SPE 23677, presented at the Second Latin American Petroleum Engineering Conference of SPE, Caracas, Venezuela (March 8-11, 1992).

Hird, K.B. and Kelkar, M.G.: "Conditional Simulation Method for Reservoir Description using Spatial and Well Performance Constraints," paper SPE 24750, presented at the SPE Annual Technical Conference and Exhibition, Washington, D.C. (October 4-8, 1992).

Kelkar, B.G.: "Ranking of Independent Projects in the Presence of Uncertainties," paper SPE 25405, unsolicited (1992).

Kerr, D.R., Martinez, G., Azof, I. and Kelkar, M.G.: "Integrated Reservoir Description Using Outcrop Studies: Example from Bartlesville Sandstone Northeast Oklahoma," presented at the Deltaic Reservoirs Workshop, Norman, OK (March 23-24, 1993).

Huang, X. and Kelkar, B.G.: "Application of Genetic Algorithm to Reservoir Description," presented at the SIAM Conference on Math and Computational Issues in Geosciences, Houston, TX (April 19-21, 1993).

Aasum, Y., Kasap, E. and Kelkar, B.G.: "Analytical Upscaling of Small Scale Permeability Using a Full Tensor," paper SPE 25913, presented at the SPE Rocky Mountain Regional/Low Permeability Reservoirs Symposium, Denver, CO (April 26-28, 1993).

Kerr, D.R., Martinez, G., Azof, I. and Kelkar, B.G.: "Integrated Reservoir Description Using Outcrop Studies: Example from Bartlesville Sandstone Northeast Oklahoma," presented at the Deltaic Reservoirs Workshop, Norman, OK (March 23-24, 1993).

Kelkar, B.G.: "Reservoir Characterization Research at The University of Tulsa," presented at BP Exploration, Houston, TX (April 20, 1993); also at Stanford University, Stanford, CA (May 24, 1993); at Exxon Production Research, Houston, TX (October 8, 1993); and at Petronas Oil Co., Kuala Lumpur, Malaysia (October 15, 1993).

Sagar, R.K., Thompson, L.G. and Kelkar, B.G.: "Reservoir Description by Integrating Well Test Data and Spatial Statistics," paper SPE 26462, presented at the SPE Annual Technical Meeting and Exhibition, Houston, TX (October 3-7, 1993).

Hird, K.B. and Kelkar, M.G.: "Incorporation of Production Data in Reservoir Description Process," paper SPE 27713, presented at the SPE Permian Basin Oil and Gas Recovery Conference, Midland, TX (March 16-18, 1994).

Huang, X. and Kelkar, B.G.: "Application of Combinatorial Algorithms for Description of Reservoir Properties," paper SPE 27803, presented at the Improved Oil Recovery Symposium, Tulsa, OK (April 17-20, 1994).

Ahuja, B.K., Bahar, A., Kerr, D.R. and Kelkar, B.G.: "Integrated Reservoir Description and Flow Performance Evaluation of Self-Unit, Glenn Pool Field," paper SPE 27748, presented at the Improved Oil Recovery Symposium, Tulsa, OK (April 17-20, 1994).

Lee, J., Kasap, E. and Kelkar, B.G.: "Analytical Upscaling of Permeability for Three-Dimensional Grid Blocks," paper SPE 27875, presented at the Western Regional Meeting, Long Beach, CA (March 23-25, 1994).

Pande, P.K., Clark, M.B., Blasingame, T.A., Kelkar, M., Vessell, R.K. and Hunt, P.E.: "Application of Integrated Reservoir Management and Reservoir Characterization to Optimize Infill Drilling," Paper SPE 27657 presented at the 1994 SPE Permian Basin Oil and Gas Recovery Conference, Midland, TX (March 16-18, 1994).

Kelkar, B.G.: "Application of Geostatistics for Reservoir Description," Invited Lecture in a Forum on Reservoir Description, presented at the SPE Permian Basin Oil and Gas Recovery Conference, Midland, TX (March 16-18, 1994).

Kelkar, B.G.: "Integration of Interdisciplinary Information for Reservoir Characterization," presented at the Symposium on Multidisciplinary Approaches to Reservoir Characterization, The University of Tulsa, Tulsa, OK (May 9-12, 1994).

Oetomo, H.K. and Kelkar, B.G.: "Incorporation of Production Data in a Reservoir Description Process," paper SPE 29316, presented at the 1995 SPE Asia Pacific Oil and Gas Conference, Kuala Lumpur (March, 1995).

Qiu, W. and Kelkar, B.G.: "Simulation of Geological Model Using Multipoint Histogram," paper SPE 30601, presented at the Annual SPE Meeting, Dallas, TX (October 22-25, 1995).

Bahar, A., Kelkar, B.G. and Thompson, L.G.: "Integrated Reservoir Description and Flow Performance Evaluation - Glenn Pool Study," paper SPE 30622, presented at the

Annual SPE Meeting, Dallas, TX (October 22-25, 1995); also presented at the AAPG Mid-Continent Section Meeting, Tulsa, OK (October 8-10, 1995).

Yang, C.T., Chopra, A.K., Chu, J., Huang, X. and Kelkar, B.G.: "Integrated Geostatistical Reservoir Description Using Petrophysical, Geological, and Seismic Data for Yachang 13-1 Gas Field," paper SPE 30566, presented at the Annual SPE Meeting, Dallas, TX (October 22-25, 1995).

Lee, J., Kasap, E. and Kelkar, B.G.: "Development and Application of a New Upscaling Technique," paper SPE 30712, presented at the Annual SPE Meeting, Dallas, TX (October 22-25, 1995).

Kantak, M., Hesketh, R.P. and Kelkar, B.G.: "Estimation of Design Parameters in Bubble Columns using Differential Pressure Fluctuations," paper presented at the Annual AIChE Meeting, Miami, FL (November, 1995).

Huang, X. and Kelkar, B.G.: "Performance Comparison of Heuristic Combinatorial Algorithms for Seismic Inversion," presented in a poster session at the SEG International Exposition and Annual Meeting, Houston, TX (October 9-12, 1995).

Huang, X., Kelkar, B.G., Chopra, A.K. and Yang, C.T.: "Wavelet Sensitivity Study on Inversion using Heuristic Combinatorial Algorithms," presented at the SEG International Exposition and Annual Meeting, Houston, TX (October 9-12, 1995).

Huang, X., Kelkar, B.G., Chopra, A.K. and Yang, C.T.: "Some Practical Considerations for Application of Heuristic Combinatorial Algorithm Inversion to Reservoir Description," presented at the SEG International Exposition and Annual Meeting, Houston, TX (October 9-12, 1995).

Kelkar, B.G. and Richmond, D.: "Implementation of Reservoir Management Plan - Self Unit, Glenn Pool. Field," paper SPE 35407, presented at the 1996 SPE/DOE Tenth Symposium on Improved Oil Recovery, Tulsa, OK (April 21-24, 1996).

Huang, X. and Kelkar, B.G.: "Reservoir Characterization by Integration of Seismic and Dynamic Data," paper SPE 35415, presented at the 1996 SPE/DOE Tenth Symposium on Improved Oil Recovery, Tulsa, OK (April 21-24, 1996). Also presented at a graduate seminar, University of Texas (February, 1996).

Jansen, F.E. and Kelkar, B.G.: "Exploratory Data Analysis of Production Data," paper SPE 35184, presented at the 1996 Permian Basin Oil and Gas Recovery Conference, Midland, TX (March 27-29, 1996).

Soeriawinata, J., Kasap, E. and Kelkar, B.G.: "Permeability Upscaling for Near-Wellbore Heterogeneities," paper SPE 36518, presented at the 1996 Annual SPE Technical Conference and Exhibition, Denver, CO (October 6-9, 1996).

Huang, X., Gajraj, A. and Kelkar, B.G.: "The Impact of Integrating Static and Dynamic Data in Quantifying Uncertainties in the Future Prediction of Multi-Phase Systems," paper SPE 36570, presented at the 1996 Annual SPE Technical Conference and Exhibition, Denver, CO (October 6-9, 1996).

Huang, X. and Kelkar, B.G.: "Integration of Dynamic Data for Reservoir Characterization in the Frequency Domain," paper SPE 36513, presented at the 1996 Annual SPE Technical Conference and Exhibition, Denver, CO (October 6-9, 1996).

Huang, X. and Kelkar, B.G.: "Direct Porosity Inversion Using Field Statistical Correlation," paper presented at the SEG International Exposition and Annual Meeting, Denver, CO (November 10-15, 1996).

Huang, X. and Kelkar, B.G.: "Seismic Inversion Using Heuristic Combinatorial Algorithm: A Hybrid Scheme," paper presented at the SEG International Exposition and Annual Meeting, Denver, CO (November 10-15, 1996).

Ates, H. and Kelkar, B.G.: "Two Phase Pressure Drop Predictions Across Gravel Pack," paper SPE 37512, paper presented at the Production Operations Symposium, Oklahoma City, OK (March 9-11, 1997).

Kelkar, B.G.: "Estimation of Turbulence Coefficient Based on Field Observations," paper SPE 37411, paper presented at the Production Operations Symposium, Oklahoma City, OK (March 9-11, 1997).

Kelkar, B.G.: "Application of Geostatistics in Reservoir Description," a seminar presented at Illinois Geological Survey Seminar Series, Urbana Champaign, IL (March 12, 1997); presented at Anadarko Petroleum Co., Houston, TX (May 1997), presented at Instituto Mexicano del Petroleo, as an invited guest to celebrate 32nd anniversery (October 23, 1997), presented at Bristol Resources, as a part of the Seminar Series, Tulsa, OK (November 11, 1997), presented at University of Pittsburgh, Graduate Seminar, Department of Petroleum and Chemical Engineering (November 14, 1997).

Kelkar, B.G.: "Reservoir Management of Self Unit- Glenn Pool Field," paper presented at Oil Recovery Conference organised by University of Kansas, Wichita, KS (March 20, 1997).

Bahar, A. and Kelkar, M.: "Integrated Lithofacies and Petrophysical Properties Simulation," SPE 38261, presented at Western Regional Meeting, Long Beach, CA (June 25-27, 1997).

Jansen, F.E. and Kelkar, M.: "Application of Wavelets to Production Data in Describing Inter-Well Relationships," paper SPE 38876, presented at SPE 72nd Annual Conference and Exhibition, San Antonio, TX (October 5-8, 1997).

Jansen, F.E. and Kelkar, M.: "Non-Stationary Estimation of Reservoir Properties Using Production Data," paper SPE 38729, presented at SPE 72nd Annual Conference and Exhibition, San Antonio, TX (October 5-8, 1997).

Bahar, A. and Kelkar, M.: "Journey from Well Logs/Cores to Integrated Geological and Petrophysical Properties Simulation: A Methodology and Application, " SPE 39565, presented at 1998 SPE India Oil and Gas Conference and Exhibition, New Delhi, India (Feb. 10-12, 1998).

Jansen, F.E. and Kelkar, M.: "Upcaling of Reservoir Properties Using Wavelets, "SPE 39495, presented at 1998 SPE India Oil and Gas Conference and Exhibition, New Delhi, India (Feb. 10-12, 1998).

Kelkar, M.: "Integrated Approach Toward the Application of Horizontal Wells to Improve Waterflooding Performance," presentation to Ft. Worth Section SPE as part of technology transfer workshop (March, 1997).

Bahar, A. and Kelkar, M.: "Integrated Lithofacies and Petrophysical Properties Simulation," SPE 38261, presented at Western Regional Meeting, Long Beach, CA (June 25-27, 1997).

Kelkar, M.: "Integration of Dynamic Data," presented in FORCE Meeting, Bergen, Norway (March, 1998).

Ates, H. and Kelkar, M.: "Incorporation of Two-Phase Production Data into Reservoir Characterization," paper SPE 48970 presented at the 1998 SPE Annual Technical Conference and Exhibition, New Orleans, Louisiana (September 27-30, 1998).

Soeriawinata, T. and Kelkar, M.: "Reservoir Management Using Production Data," paper SPE 52224, to be presented at the 1999 SPE Mid-Continent Operations Symposium, Oklahoma City, Oklahoma (March 28-31, 1999).

Bitsindou, A. and Kelkar, M.: "Gas Well Production Optimization Using Dynamic Nodal Analysis," paper SPE 52170, to be presented at the 1999 SPE Mid-Continent Operations Symposium, Oklahoma City, Oklahoma (March 28-31, 1999).

Kelkar, M.: "History Matching through Integration of Multi-Phase Production Data," presented at the EAGE/SPE International Symposium on Petroleum Geostatistics, Toulouse, France (April 20-23, 1999).

Kelkar, M.: "Integrated Approach Towards the Application of Horizontal Wells to Improve Waterflooding Performance," 1999 Oil and Gas Conference, US DOE, Dallas, TX (June 28-30, 1999).

Kelkar, M.: "Integration of Two Phase Production Data using the Dual Loop Method," The Statoil Research Summit, Invited Lecture, Trondheim, Norway (September 13-14, 1999).

Kelkar, M.: "Estimation of Turbulence Coefficient Based on Field Observations," paper SPE 62488 was revised for publication from paper SPE 37411, first presented at the 1997 SPE Production Operations Symposium, Oklahoma City, March 9-11. Original manuscript received for review April 17, 1997. Revised manuscript received December 7, 1999. Paper peer approved January 10, 2000.

Tanakov, M. and Kelkar, M.: "Integrated Reservoir Description for Boonsville, Texas Field Using 3-D seismic Well and Production Data," SPE 59693, presented at the SPE Permian Basin Oil and Gas Recovery Conference, Midland, TX (March 21-23, 2000); paper SPE 59349 also presented at the SPE/DOE Improved Oil Recovery Symposium, Tulsa, OK (April 3-6, 2000).

Ates, H. and Kelkar, M. "History Matching using Dual Loop Techniques," SPE 59371, presented at the SPE/DOE Improved Oil Recovery Symposium, Tulsa, OK (April 3-6, 2000).

Kelkar, M. "Advantages of Integrated Reservoir Description," presented at Geophysical Trends in the New Millennium, Invited Lecture, Bartlesville, OK (April 13, 2000).

Bahar, A., and Kelkar, M.: "Journey from Well Logs/Cores to Integrated Geological and Petrophysical Properties Simulation: A Methodology and Application," was revised for publication from paper SPE 39565, first presented at the 1998 SPE India Oil and Gas Conference and Exhibition, New Delhi, India, February 17-19, 1998. Original manuscript received for review March 31, 1998. Revised manuscript received August 30, 1999. Paper peer approved July 10, 2000.

Tang, Y., Ozkan, E., Kelkar, M., Sarica, C. and Yildiz, T.: "Performance of Horizontal Wells Completed with Slotted Liners and Perforations," paper SPE 65516, presented at the 2000 SPE/Petroleum Society of CIM International Conference on Horizontal Well Technology, Calgary, Alberta, Canada (November 6-8, 2000).

Bahar, A., Ates, H., Kelkar, M., and Al-Deeb, M.: "Methodology to Incorporate Geological Knowledge in Variogram Modeling," SPE 68704, presented at SPE Asia Pacific Oil and Gas Conference and Exhibition, Jakarta, Indonesia (April 17-19, 2001).

Tang, Y., Ozkan, E., Kelkar, M., and Yildiz, T.: "Fast and Accurate Correlations to Compute the Perforation Pseudoskin and Productivity of Horizontal Wells," SPE 71638, presented at SPE Annual Conference and Exhibition, New Orleans, LA (September 30 - October 3, 2001).

Kho, T.S. and Kelkar, M.: "The Effect of Using Scale-Splitting Technique on Two Phase, Two Dimensional Automatic History Matching," SPE 75220, presented at SPE/DOE Thirteenth Symposium on Improved Oil Recovery, Tulsa, OK (April 13-17, 2002).

Frederick, J., Kelkar, M., and Keefer, B.: "Production Type Curves for Hunton Formation," SPE 75248, presented at SPE/DOE Thirteenth Symposium on Improved Oil Recovery, Tulsa, OK (April 13-17, 2002).

Marwah, V., Kelkar, M., and Keefer, B.: "Reservoir Mechanism for Hunton Formation Production," SPE 75127, presented at Thirteenth Symposium on Improved Oil Recovery, Tulsa, OK (April 13-17, 2002).

Ates, H., Bahar, A., and Kelkar, M.: "Integration of 3-D Seismic, Well Test and Core Data to Simulate Permeability Descriptions," presented at Conference on Naturally Fractured Reservoirs, University of Oklahoma, Norman, OK (June 1-3, 2002).

Tang, Y., Yildiz, T., Kelkar, M.: "Effects of Formation Damage and High-Velocity Flow on the Productivity of Perforated Horizontal Wells," SPE 77534, presented at the SPE Annual Technical Conference and Exhibition, San Antonio, TX (September 29 – October 2, 2002).

Charfeddinne, M., Al-Deeb, M., El-Abd, S., Bahar, A., Ates, H., Soeriawinata, T., and Kelkar, M., "Reconciling Well Test and Core Derived Permeabilities using Fracture Network : A Field Case Example", paper SPE 78499 presented at the 10th Abu Dhabi International Petroleum Exhibition and Conference held in Abu Dhabi (October 13-16, 2002).

Al-Deeb, M., Bloch, G., El-Abd, S., Charfeddinne, M., Bahar, A., Ates, H., Soeriawinata, T., and Kelkar, M., "Fully Integrated 3D Reservoir Characterization and Flow Simulation Study: A Field Case Example", paper SPE 78510 presented at the 10th Abu

Dhabi International Petroleum Exhibition and Conference held in Abu Dhabi (October 13-16, 2002).

Kelkar, M.: "Simplified History Matching," a Graduate Seminar presented at Texas A&M University (November, 2002) and The University of Tulsa (November, 2002).

Ramakrishna, S., Kelkar, M. and Keefer, B.: "Correlating Static Data to Dynamic Characteristics: Hunton Reservoir" presented at TOPR Oil Recovery Conference, Wichita, KS (March 17, 2003).

Ates, H., Bahar, A., El-Abd., S., Charfeddine, M., Kelkar, M., Datta-Gupta, A., "Ranking and Upscaling Optimization of the Geostatistical Reservoir Models using Streamline Simulation : A Field Case Study", paper SPE 81497 presented at the SPE 13th Middle East Oil Show & Conference, held in Bahrain, (April 5-8, 2003).

Bahar, A., Ates, H., Al-Deeb, M., Salem, S. E., Badaam, H., and Kelkar, M., "Practical Approach in Modeling of Naturally Fractured Reservoir: A Field Case Study", paper SPE 84078 presented at the SPE Annual Technical Conference and Exhibition held in Denver, Colorado (October 5-8, 2003)

Bahar, A., Ates, H., Al-Deeb, M., Salem, S. E., Badaam, H., Linthorst, S., and Kelkar, M., "An Innovative Approach to Integrate Fracture, Well Test, and Production Data into Reservoir Models", paper SPE 84876 presented at the SPE International Improved Oil Recovery Conference in Asia Pacific, held in Kuala Lumpur, Malaysia (October 20-21, 2003).

Ates, H., Bahar, A., El-Abd, S., Charfeddine, M., Kelkar, M., and Datta-Gupta, A.: "Ranking and Upscaling of Geostatistical Reservoir Models by Use of Streamline Simulation: A Field Case Study," SPE 81497 presented at the 2003 SPE Middle East Oil Show and Conference, Bahrain (April 5-8, 2004).

Joshi, R., and Kelkar, M., "Production Performance Study of West Carney Field, Lincoln County, Oklahoma", paper SPE 89461 presented at the SPE/DOE Fourteenth Symposium on Improved Oil Recovery held in Tulsa, Oklahoma (April 17-21, 2004).

Patwardhan, S., Kelkar, M., and Keefer, B., "Dewatering in Hunton Reservoir – Drill Vertical or Horizontal Well?", paper SPE 89462 presented at the SPE/DOE Fourteenth Symposium on Improved Oil Recovery held in Tulsa, Oklahoma (April 17-21, 2004).

Zubarev, D., Patwardhan, S., Kelkar, M., and Keefer, B., "Dewatering in Hunton Reservoir - Drill Vertical or Horizontal Well?", paper SPE 89462 presented at the, SPE/DOE Fourteenth Symposium on Improved Oil Recovery held in Tulsa, Oklahoma (April 17-21, 2004).

Salem, S. E., Al-Deeb, M., Abdou, M, Linthorst, S., Bahar, A., and Kelkar, M.: "Practical Flow Simulation Method for a Naturally Fractured Reservoir: A Field Study," SPE 88761, paper presented at 11th Abu Dhabi international Petroleum Exhibition and Conference held in Abu Dhabi, U.A.E. (October 10–13, 2004).

Bahar, A., Abdel-Aal, O., Ghani, A., Silva, F. P., and Kelkar, M.: "Seismic Integration for Better Modeling of Rock Type Based Reservoir Characterization: A Field Case

Example," SPE 88793, paper presented at 11th Abu Dhabi international Petroleum Exhibition and Conference held in Abu Dhabi, U.A.E. (October 10-23, 2004).

Kelkar, M.: "Hunton Formation: Production Performance and Solutions," presented at Graduate Seminar at the University of Missouri, Rolla, MO (December 2, 2004)

Kelkar, M.: "Improving Reservoir Performance using Integrated Reservoir Modeling," Key Note Speaker, West Coast PTTC Workshop, Valencia, CA (January 27, 2005)

Kelkar, M.: "Integrated Reservoir Modeling Using Geostatistics" presented at University of Alaska, Fairbanks, AK (February 24-25, 2005).

Cui, H. and Kelkar, M.: "Automatic History Matching of Naturally Fractured Reservoirs and a Case Study," SPE 94037, presented at SPE Western Regional Meeting, Irvine, CA (March 30 – April 1, 2005).

Kelkar, M.: "Dewatering of Hunton Reservoir - What Makes It Work?" presented at SPE Mid-Continent Section Luncheon and Workshop (March 3, 2005); also presented as SPE 94347, SPE Production Symposium, OK City, OK (April 17-19, 2005).

Kelkar, M.: "Integrated Reservoir Modeling: Solutions and Challenges," invited speaker at Shell International Reservoir Engineering Focus Group, Houston, TX (April 7, 2005); also presented the same talk at Shell International, The Hague, Netherlands (February 17, 2005).

Frederick, J. and Kelkar, M.: "Decline Curve Analysis for Solution Gas Drives," paper SPE 94859 to be presented at the 2005 SPE Annual Technical Conference and Exhibition held in Dallas, TX (October 9-12, 2005).

Gang, T. and Kelkar, M.: "Efficient History Matching in Naturally Fractured Reservoirs," SPE 99578, presented at SPE/DOE IOR Symposium, Tulsa, OK (April 22-24, 2006).

Zubarev, D. and Kelkar, M.: "New Parallel Algorithm for Multiple History Matching of Realizations," SPE 101333, paper presented at SPE Ann. Tech. Conference and Exhibition, San Antonio, TX (Sept 24-27, 2006); also presented at ADIPEC Conference and Exhibition, Abu Dhabi, UAE (Nov 5-8, 2006).

Gang, T. and Kelkar, M.: "History Matching for Determination of Fracture Permeability and Capillary Pressure," SPE 101052, paper presented at SPE Ann. Tech. Conference and Exhibition, San Antonio, TX (Sept 24-27, 2006).

Kelkar, M.: "Dewatering of Hunton Reservoir - What Makes It Work?" presented at University of Southern California, Los Angeles, CA (Nov 30, 2006).

Kelkar, M.: "Barnett Shale – Production Opportunities and Challenges," presented at Williams Energy Company, Tulsa, OK (October 4, 2006); Apache Corporation, Tulsa, OK (December 6, 2006); Marathon Oil Company, Houston, TX (January 11, 2007); Pioneer Resources, Dallas, TX (June 1, 2007); St Mary's Land and Production (June 15, 2007).

Tang, Y., Yildiz, T. and Ozkan, E. and Kelkar, M.: " Effects of Formation Damage of High Velocity Flow on the Productivity of Slotted Liner Completed Horizontal Wells," SPE

101987, paper presented at SPE Intl. Oil and Gas Exhibition, Beijing, China (Dec 5-7, 2006).

Faskhoodi, M. and Kelkar, M.: "Using the Low Frequency Observation Data in Automatic History Matching," SPE 105252, presented at SPE Middle East Oil and Gas Show and Conference, Bahrain (March 11-14, 2007).

Kelkar, M.: "Biofuels – Myth or Reality?" presented at AIChE Meeting, Student Chapter, The University of Tulsa, Tulsa, OK (March 19, 2007).

Liu, B., Kelkar, M., Gang, T., and Dixon, T.: "Efficient Automatic History Matching through Production Data Selection," SPE 106157, paper presented at SPE Production Symposium, Oklahoma City, OK (April 10-11, 2007).

Kelkar, M.: "Biofuels – Myth or Reality?" presented at Desk and Derrick Club of Tulsa, Tulsa, OK (April 11, 2007).

Gang, T. and Kelkar, M.: "A More General Capillary Pressure Curve and Its Estimation from Production Data," SPE 108180, presented at SPE Rocky Mountain Oil and Gas Technology Symposium, Denver, CO (April 16-18, 2007).

Kelkar, M.: "Biofuels – Myth or Reality?" presented at the Tulsa Association of Petroleum Landmen Spring Seminar, Tulsa, OK (April 19, 2007).

Kelkar, M.: "Biofuels – Myth or Reality?" presented at Anadarko Petroleum, Denver, CO (July 13, 2007).

Kelkar, M.: "Biofuels – Myth or Reality?" presented at the Tulsa Association of Petroleum Landmen Fall Seminar, Tulsa, OK (November 8, 2007).

Al-Safran, E.M. and Kelkar, M.: "Prediction of Two Phase Critical Flow Boundary and Mass Flow Rate across Chokes," SPE 109243, paper presented at SPE Ann Tech Conference and Exhibition, Anaheim, CA (Nov 11-14, 2007).

Khasanov, M., Krasnov, V., Petrov, A., Kelkar, M. and Bahar, A.: "Reconciling Production and Well Test Data in Mapping kh Trends: Field Study," SPE 116087, presented at SPE Ann Tech Conference and Exhibition, Denver, CO (Sept 21-24, 2008).

Hosseini, S. and Kelkar, M.: "Analytical Upgridding Method to Preserve Dynamic Flow Behavior," SPE 116113, presented at SPE Ann Tech Conference and Exhibition, Denver, CO (Sept 21-24, 2008).

Khasanov, M., Krasnov, V., Petrov, A., Kelkar, M. and Bahar, A.: "Reconciling Production Decline with Reservoir Connectivity: Field Study," SPE 117756, presented at SPE Eastern Regional Meeting, Pittsburgh, PA (October 11-15, 2008).

Liu, B., McMillan, K., Dessenberger, R. and Kelkar, M.: "Waterflooding Incremental Oil Recovery Study in Middle Miocene to Paleocene Reservoirs, Deep Water Gulf of Mexico," SPE 115669, presented at SPE Asia Pacific Oil and Gas Conference and Exhibition, Perth, Australia (October 20-22, 2008).

Uvarov., I., Petrov, A., Kelkar, M. and Ates, H.: "Constraining 2D Maps to 3D Reservoir Description," IPTC 12181, presented at International Petroleum Technology Conference, Kuala Lumpur, Malaysia (Dec 3-5, 2008).

Kelkar, M.: "Integration of Geophysical Data to Describe Reservoir Properties," presentation at Geophysical Society of Tulsa, Tulsa, OK (January 8, 2009).

Soni, S., Kelkar, M. and Perez, C.: "Pressure Drop Predictions in Tubing in the Presence of Surfactants," presented at 7th Annual Gas Well Deliquification Workshop, Denver, CO (Feb 23-26, 2009); also SPE 120042, presented at SPE Production and Operations Symposium, Oklahoma City, OK (April 4-8, 2009).

Faskhoodi, M., Ates, H., Soeriawinata, T., Britsch, X., Vert, M. and Kelkar, M. : "Incorporation of Static and Dynamic Constraints in Optimum Upscaling," SPE 121612, presented at SPE EUROPEC/EAGE Conference and Exhibition, Amsterdam, Netherlands (June 8-11, 2009).

Ates, H., Bahar, A., Krasnov, V. and Kelkar, M.: "Dynamic Updating of Reservoir Models," SPE 123671, presented at the SPE Ann Meeting and Exhibition, New Orleans, LA (Sept 2009); Also, published in abbreviated form in JPT (July 2010).

Kelkar, M.: "Upgridding in the Presence of Gravity Dominated Displacement," Invited Lecture, History Matching Advanced Technology Workshop, Galveston, TX (Nov 2010).

Rittirong, A. and Kelkar, M.: "Upgridding of Geocellular Models in the Presence of Gravity Dominated Displacement," SPE 129774, presented at the SPE IOR Meeting, Tulsa, OK (April 2010).

Atiq, M. and Kelkar, M.: "Upgridding Method for Tight Gas reservoirs," SPE 133301, paper presented at SPE Annual Tech Conference and Exhibition, Florence, Italy (September 19-22, 2010).

Luo, S. and Kelkar, M.: "Infill Drilling Potential in Tight Gas Reservoirs," SPE 134249, paper presented at SPE Annual Tech Conference and Exhibition, Florence, Italy (September 19-22, 2010).

Kelkar M. and Bonney, K.: "Prediction of Uncertainty in Exploration of Unconventional Reservoirs," SPE 133299, paper presented at SPE Annual Tech Conference and Exhibition, Florence, Italy (September 19-22, 2010).

Kelkar M. and Bonney, K.: "Prediction of Uncertainty in Exploration of Unconventional Reservoirs," SPE 133299, paper presented at SPE Annual Tech Conference and Exhibition, Florence, Italy (September 19-22, 2010). Appeared in Journal of Petroleum Technology (July 2011).

Kelkar, M.: "Interference Study in Shale Plays," presented at SPE Mid-Continent Section, Tulsa (May 12, 2011); presented at SPE Lou-Ark Section, Shreveport (April 23, 2011); presented at SPE Dallas Section (August 17, 2011).

BOOKS

Kelkar, M. and Perez, G: "Application of Geostatistics for Reservoir Characterization," SPE Publications, Richardson, TX (2002).

Kelkar, M.: "The Future of Oil as a Source of Energy," Chapter 7 – New Developments in the Upstream Oil Industry, The Emirates Center for Strategic Studies and Research, Abu Dhabi, UAE (2003).

Kelkar, M.: "Natural Gas Production Engineering," PennWell Publications, Tulsa, OK (2008).

TECHNICAL REPORTS

"Thermal and Hydrodynamic Behavior of Multiphase Reactors", DOE Report DOE/ET/10104-29 (February, 1982).

"Reservoir Characterization of Pennsylvanian Sandstone Reservoirs," DOE Report DOE/BC/14651-5 (September, 1992).

"Downhole Permeability: Experiments and Simulation," with E. Kasap, Oklahoma Center for Advancement of Science and Technology Final Report (July, 1997)

"Application of Artificial Intelligence to Reservoir Characterization: An Interdisciplinary Approach," DOE Final Report DOE/DE-AC22-93BC14894 (September, 1997).

"Application of Integrated Reservoir Management and Reservoir Characterization to Optimize Infill Drilling," DOE Report DOE/DE-FC22-94BC14989 (1997).

"Reservoir Architecture Modeling: Nonstationary Models for Quantitative Geological Characterization," BDM Oklahoma Report, Contract No. 93-0001, Delivery Order No. 47 (1997).

"Estimation of Reservoir Properties and Well Parameters from Priori Information and Production Data under Multi-Phase Flow Conditions," BDM Oklahoma Report, Contract No. 93-0001, Delivery Order No. 54 (1997).

OTHER PUBLICATIONS

"Study of Hydrodynamics and Mixing Characteristics in Concurrent Bubble Column," Ph.D. Dissertation, University of Pittsburgh, PA (1982).

Kelkar, B.G. and Olsen, R.: "Knowledge of the Business Side of the Industry is Extremely Critical for the Productive Engineer," *Engineering Horizons* (Spring, 1996).

CONTINUING EDUCATION/SHORT COURSE ACTIVITIES

Taught short course on "Water Flooding" for Kuwait Oil Company (April, 1987).

Taught short course on "Geostatistics" for OXY USA, Inc., Phillips Petroleum Company, Amoco Production Company, Conoco, Caltex, Unocal, Texaco, ADNOC, Bechtel Petroleum Company, and for OGCI (1989-Present).

Taught short course on "Risk Analysis" to Caltex, Indonesia, Fletcher Challange, Singapore.

Taught Schlumberger PERF short courses. Responsible for Economics, Reservoir Management, Principles of Geology, and Volumetric Analysis Sections of comprehensive short course for Schlumberger professionals through The University of Tulsa's Continuing Education (1994-Present).

Taught short course on "Natural Gas Production Engineering" for Pertamina, Indonesia and for OGCI (1995 -Present).

Taught short course on "Natural Gas Production Engineering" for Texaco through The University of Tulsa's Continuing Education Division.

Taught Schlumberger Stim LEADER short courses (November 2002 - Present).

TECHNICAL CONSULTING

Triton Engineering, Houston, TX

Amoco Production Company, Tulsa, OK

Robert Hanson, Independent, Minneapolis, MN

John Kane, Attorney at Law, Pawhuska, OK

SAFECO, Tulsa, OK

Oil and Natural Gas Commission, INDIA

PROFESSIONAL/CIVIC ACTIVITIES

Served on Oklahoma Governor's Task Force Subcommittee for "Application of Enhanced Oil Recovery in Oklahoma" (1984).

Reviewed refereed articles for *AIChE Journal*, *Chem. Eng. Communications, Canadian Journal of Chemical Engineering*, *Journal of Petroleum Technology*, and *In Situ*.

Reviewed research proposals for National Science Foundation, American Petroleum Fund and Department of Energy.

Served as External Reviewer on various Tenure and Promotion Committees at other Petroleum and Chemical Engineering Departments (1990- present)

Served as a Technical Editor for Journal of Petroleum Technology (1991-1994).

Served on SPE Ad Hoc Committee on Interdisciplinary Programming (1993-1996).

Served on a Program Committee for Improved Oil Recovery Symposium, Tulsa, OK (1994, 2004).

Served on an Executive Committee for University of Tulsa Centennial Petroleum Engineering Symposium (1993-1994).

Served on a technical committee on a joint SPE/SEG Forum on Integration of Seismic Data into Reservoir Description (1996).

Served on a steering committee on Fourth International Reservoir Characterization Technical Committee (1996).

Served as Technical Editor, SPE Reservoir and Formation Evaluation (1997-2001, 2006 - present).

Served as Review Chairman for SPE Reservoir Evaluation and Engineering (2000-2006t)

Served on SPE Education and Accreditation Committee (2001-2003)

Served as General Chairman of the SPE/IOR Fifteenth Symposium on Improved Oil Recovery (2006)

Served as member of Steering Committee of the SPE/IOR Sixteenth Symposium on Improved Oil Recovery (2008, 2010)

Served on Board of Directors, SPE Mid Continent Section (2008-09).

Served on SPE Ferguson Awards Committee, currently serving as a Chairman of the Committee (2006-09).

Served as Distinguished SPE Speaker (2007-08).

Served on the External Evaluation Committee, Tertiary Oil Recovery Program, University of Kansas (2008)

Served on Steering Committee, IOR Symposium, Tulsa (2010).

Served on Steering Committee, SPE Education Colloquium (2010); also was an invited speaker

Served on various committees as member of PE Chairmans' Committee (2010)

Served on SPE International Board of Directors (2010-2013)

THE UNIVERSITY OF TULSA SERVICE ACTIVITIES

Undergraduate Coordinator for Petroleum Engineering Department (1990-92, 2001-2002).

Served on a Program Implementation Team for BDM-TU Joint Project for the National Oil and Related Program (1993-1994).

Served on a Planning Committee as a TU representative for the area of "Risk Analysis in Exploration," jointly funded by BDM and DOE (1994).

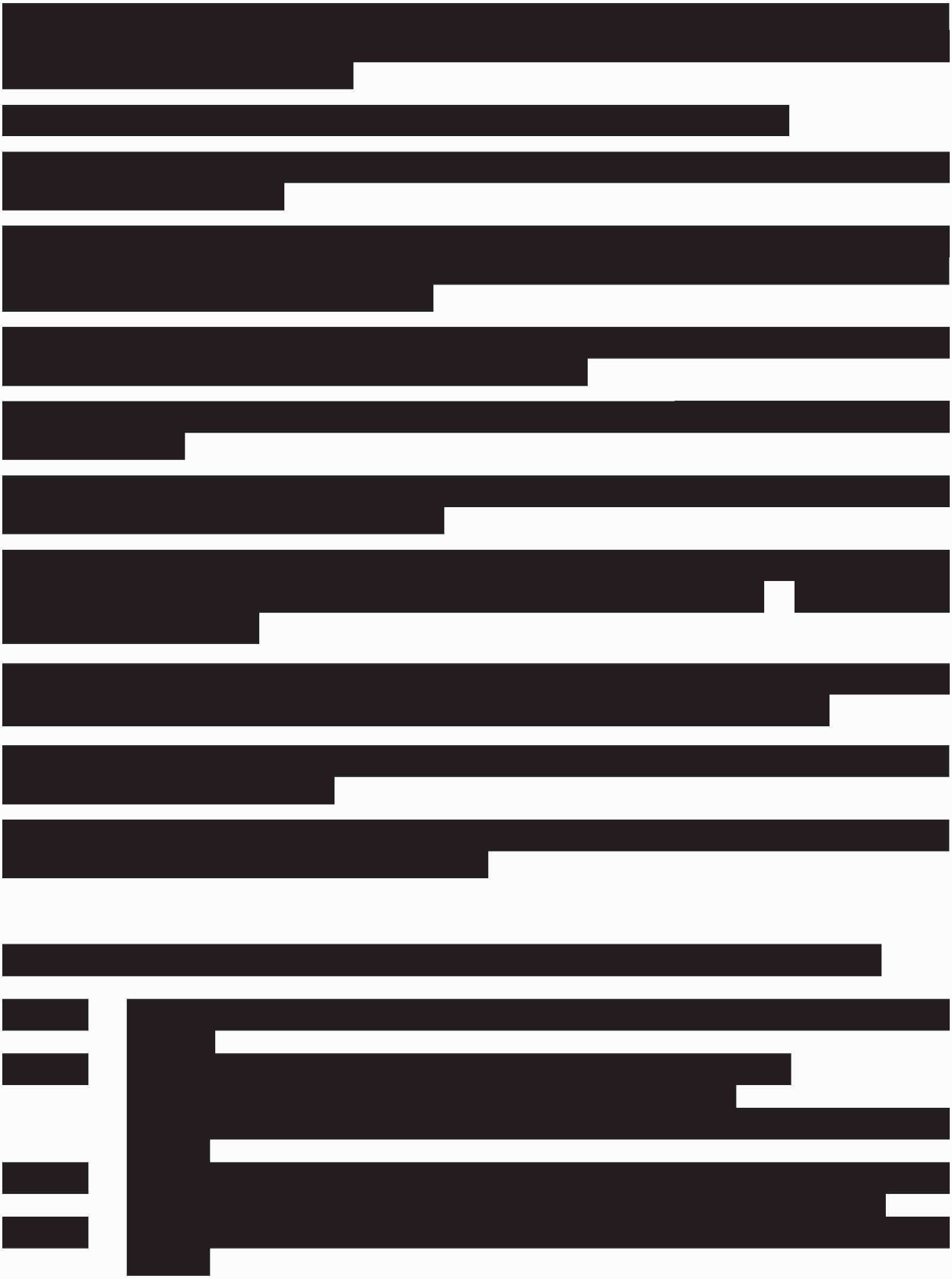

APPENDIX F. FACTS AND DATA WE CONSIDERED IN FORMING OUR OPINIONS

NDX001-0202088-NDX001-0202137
ETL078-005529-ETL078-010078
SNL046-82640
SES-00026218
BP-HZN-2179MDL02114983
BP-HZN-2179MDL00554375 - 00554414
SNL021-7543-SNL021-7548
SNL046-70150- SNL046-70162
SNL046-000421- SNL046-000424
SNL084-58529- SNL084-58532
ETL065-000134-ETL065-000146
BP-HZN-CEC011954 - 011958
BP-HZN-CEC012072 - 012074
BP-HZN-CEC011581 - 011584
BP-HZN-MBI00178699 - 8707
BP-HZN-CEC011710 - 011716
BP-HZN-CEC012008 - 012013
BP-HZN-CEC011717 - 011723
BP-HZN-CEC011724 - 011729
BP-HZN-CEC011730 - 011735
BP-HZN-CEC011736 - 011741
BP-HZN-CEC011742 - 011747
BP-HZN-CEC011748 - 011752
BP-HZN-CEC011753 - 011758
BP-HZN-CEC012014 - 012019
BP-HZN-CEC011759 - 011765
BP-HZN-CEC011766 - 011770
BP-HZN-CEC011771 - 011775
BP-HZN-CEC011761 - 011781
BP-HZN-CEC011782 - 011784
BP-HZN-CEC011785 - 011791
BP-HZN-CEC011792 - 011797
BP-HZN-CEC011798 - 011803
BP-HZN-CEC011804 - 011809
BP-HZN-CEC011810 - 011815
BP-HZN-CEC011816 - 011822
BP-HZN-CEC011823 - 011827
BP-HZN-CEC011828 - 011832
BP-HZN-CEC011833 - 011838
BP-HZN-CEC011839 - 011844
BP-HZN-CEC011845 - 011851
BP-HZN-CEC011852 - 011856
BP-HZN-CEC011857 - 011862
BP-HZN-CEC011863 - 011867
BP-HZN-CEC011868 - 011872
BP-HZN-CEC011879 - 011885
BP-HZN-CEC011886 - 011893
BP-HZN-CEC011894 - 011899
BP-HZN-CEC012371 - 012375
BP-HZN-CEC012376 - 012380
BP-HZN-CEC012381 - 012385
BP-HZN-CEC012386 - 012394
BP-HZN-CEC012395 - 012400
BP-HZN-CEC012401 - 012406
BP-HZN-CEC012407 - 012410
BP-HZN-CEC012411 - 012414
BP-HZN-CEC012415 - 012419
BP-HZN-CEC012420 - 012424
BP-HZN-CEC012425 - 012429
BP-HZN-CEC011964 - 011968
BP-HZN-CEC011585 - 011587
BP-HZN-CEC011969 - 011974
BP-HZN-CEC011610 - 011613
BP-HZN-CEC011975 - 011979
BP-HZN-CEC011588 - 011591
BP-HZN-CEC011574 - 011580
BP-HZN-CEC011606 - 011609
BP-HZN-2179MDL00357010 - 7012
BP-HZN-CEC011980 - 011983
BP-HZN-CEC011596 - 011599

BP-HZN-CEC011592 - 011595
BP-HZN-CEC011600 - 011605
BP-HZN-CEC011614 - 011618
BP-HZN-CEC011619 - 011624
BP-HZN-CEC011625 - 011631
BP-HZN-CEC011632 - 011637
BP-HZN-CEC011638 - 011643
BP-HZN-CEC011644 - 011649
BP-HZN-CEC011650 - 011654
BP-HZN-CEC011655 - 011661
BP-HZN-CEC011662 - 011668
BP-HZN-CEC011669 - 011675
BP-HZN-CEC011676 - 011682
BP-HZN-CEC011683 - 011688
BP-HZN-CEC011689 - 011695
BP-HZN-CEC011984 - 011990
BP-HZN-CEC011696 - 011702
BP-HZN-CEC011703 - 011709
BP-HZN-CEC011991 - 011995
BP-HZN-CEC011996 - 012001
BP-HZN-CEC012002 - 012007
BP-HZN-CEC012028 - 012052
BP-HZN-CEC012020 - 012064; BP-HZN-CEC017024 - 017039
BP-HZN-CEC012075 - 012202
BP-HZN-CEC012203 - 012309
BP-HZN-CEC012069 - 012370
SNL046-082105 - 2141
SNL-008-002541
SNL042-02687- 2688
SNL075-028330- 8330
SNL110-012087
SNL110-017071
SNL046-073422 - 3439
SNL087-001149 - 1171
BP-HZN-2179MDL02564596 - 4602
ETL078-005529 - 0078
PNL001-006184 - 6215
PNL001-006216 - 6217
SNL059-000136 - 0137
PNL001-006218 -PNL001-006296
PNL001-006297-PNL001-006337
SNL048-005360- SNL048-005375
TRN-USCG_MMS-00011510 - 00011513
BP-HZN-CEC-019162 - 019164
BP-HZN-JUD000198 - 000203
TRN-USCG_MMS-00011586 - 00011590
BP-HZN-CEC-019217 - 019219
TRN-USCG_MMS-00011542 - 00011545
BP-HZN-CEC-019097 - 019100
BP-HZN-CEC-019223 - 019225
BP-HZN-CEC-019104 - 019108
BP-HZN-CEC-019226 - 019228
BP-HZN-CEC-019112 - 019116
BP-HZN-CEC-019229 - 019231
BP-HZN-CEC-019121 - 019124
BP-HZN-CEC-019232 - 019234
HCG009-015700
BP-HZN-MBI00143483 - 0014387
HCG009-015704
BP-HZN-CEC-019136 - 019139
TRN-USCG_MMS-00011591 - 00011595
BP-HZN-CEC-019143 - 019146
HCG009-015713
TRN-USCG_MMS-00011546 - 00011549
HCG009-015717
TRN-USCG_MMS-00011550 - 00011553
TRN-USCG_MMS-00011514 - 00011517
BP-HZN-CEC-019168 - 019170
TRN-USCG_MMS-00011554 - 00011557

HCG009-015721
TRN-USCG_MMS-00011558 - 00011561
HCG009-015729
BP-HZN-CEC-019177 - 019179
TRN-USCG_MMS-00011596 - 00011599
BP-HZN-FIN00000192 - 00000194
TRN-USCG_MMS-00011600 - 00011604
BP-HZN-CEC-019189 - 019192
TRN-USCG_MMS-00011605 - 00011608
TRN-USCG_MMS-00011562 - 00011565
TRN-USCG_MMS-00011609 - 00011612
TRN-USCG_MMS-00011566 - 00011569
TRN-USCG_MMS-00011613 - 00011616
BP-HZN-CEC-019208 - 019210
TRN-USCG_MMS-00011617 - 00011620
BP-HZN-CEC-019214 - 019216
TRN-USCG_MMS-00011621 - 00011624
BP-HZN-CEC-019220 - 019222
TRN-USCG_MMS-00011518 - 00011521
BP-HZN-FIN00000183 - 00000185
TRN-USCG_MMS-00011625 - 00011628
BP-HZN-CEC-019026 - 019029
TRN-USCG_MMS-00011629 - 00011633
BP-HZN-CEC-019035 - 019037
TRN-USCG_MMS-00011634 - 00011637
BP-HZN-CEC-019043 - 019045
TRN-USCG_MMS-00011638 - 00011643
TRN-USCG_MMS-00011570 - 00011573
TRN-USCG_MMS-00011644 - 00011648
BP-HZN-BLY00101690 - 001694
BP-HZN-BLY00101695 - 001698
BP-HZN-CEC-019076 - 019078
BP-HZN-BLY00101703 - 00101706
BP-HZN-SNR00001109 - 00001112
BP-HZN-CEC-019101 - 019103
TRN-USCG_MMS-00011522 - 00011525
BP-HZN-BLY00215713 - 00215715
BP-HZN-FIN00000118 - 00000120
BP-HZN-CEC-019117 - 019120
BP-HZN-CEC-019125 - 019127
BP-HZN-FIN00000142 - 00000144
TRN-USCG_MMS-00011574 - 00011577
BP-HZN-CEC-019147 - 019149
BP-HZN-FIN00000163 - 00000165
BP-HZN-CEC-019046 - 019050
TRN-USCG_MMS-00011578 - 00011581
TRN-USCG_MMS-00011526 - 00011529
BP-HZN-CEC-019193 - 019195
TRN-USCG_MMS-00011530 - 00011533
BP-HZN-FIN00000208 - 00000210
TRN-USCG_MMS-00011534 - 00011537
BP-HZN-CEC-019205 - 019207
TRN-USCG_MMS-00011538 - 00011541
TRN-USCG_MMS-00011582 - 00011585
SNL045-01583-SNL045-01611
BP-HZN-2179MDL02114983
In re. Deepwater Horizon MDL 2179 Reservoir Experts Materials (BP MDL2179VOL000001-011 thru BP MDL2179VOL000001-013; BP MDL2179VOL000001-014, BP MDL2179VOL000001-015, and BP MDL2179VOL000001-018)
File- Deepwater DVD Label.2: In re. Deepwater Horizon MDL 2179 Reservoir Experts Materials (BP MDL2179VOL000001-016; BP MDL2179VOL000001-017)
File- Deepwater DVD Label.3: In re. Deepwater Horizon MDL 2179 Reservoir Experts Materials BPD248 and Pencor PVT thru Skripnikova 20110708 Depo Ex3533
SUBFOLDER- BP Macondo High Quality Dips (Depth, Dip, Azimuth, Quality and Type).Excel BP_Macondo_32306_1_ST00BP01_OBMI_Dips_HandPicked_Hi_Quality (BP MDL2179VOL000001-003)

File- BP Macondo Low Quality Dips (Depth, Dip, Azimuth, Quality and Type).Excel BP_Macondo_32306_1_ST00BP01_OBMI_Dips_HandPicked_Low_Quality (BP MDL2179VOL000001-003)
File- BP Macondo Posssible Faults (Depth, Dip, Azimuth, Quality and Type).Excel BP_Macondo_32306_1_ST00BP01_OBMI_Dips_PossibleFault (BP MDL2179VOL000001-003)
File- BP Macondo Possible Fractures (Depth, Dip, Azimuth, Quality and Type).Excel BP_Macondo_32306_1_ST00BP01_OBMI_Dips_PossibleFractures (BP MDL2179VOL000001-003)
File- Geo TAP LWD DATA; MC252_001_ST00BP01_GEOTAP_LOG (BP MDL2179VOL000001-004)
File- BP Exploratory and Production (OCS-G 32306 001 ST00BP01 Mississippi Canyon 252) Pressure Transient Summary.Excel MC252_001_ST00BP01_GEOTAP_MMS (BP MDL2179VOL000001-004)
File- BP Exploratory and Production (OCS-G 32306 001 ST00BP01 Mississippi Canyon 252) Pressure Transient Summary.Text Notepad MC252_001_ST00BP01_GEOTAP_Pressures (BP MDL2179VOL000001-004)
File- Halliburton Report/GEO Tap Pressure Transient Analysis for Well OCS-G 32306 001 ST00BP01, Field Mississippi Canyon 252, Deepwater Horizon.MS Word MC252_001_ST00BP01_GEOTAP_REPORT (BP MDL2179VOL000001-004)
File- Deepwater Horizon Well: OCS-G 32306 001 ST00BP01 Mississippi Canyon Block 252 Full Service PWD Time-Based Data Log Report - RUN NO. 1100.Text Notepad MC252_001_ST00BP01_PWD_DDS_RUN_1100_ASCII (BP MDL2179VOL000001-004)
File- Deepwater Horizon Well: OCS-G 32306 001 ST00BP01 Mississippi Canyon Block 252 Full Service PWD Time-Based Data Log Report - RUN NO. 1200.Text Notepad MC252_001_ST00BP01_PWD_DDS_RUN_1200_ASCII (BP MDL2179VOL000001-004)
File- Deepwater Horizon Well: OCS-G 32306 001 ST00BP01 Mississippi Canyon Block 252 Full Service PWD Time-Based Data Log Report - RUN NO. 1300.Text Notepad MC252_001_ST00BP01_PWD_DDS_RUN_1300_ASCII (BP MDL2179VOL000001-004)
File-Deepwater Horizon Well: OCS-G 32306 001 ST00BP01 Mississippi Canyon Block 252 Full Service PWD Time-Based Data Log Report - RUN NO. 1400.Text Notepad MC252_001_ST00BP01_PWD_DDS_RUN_1400_ASCII (BP MDL2179VOL000001-004)
File- Deepwater Horizon Well: OCS-G 32306 001 ST00BP01 Mississippi Canyon Block 252 Full Service PWD Time-Based Data Log Report - RUN NO. 1500.Text Notepad MC252_001_ST00BP01_PWD_DDS_RUN_1500_ASCII (BP MDL2179VOL000001-004)
File- Deepwater Horizon Well: OCS-G 32306 001 ST00BP01 Mississippi Canyon Block 252 Full Service PWD Time-Based Data Log Report - RUN NO. 1600.Text Notepad MC252_001_ST00BP01_PWD_DDS_RUN_1600_ASCII (BP MDL2179VOL000001-004)
File- Survey Containing Information about Deepwater Horizon - Version, Well, Parameter and Curve.Excel MC252_001_ST00BP01_SURVEY (BP MDL2179VOL000001-004)
File- Halliburton Sperry Drilling Services Geodetic Report for North America Exploration - BP Macondo Well MC252 Design: OCS-G 32306 MC252#1ST00BP01.pdf OCSG32306_001_ST00BP01_GEODETIC_SURVEY (BP MDL2179VOL000001-004)
File- Deepwater Horizon Well: OCS-G 32306 001 ST00BP01 (Measured Depth, Inclination, Azimuth, Tool Type and Station Type).Text Notepad OCSG32306_001_ST00BP01_MMS (BP MDL2179VOL000001-004)
File- End-User License Agreement Supplied by Halliburton Under Rights of Sublicense from Larson Software Technology, Inc.pdf HalliburtonLogViewerPro9.50_EndUserLicense (BP MDL2179VOL000001-004)
File- Halliburton Log Viewer Pro V9.5.0 Release Notes and Installation / Operation Instructions.pdf HalliburtonLogViewerPro9.50_ReleaseNotes (BP MDL2179VOL000001-004)
File- Installation Link for Installing Halliburton Log Viewer Pro9.50.Install Wizard HalliburtonLogViewerPro950Install (BP MDL2179VOL000001-004)
File- Instructions for Installing Halliburton Log Viewer Pro9.50.pdf InstallingHalliburtonLogViewerPro9.50 (BP MDL2179VOL000001-004)
File- Halliburton Sperry Drilling Services/BP OCSG-32306 Macondo Prospect Daily Operations Report.Excel MC252 001 ST00BP00 Sperry Rpt 043 (BP MDL2179VOL000001-005)
File- Halliburton Sperry Drilling Services/BP OCSG-32306 Macondo Prospect Daily Operations Report.Excel MC252 001 ST00BP00 Sperry Rpt 043A (BP MDL2179VOL000001-005)
File- Halliburton Sperry Drilling Services/BP OCSG-32306 Macondo Prospect Daily Operations Report.Excel MC252 001 ST00BP00 Sperry Rpt 044 (BP MDL2179VOL000001-005)
File- Halliburton Sperry Drilling Services/BP OCSG-32306 Macondo Prospect Daily Operations Report.Excel MC252 001 ST00BP00 Sperry Rpt 044A (BP MDL2179VOL000001-005)
File- Halliburton Sperry Drilling Services/BP OCSG-32306 Macondo Prospect Daily Operations Report.Excel MC252 001 ST00BP00 Sperry Rpt 045 (BP MDL2179VOL000001-005)
File- Halliburton Sperry Drilling Services/BP OCSG-32306 Macondo Prospect Daily Operations Report.Excel MC252 001 ST00BP00 Sperry Rpt 045A (BP MDL2179VOL000001-005)
File- Halliburton Sperry Drilling Services/BP OCSG-32306 Macondo Prospect Daily Operations Report. Excel MC252 001 ST00BP01 Sperry Rpt 046 (BP MDL2179VOL000001-005)
File- Halliburton Sperry Drilling Services/BP OCSG-32306 Macondo Prospect Daily Operations Report. Excel MC252 001 ST00BP01 Sperry Rpt 046A (BP MDL2179VOL000001-005)
File- Halliburton Sperry Drilling Services/BP OCSG-32306 Macondo Prospect Daily Operations Report. Excel MC252 001 ST00BP01 Sperry Rpt 047 (BP MDL2179VOL000001-005)
File- Halliburton Sperry Drilling Services/BP OCSG-32306 Macondo Prospect Daily Operations Report. Excel MC252 001 ST00BP01 Sperry Rpt 047A (BP MDL2179VOL000001-005)
File- Halliburton Sperry Drilling Services/BP OCSG-32306 Macondo Prospect Daily Operations Report. Excel MC252 001 ST00BP00 Sperry Rpt 048 (BP MDL2179VOL000001-005)
File- Halliburton Sperry Drilling Services/BP OCSG-32306 Macondo Prospect Daily Operations Report. Excel MC252 001 ST00BP00 Sperry Rpt 048A (BP MDL2179VOL000001-005)

File- Halliburton Sperry Drilling Services/BP OCSG-32306 Macondo Prospect Daily Operations Report. Excel MC252 001 ST00BP00 Sperry Rpt 049 (BP MDL2179VOL000001-005)
File- Halliburton Sperry Drilling Services/BP OCSG-32306 Macondo Prospect Daily Operations Report. Excel MC252 001 ST00BP00 Sperry Rpt 049A (BP MDL2179VOL000001-005)
File- Halliburton Sperry Drilling Services/BP OCSG-32306 Macondo Prospect Daily Operations Report. Excel MC252 001 ST00BP00 Sperry Rpt 050 (BP MDL2179VOL000001-005)
File- Halliburton Sperry Drilling Services/BP OCSG-32306 Macondo Prospect Daily Operations Report. Excel MC252 001 ST00BP00 Sperry Rpt 050A (BP MDL2179VOL000001-005)
File- Halliburton Sperry Drilling Services/BP OCSG-32306 Macondo Prospect Daily Operations Report. Excel MC252 001 ST00BP00 Sperry Rpt 051 (BP MDL2179VOL000001-005)
File- Halliburton Sperry Drilling Services/BP OCSG-32306 Macondo Prospect Daily Operations Report. Excel MC252 001 ST00BP00 Sperry Rpt 051A (BP MDL2179VOL000001-005)
File- Halliburton Sperry Drilling Services/BP OCSG-32306 Macondo Prospect Daily Operations Report. Excel MC252 001 ST00BP00 Sperry Rpt 052 (BP MDL2179VOL000001-005)
File- Halliburton Sperry Drilling Services/BP OCSG-32306 Macondo Prospect Daily Operations Report. Excel MC252 001 ST00BP00 Sperry Rpt 052A (BP MDL2179VOL000001-005)
File- Halliburton Sperry Drilling Services/BP OCSG-32306 Macondo Prospect Daily Operations Report. Excel MC252 001 ST00BP00 Sperry Rpt 053 (BP MDL2179VOL000001-005)
File- Halliburton Sperry Drilling Services/BP OCSG-32306 Macondo Prospect Daily Operations Report. Excel MC252 001 ST00BP00 Sperry Rpt 053A (BP MDL2179VOL000001-005)
File- Halliburton Sperry Drilling Services/BP OCSG-32306 Macondo Prospect Daily Operations Report. Excel MC252 001 ST00BP00 Sperry Rpt 054 (BP MDL2179VOL000001-005)
File- Halliburton Sperry Drilling Services/BP OCSG-32306 Macondo Prospect Daily Operations Report. Excel MC252 001 ST00BP00 Sperry Rpt 054A (BP MDL2179VOL000001-005)
File- Halliburton Sperry Drilling Services/BP OCSG-32306 Macondo Prospect Daily Operations Report. Excel MC252 001 ST00BP00 Sperry Rpt 055 (BP MDL2179VOL000001-005)
File- Halliburton Sperry Drilling Services/BP OCSG-32306 Macondo Prospect Daily Operations Report. Excel MC252 001 ST00BP00 Sperry Rpt 055A (BP MDL2179VOL000001-005)
File- Halliburton Sperry Drilling Services/BP OCSG-32306 Macondo Prospect Daily Operations Report. Excel MC252 001 ST00BP00 Sperry Rpt 056 (BP MDL2179VOL000001-005)
File- Halliburton Sperry Drilling Services/BP OCSG-32306 Macondo Prospect Daily Operations Report. Excel MC252 001 ST00BP00 Sperry Rpt 056A (BP MDL2179VOL000001-005)
File- Halliburton Sperry Drilling Services/BP OCSG-32306 Macondo Prospect Daily Operations Report. Excel MC252 001 ST00BP00 Sperry Rpt 057 (BP MDL2179VOL000001-005)
File- Halliburton Sperry Drilling Services/BP OCSG-32306 Macondo Prospect Daily Operations Report. Excel MC252 001 ST00BP00 Sperry Rpt 057A (BP MDL2179VOL000001-005)
File- Halliburton Sperry Drilling Services/BP OCSG-32306 Macondo Prospect Daily Operations Report. Excel MC252 001 ST00BP00 Sperry Rpt 058 (BP MDL2179VOL000001-005)
File- Halliburton Sperry Drilling Services/BP OCSG-32306 Macondo Prospect Daily Operations Report. Excel MC252 001 ST00BP00 Sperry Rpt 058A (BP MDL2179VOL000001-005)
File-Halliburton Sperry Drilling Services/BP OCSG-32306 Macondo Prospect Daily Operations Report. Excel MC252 001 ST00BP00 Sperry Rpt 059 (BP MDL2179VOL000001-005)
File- Halliburton Sperry Drilling Services/BP OCSG-32306 Macondo Prospect Daily Operations Report. Excel MC252 001 ST00BP00 Sperry Rpt 059A (BP MDL2179VOL000001-005)
File- Halliburton Sperry Drilling Services/BP OCSG-32306 Macondo Prospect Daily Operations Report. Excel MC252 001 ST00BP00 Sperry Rpt 060 (BP MDL2179VOL000001-005)
File- Halliburton Sperry Drilling Services/BP OCSG-32306 Macondo Prospect Daily Operations Report. Excel MC252 001 ST00BP00 Sperry Rpt 060A (BP MDL2179VOL000001-005)
File- Halliburton Sperry Drilling Services/BP OCSG-32306 Macondo Prospect Daily Operations Report. Excel MC252 001 ST00BP00 Sperry Rpt 061 (BP MDL2179VOL000001-005)
File- Halliburton Sperry Drilling Services/BP OCSG-32306 Macondo Prospect Daily Operations Report. Excel MC252 001 ST00BP00 Sperry Rpt 061A (BP MDL2179VOL000001-005)
File- Halliburton Sperry Drilling Services/BP OCSG-32306 Macondo Prospect Daily Operations Report. Excel MC252 001 ST00BP00 Sperry Rpt 062 (BP MDL2179VOL000001-005)
File- Halliburton Sperry Drilling Services/BP OCSG-32306 Macondo Prospect Daily Operations Report. Excel MC252 001 ST00BP00 Sperry Rpt 062A (BP MDL2179VOL000001-005)
File- Halliburton Sperry Drilling Services/BP OCSG-32306 Macondo Prospect Daily Operations Report. Excel MC252 001 ST00BP00 Sperry Rpt 063 (BP MDL2179VOL000001-005)
File- Halliburton Sperry Drilling Services/BP OCSG-32306 Macondo Prospect Daily Operations Report. Excel MC252 001 ST00BP00 Sperry Rpt 063A (BP MDL2179VOL000001-005)
File- Halliburton Sperry Drilling Services/BP OCSG-32306 Macondo Prospect Daily Operations Report. Excel MC252 001 ST00BP00 Sperry Rpt 064 (BP MDL2179VOL000001-005)
File- Halliburton Sperry Drilling Services/BP OCSG-32306 Macondo Prospect Daily Operations Report. Excel MC252 001 ST00BP00 Sperry Rpt 064A (BP MDL2179VOL000001-005)
File- Halliburton Sperry Drilling Services/BP OCSG-32306 Macondo Prospect Daily Operations Report. Excel MC252 001 ST00BP00 Sperry Rpt 065 (BP MDL2179VOL000001-005)
File- Halliburton Sperry Drilling Services/BP OCSG-32306 Macondo Prospect Daily Operations Report. Excel MC252 001 ST00BP00 Sperry Rpt 065A (BP MDL2179VOL000001-005)
File- Halliburton Sperry Drilling Services/BP OCSG-32306 Macondo Prospect Daily Operations Report. Excel MC252 001 ST00BP00 Sperry Rpt 066 (BP MDL2179VOL000001-005)

APPENDIX F. FACTS AND DATA WE CONSIDERED IN FORMING OUR OPINIONS

File- Halliburton Sperry Drilling Services/BP OCSG-32306 Macondo Prospect Daily Operations Report. Excel MC252 001 ST00BP00 Sperry Rpt 066A (BP MDL2179VOL000001-005)
File- Halliburton Sperry Drilling Services/BP OCSG-32306 Macondo Prospect Daily Operations Report. Excel MC252 001 ST00BP00 Sperry Rpt 067 (BP MDL2179VOL000001-005)
File- Halliburton Sperry Drilling Services/BP OCSG-32306 Macondo Prospect Daily Operations Report. Excel MC252 001 ST00BP00 Sperry Rpt 067A (BP MDL2179VOL000001-005)
File- Halliburton Sperry Drilling Services/BP OCSG-32306 Macondo Prospect Daily Operations Report. Excel MC252 001 ST00BP00 Sperry Rpt 068 (BP MDL2179VOL000001-005)
File- Halliburton Sperry Drilling Services/BP OCSG-32306 Macondo Prospect Daily Operations Report. Excel MC252 001 ST00BP00 Sperry Rpt 068A (BP MDL2179VOL000001-005)
File- Halliburton Sperry Drilling Services/BP OCSG-32306 Macondo Prospect Daily Operations Report. Excel MC252 001 ST00BP00 Sperry Rpt 069 (BP MDL2179VOL000001-005)
File- Halliburton Sperry Drilling Services/BP OCSG-32306 Macondo Prospect Daily Operations Report. Excel MC252 001 ST00BP00 Sperry Rpt 069A (BP MDL2179VOL000001-005)
File- Halliburton Sperry Drilling Services/BP OCSG-32306 Macondo Prospect Daily Operations Report. Excel MC252 001 ST00BP00 Sperry Rpt 070 (BP MDL2179VOL000001-005)
File- Halliburton Sperry Drilling Services/BP OCSG-32306 Macondo Prospect Daily Operations Report. Excel MC252 001 ST00BP00 Sperry Rpt 070A (BP MDL2179VOL000001-005)
File- Halliburton Sperry Drilling Services/BP OCSG-32306 Macondo Prospect Daily Operations Report. Excel MC252 001 ST00BP00 Sperry Rpt 071 (BP MDL2179VOL000001-005)
File- Halliburton Sperry Drilling Services/BP OCSG-32306 Macondo Prospect Daily Operations Report. Excel MC252 001 ST00BP00 Sperry Rpt 071A (BP MDL2179VOL000001-005)
File- Halliburton Sperry Drilling Services/BP OCSG-32306 Macondo Prospect Daily Operations Report. Excel MC252 001 ST00BP00 Sperry Rpt 072 (BP MDL2179VOL000001-005)
File- Halliburton Sperry Drilling Services/BP OCSG-32306 Macondo Prospect Daily Operations Report. Excel MC252 001 ST00BP00 Sperry Rpt 072A (BP MDL2179VOL000001-005)
File- Halliburton Sperry Drilling Services/BP OCSG-32306 Macondo Prospect Daily Operations Report. Excel MC252 001 ST00BP01 Sperry Rpt 073 (BP MDL2179VOL000001-005)
File- Halliburton Sperry Drilling Services/BP OCSG-32306 Macondo Prospect Daily Operations Report. Excel MC252 001 ST00BP01 Sperry Rpt 073A (BP MDL2179VOL000001-005)
File- Halliburton Sperry Drilling Services/BP OCSG-32306 Macondo Prospect Daily Operations Report. Excel MC252 001 ST00BP01 Sperry Rpt 074 (BP MDL2179VOL000001-005)
File- Halliburton Sperry Drilling Services/BP OCSG-32306 Macondo Prospect Daily Operations Report. Excel MC252 001 ST00BP01 Sperry Rpt 074A (BP MDL2179VOL000001-005)
File- Halliburton Sperry Drilling Services/BP OCSG-32306 Macondo Prospect Daily Operations Report. Excel MC252 001 ST00BP01 Sperry Rpt 075 (BP MDL2179VOL000001-005)
File- Halliburton Sperry Drilling Services/BP OCSG-32306 Macondo Prospect Daily Operations Report. Excel MC252 001 ST00BP01 Sperry Rpt 075A (BP MDL2179VOL000001-005)
File- Halliburton Sperry Drilling Services/BP OCSG-32306 Macondo Prospect Daily Operations Report. Excel MC252 001 ST00BP01 Sperry Rpt 076 (BP MDL2179VOL000001-005)
File- Halliburton Sperry Drilling Services/BP OCSG-32306 Macondo Prospect Daily Operations Report. Excel MC252 001 ST00BP01 Sperry Rpt 076A (BP MDL2179VOL000001-005)
File- Halliburton Sperry Drilling Services/BP OCSG-32306 Macondo Prospect Daily Operations Report. Excel MC252 001 ST00BP01 Sperry Rpt 077 (BP MDL2179VOL000001-005)
File- Halliburton Sperry Drilling Services/BP OCSG-32306 Macondo Prospect Daily Operations Report. Excel MC252 001 ST00BP01 Sperry Rpt 077A (BP MDL2179VOL000001-005)
File- Halliburton Sperry Drilling Services/BP OCSG-32306 Macondo Prospect Daily Operations Report. Excel MC252 001 ST00BP01 Sperry Rpt 078 (BP MDL2179VOL000001-005)
File- Halliburton Sperry Drilling Services/BP OCSG-32306 Macondo Prospect Daily Operations Report. Excel MC252 001 ST00BP01 Sperry Rpt 078A (BP MDL2179VOL000001-005)
File- Halliburton Sperry Drilling Services/BP OCSG-32306 Macondo Prospect Daily Operations Report. Excel MC252 001 ST00BP01 Sperry Rpt 079 (BP MDL2179VOL000001-005)
File- Halliburton Sperry Drilling Services, BP Exploration & Production Summary: OCS-G 32306 001 ST00BP00 & BP01 Mississippi Canyon Block 252 surface data logging and pore pressure prediction services. MS Word MC252_001_ST00BP01_EOWR (BP MDL2179VOL000001-005)
File- Sperry Drilling Services ZOI / Show Report for Well: OCS-G-32306 001 ST00BP01 Mississippi Canyon 252 No1 ST00BP01, Prepared By Josph Keith. Excel MC252_001_ST00BP01_SHOW_REPORT_#1 (BP MDL2179VOL000001-005)
File- Sperry Drilling Services ZOI / Show Report for Well: OCS-G-32306 001 ST00BP01 Mississippi Canyon 252 No1 ST00BP01, Prepared By Josph Keith. Excel MC252_001_ST00BP01_ZOI_A (BP MDL2179VOL000001-005)
File- MC252_001_ST00BP01_1MD_COMBO. MS Word (BP MDL2179VOL000001-005)
File- MC252_001_ST00BP01_1MD_ENGINEERING. MS Word (BP MDL2179VOL000001-005)
File- MC252_001_ST00BP01_1TVD_COMBO. MS Word (BP MDL2179VOL000001-005)
File- MC252_001_ST00BP01_1TVD_PRESSURE. MS Word (BP MDL2179VOL000001-005)
File- MC252_001_ST00BP01_5MD_COMBO. MS Word (BP MDL2179VOL000001-005)
File- MC252_001_ST00BP01_5MD_SHOW_1. MS Word (BP MDL2179VOL000001-005)
File- MC252_001_ST00BP01_5TVD_COMBO. MS Word (BP MDL2179VOL000001-005)

APPENDIX F. FACTS AND DATA WE CONSIDERED IN FORMING OUR OPINIONS

File- Deepwater Horizon Well: OCS-G 32306 001 ST00BP00 Mississippi Canyon Block 252 Full Service PWD Time-Based Data Log Report - RUN NO. 500. Text Notepad MC252_001_ST00BP00_PWD_DDS_RUN_500_ASCII (BP MDL2179VOL000001-006)
File- Deepwater Horizon Well: OCS-G 32306 001 ST00BP00 Mississippi Canyon Block 252 Full Service PWD Time-Based Data Log Report - RUN NO. 600. Text Notepad MC252_001_ST00BP00_PWD_DDS_RUN_600_ASCII (BP MDL2179VOL000001-006)
File- Deepwater Horizon Well: OCS-G 32306 001 ST00BP00 Mississippi Canyon Block 252 Full Service PWD Time-Based Data Log Report - RUN NO. 700. Text Notepad MC252_001_ST00BP00_PWD_DDS_RUN_700_ASCII (BP MDL2179VOL000001-006)
File- Deepwater Horizon Well: OCS-G 32306 001 ST00BP00 Mississippi Canyon Block 252 Full Service PWD Time-Based Data Log Report - RUN NO. 800. Text Notepad MC252_001_ST00BP00_PWD_DDS_RUN_800_ASCII (BP MDL2179VOL000001-006)
File- Deepwater Horizon Well: OCS-G 32306 001 ST00BP00 Mississippi Canyon Block 252 Full Service PWD Time-Based Data Log Report - RUN NO. 900. Text Notepad MC252_001_ST00BP00_PWD_DDS_RUN_900_ASCII (BP MDL2179VOL000001-006)
File- Deepwater Horizon Well: OCS-G 32306 001 ST00BP00 Mississippi Canyon Block 252 Full Service PWD Time-Based Data Log Report - RUN NO. 1000. Text Notepad MC252_001_ST00BP00_PWD_DDS_RUN_1000_ASCII (BP MDL2179VOL000001-006)
File- Survey Containing Information about Deepwater Horizon - Version, Well, Parameter and Curve. Text Notepad MC252_001_ST00BP00_RAW_SURVEY_ASCII (BP MDL2179VOL000001-006)
File- Survey Containing Information about Deepwater Horizon - Version, Well, Parameter and Curve. Excel MC252_001_ST00BP00_SURVEY (BP MDL2179VOL000001-006)
File- Survey Containing Information about Deepwater Horizon - Version, Well, Parameter and Curve. Excel MC252_001_ST00BP00_UT (BP MDL2179VOL000001-006)
File- Halliburton Sperry Drilling Services Geodetic Report for North America Exploration - BP Macondo Well MC252 Design: OCS-G 32306 MC252#1ST00BP01. pdf OCSG32306_001_ST00BP00_GEODETIC_SURVEY (BP MDL2179VOL000001-006)
File- Deepwater Horizon Well: OCS-G 32306 001 ST00BP01 (Measured Depth, Inclination, Azimuth, Tool Type and Station Type). Text Notepad OCSG32306_001_ST00BP00_MMS (BP MDL2179VOL000001-006)
File- End-User License Agreement Supplied by Halliburton Under Rights of Sublicense from Larson Software Technology, Inc. pdf HalliburtonLogViewerPro9.50_EndUserLicense (BP MDL2179VOL000001-006)
File- Halliburton Log Viewer Pro V9.5.0 Release Notes and Installation / Operation Instructions.pdf HalliburtonLogViewerPro9.50_ReleaseNotes (BP MDL2179VOL000001-006)
File- Installation Link for Installing Halliburton Log Viewer Pro9.50. Install Wizard HalliburtonLogViewerPro950Install (BP MDL2179VOL000001-006)
File- Instructions for Installing Halliburton Log Viewer Pro9.50. pdf InstallingHalliburtonLogViewerPro9.50 (BP MDL2179VOL000001-006)
File- MC252_001_ST00BP00_ALL_RUNS (BP MDL2179VOL000001-006)
File- Halliburton End of Well Report for BP Exploration and Production for Rig: Deepwater Horizon, Well: OCS-G 32306 001 ST00BP00 MC252_001_ST00BP00_EOWR (BP MDL2179VOL000001-006)
File- MC252_001_ST00BP00_RUN_500 (BP MDL2179VOL000001-006)
File- MC252_001_ST00BP00_RUN_600 (BP MDL2179VOL000001-006)
File- MC252_001_ST00BP00_RUN_700 (BP MDL2179VOL000001-006)
File- MC252_001_ST00BP00_RUN_800 (BP MDL2179VOL000001-006)
File- MC252_001_ST00BP00_RUN_900 (BP MDL2179VOL000001-006)
File- MC252_001_ST00BP00_RUN_1000 (BP MDL2179VOL000001-006)
File- MC252_ST00BP00_1MD_CORRELATION (BP MDL2179VOL000001-006)
File- MC252_ST00BP00_5MD_PHASE_ATTEN (BP MDL2179VOL000001-006)
File- Halliburton Sperry Drilling Services/BP OCSG-32306 Macondo Prospect Daily Operations Report. Excel MC252 001 ST00BP00 Sperry Rpt 001 (BP MDL2179VOL000001-007)
File- Halliburton Sperry Drilling Services/BP OCSG-32306 Macondo Prospect Daily Operations Report. Excel MC252 001 ST00BP00 Sperry Rpt 001A (BP MDL2179VOL000001-007)
File- Halliburton Sperry Drilling Services/BP OCSG-32306 Macondo Prospect Daily Operations Report. Excel MC252 001 ST00BP00 Sperry Rpt 002 (BP MDL2179VOL000001-007)
File- Halliburton Sperry Drilling Services/BP OCSG-32306 Macondo Prospect Daily Operations Report. Excel MC252 001 ST00BP00 Sperry Rpt 002A (BP MDL2179VOL000001-007)
File- Halliburton Sperry Drilling Services/BP OCSG-32306 Macondo Prospect Daily Operations Report. Excel MC252 001 ST00BP00 Sperry Rpt 003 (BP MDL2179VOL000001-007)
File- Halliburton Sperry Drilling Services/BP OCSG-32306 Macondo Prospect Daily Operations Report. Excel MC252 001 ST00BP00 Sperry Rpt 003A (BP MDL2179VOL000001-007)
File- Halliburton Sperry Drilling Services/BP OCSG-32306 Macondo Prospect Daily Operations Report. Excel MC252 001 ST00BP00 Sperry Rpt 004 (BP MDL2179VOL000001-007)
File- Halliburton Sperry Drilling Services/BP OCSG-32306 Macondo Prospect Daily Operations Report. Excel MC252 001 ST00BP00 Sperry Rpt 004A (BP MDL2179VOL000001-007)
File- Halliburton Sperry Drilling Services/BP OCSG-32306 Macondo Prospect Daily Operations Report. Excel MC252 001 ST00BP00 Sperry Rpt 005 (BP MDL2179VOL000001-007)
File- Halliburton Sperry Drilling Services/BP OCSG-32306 Macondo Prospect Daily Operations Report. Excel MC252 001 ST00BP00 Sperry Rpt 005A (BP MDL2179VOL000001-007)
File- Halliburton Sperry Drilling Services/BP OCSG-32306 Macondo Prospect Daily Operations Report. Excel MC252 001 ST00BP00 Sperry Rpt 006 (BP MDL2179VOL000001-007)

APPENDIX F. FACTS AND DATA WE CONSIDERED IN FORMING OUR OPINIONS

File- Halliburton Sperry Drilling Services/BP OCSG-32306 Macondo Prospect Daily Operations Report. Excel MC252 001 ST00BP00 Sperry Rpt 006A (BP MDL2179VOL000001-007)
File- Halliburton Sperry Drilling Services/BP OCSG-32306 Macondo Prospect Daily Operations Report. Excel MC252 001 ST00BP00 Sperry Rpt 007 (BP MDL2179VOL000001-007)
File- Halliburton Sperry Drilling Services/BP OCSG-32306 Macondo Prospect Daily Operations Report. Excel MC252 001 ST00BP00 Sperry Rpt 007A (BP MDL2179VOL000001-007)
File- Halliburton Sperry Drilling Services/BP OCSG-32306 Macondo Prospect Daily Operations Report. Excel MC252 001 ST00BP00 Sperry Rpt 008 (BP MDL2179VOL000001-007)
File- Halliburton Sperry Drilling Services/BP OCSG-32306 Macondo Prospect Daily Operations Report. Excel MC252 001 ST00BP00 Sperry Rpt 008A (BP MDL2179VOL000001-007)
File- Halliburton Sperry Drilling Services/BP OCSG-32306 Macondo Prospect Daily Operations Report. Excel MC252 001 ST00BP00 Sperry Rpt 009 (BP MDL2179VOL000001-007)
File- Halliburton Sperry Drilling Services/BP OCSG-32306 Macondo Prospect Daily Operations Report. Excel MC252 001 ST00BP00 Sperry Rpt 009A (BP MDL2179VOL000001-007)
File- Halliburton Sperry Drilling Services/BP OCSG-32306 Macondo Prospect Daily Operations Report. Excel MC252 001 ST00BP00 Sperry Rpt 010 (BP MDL2179VOL000001-007)
File- Halliburton Sperry Drilling Services/BP OCSG-32306 Macondo Prospect Daily Operations Report. Excel MC252 001 ST00BP00 Sperry Rpt 010A (BP MDL2179VOL000001-007)
File- Halliburton Sperry Drilling Services/BP OCSG-32306 Macondo Prospect Daily Operations Report. Excel MC252 001 ST00BP00 Sperry Rpt 011 (BP MDL2179VOL000001-007)
File- Halliburton Sperry Drilling Services/BP OCSG-32306 Macondo Prospect Daily Operations Report. Excel MC252 001 ST00BP00 Sperry Rpt 011A (BP MDL2179VOL000001-007)
File- Halliburton Sperry Drilling Services/BP OCSG-32306 Macondo Prospect Daily Operations Report. Excel MC252 001 ST00BP00 Sperry Rpt 012 (BP MDL2179VOL000001-007)
File- Halliburton Sperry Drilling Services/BP OCSG-32306 Macondo Prospect Daily Operations Report. Excel MC252 001 ST00BP00 Sperry Rpt 012A (BP MDL2179VOL000001-007)
File- Halliburton Sperry Drilling Services/BP OCSG-32306 Macondo Prospect Daily Operations Report. Excel MC252 001 ST00BP00 Sperry Rpt 013 (BP MDL2179VOL000001-007)
File- Halliburton Sperry Drilling Services/BP OCSG-32306 Macondo Prospect Daily Operations Report. Excel MC252 001 ST00BP00 Sperry Rpt 013A (BP MDL2179VOL000001-007)
File- Halliburton Sperry Drilling Services/BP OCSG-32306 Macondo Prospect Daily Operations Report. Excel MC252 001 ST00BP00 Sperry Rpt 014 (BP MDL2179VOL000001-007)
File- Halliburton Sperry Drilling Services/BP OCSG-32306 Macondo Prospect Daily Operations Report. Excel MC252 001 ST00BP00 Sperry Rpt 014A (BP MDL2179VOL000001-007)
File- Halliburton Sperry Drilling Services/BP OCSG-32306 Macondo Prospect Daily Operations Report. Excel MC252 001 ST00BP00 Sperry Rpt 015 (BP MDL2179VOL000001-007)
File- Halliburton Sperry Drilling Services/BP OCSG-32306 Macondo Prospect Daily Operations Report. Excel MC252 001 ST00BP00 Sperry Rpt 015A (BP MDL2179VOL000001-007)
File- Halliburton Sperry Drilling Services/BP OCSG-32306 Macondo Prospect Daily Operations Report. Excel MC252 001 ST00BP00 Sperry Rpt 016 (BP MDL2179VOL000001-007)
File- Halliburton Sperry Drilling Services/BP OCSG-32306 Macondo Prospect Daily Operations Report. Excel MC252 001 ST00BP00 Sperry Rpt 016A (BP MDL2179VOL000001-007)
File- Halliburton Sperry Drilling Services/BP OCSG-32306 Macondo Prospect Daily Operations Report. Excel MC252 001 ST00BP00 Sperry Rpt 017 (BP MDL2179VOL000001-007)
File- Halliburton Sperry Drilling Services/BP OCSG-32306 Macondo Prospect Daily Operations Report. Excel MC252 001 ST00BP00 Sperry Rpt 017A (BP MDL2179VOL000001-007)
File- Halliburton Sperry Drilling Services/BP OCSG-32306 Macondo Prospect Daily Operations Report. Excel MC252 001 ST00BP00 Sperry Rpt 018 (BP MDL2179VOL000001-007)
File- Halliburton Sperry Drilling Services/BP OCSG-32306 Macondo Prospect Daily Operations Report. Excel MC252 001 ST00BP00 Sperry Rpt 018A (BP MDL2179VOL000001-007)
File- Halliburton Sperry Drilling Services/BP OCSG-32306 Macondo Prospect Daily Operations Report. Excel MC252 001 ST00BP00 Sperry Rpt 019 (BP MDL2179VOL000001-007)
File- Halliburton Sperry Drilling Services/BP OCSG-32306 Macondo Prospect Daily Operations Report. Excel MC252 001 ST00BP00 Sperry Rpt 019A (BP MDL2179VOL000001-007)
File- Halliburton Sperry Drilling Services/BP OCSG-32306 Macondo Prospect Daily Operations Report. Excel MC252 001 ST00BP00 Sperry Rpt 020 (BP MDL2179VOL000001-007)
File- Halliburton Sperry Drilling Services/BP OCSG-32306 Macondo Prospect Daily Operations Report. Excel MC252 001 ST00BP00 Sperry Rpt 020A (BP MDL2179VOL000001-007)
File- Halliburton Sperry Drilling Services/BP OCSG-32306 Macondo Prospect Daily Operations Report. Excel MC252 001 ST00BP00 Sperry Rpt 021 (BP MDL2179VOL000001-007)
File- Halliburton Sperry Drilling Services/BP OCSG-32306 Macondo Prospect Daily Operations Report. Excel MC252 001 ST00BP00 Sperry Rpt 021A (BP MDL2179VOL000001-007)
File- Halliburton Sperry Drilling Services/BP OCSG-32306 Macondo Prospect Daily Operations Report. Excel MC252 001 ST00BP00 Sperry Rpt 022 (BP MDL2179VOL000001-007)
File- Halliburton Sperry Drilling Services/BP OCSG-32306 Macondo Prospect Daily Operations Report. Excel MC252 001 ST00BP00 Sperry Rpt 022A (BP MDL2179VOL000001-007)
File- Halliburton Sperry Drilling Services/BP OCSG-32306 Macondo Prospect Daily Operations Report. Excel MC252 001 ST00BP00 Sperry Rpt 023 (BP MDL2179VOL000001-007)
File- Halliburton Sperry Drilling Services/BP OCSG-32306 Macondo Prospect Daily Operations Report. Excel MC252 001 ST00BP00 Sperry Rpt 023A (BP MDL2179VOL000001-007)

File- Halliburton Sperry Drilling Services/BP OCSG-32306 Macondo Prospect Daily Operations Report. Excel MC252 001 ST00BP00 Sperry Rpt 024 (BP MDL2179VOL000001-007)
File- Halliburton Sperry Drilling Services/BP OCSG-32306 Macondo Prospect Daily Operations Report. Excel MC252 001 ST00BP00 Sperry Rpt 024A (BP MDL2179VOL000001-007)
File- Halliburton Sperry Drilling Services/BP OCSG-32306 Macondo Prospect Daily Operations Report. Excel MC252 001 ST00BP00 Sperry Rpt 025 (BP MDL2179VOL000001-007)
File- Halliburton Sperry Drilling Services/BP OCSG-32306 Macondo Prospect Daily Operations Report. Excel MC252 001 ST00BP00 Sperry Rpt 025A (BP MDL2179VOL000001-007)
File- Halliburton Sperry Drilling Services/BP OCSG-32306 Macondo Prospect Daily Operations Report. Excel MC252 001 ST00BP00 Sperry Rpt 026 (BP MDL2179VOL000001-007)
File- Halliburton Sperry Drilling Services/BP OCSG-32306 Macondo Prospect Daily Operations Report. Excel MC252 001 ST00BP00 Sperry Rpt 026A (BP MDL2179VOL000001-007)
File- Halliburton Sperry Drilling Services/BP OCSG-32306 Macondo Prospect Daily Operations Report. Excel MC252 001 ST00BP00 Sperry Rpt 027 (BP MDL2179VOL000001-007)
File- Halliburton Sperry Drilling Services/BP OCSG-32306 Macondo Prospect Daily Operations Report. Excel MC252 001 ST00BP00 Sperry Rpt 027A (BP MDL2179VOL000001-007)
File- Halliburton Sperry Drilling Services/BP OCSG-32306 Macondo Prospect Daily Operations Report. Excel MC252 001 ST00BP00 Sperry Rpt 028 (BP MDL2179VOL000001-007)
File- Halliburton Sperry Drilling Services/BP OCSG-32306 Macondo Prospect Daily Operations Report. Excel MC252 001 ST00BP00 Sperry Rpt 028A (BP MDL2179VOL000001-007)
File- Halliburton Sperry Drilling Services/BP OCSG-32306 Macondo Prospect Daily Operations Report. Excel MC252 001 ST00BP00 Sperry Rpt 029 (BP MDL2179VOL000001-007)
File- Halliburton Sperry Drilling Services/BP OCSG-32306 Macondo Prospect Daily Operations Report. Excel MC252 001 ST00BP00 Sperry Rpt 029A (BP MDL2179VOL000001-007)
File- Halliburton Sperry Drilling Services/BP OCSG-32306 Macondo Prospect Daily Operations Report. Excel MC252 001 ST00BP00 Sperry Rpt 030 (BP MDL2179VOL000001-007)
File- Halliburton Sperry Drilling Services/BP OCSG-32306 Macondo Prospect Daily Operations Report. Excel MC252 001 ST00BP00 Sperry Rpt 030A (BP MDL2179VOL000001-007)
File- Halliburton Sperry Drilling Services/BP OCSG-32306 Macondo Prospect Daily Operations Report. Excel MC252 001 ST00BP00 Sperry Rpt 031 (BP MDL2179VOL000001-007)
File- Halliburton Sperry Drilling Services/BP OCSG-32306 Macondo Prospect Daily Operations Report. Excel MC252 001 ST00BP00 Sperry Rpt 031A (BP MDL2179VOL000001-007)
File- Halliburton Sperry Drilling Services/BP OCSG-32306 Macondo Prospect Daily Operations Report. Excel MC252 001 ST00BP00 Sperry Rpt 032 (BP MDL2179VOL000001-007)
File- Halliburton Sperry Drilling Services/BP OCSG-32306 Macondo Prospect Daily Operations Report. Excel MC252 001 ST00BP00 Sperry Rpt 032A (BP MDL2179VOL000001-007)
File- Halliburton Sperry Drilling Services/BP OCSG-32306 Macondo Prospect Daily Operations Report. Excel MC252 001 ST00BP00 Sperry Rpt 033 (BP MDL2179VOL000001-007)
File- Halliburton Sperry Drilling Services/BP OCSG-32306 Macondo Prospect Daily Operations Report. Excel MC252 001 ST00BP00 Sperry Rpt 033A (BP MDL2179VOL000001-007)
File- Halliburton Sperry Drilling Services/BP OCSG-32306 Macondo Prospect Daily Operations Report. Excel MC252 001 ST00BP00 Sperry Rpt 034 (BP MDL2179VOL000001-007)
File- Halliburton Sperry Drilling Services/BP OCSG-32306 Macondo Prospect Daily Operations Report. Excel MC252 001 ST00BP00 Sperry Rpt 034A (BP MDL2179VOL000001-007)
File- Halliburton Sperry Drilling Services/BP OCSG-32306 Macondo Prospect Daily Operations Report. Excel MC252 001 ST00BP00 Sperry Rpt 035 (BP MDL2179VOL000001-007)
File- Halliburton Sperry Drilling Services/BP OCSG-32306 Macondo Prospect Daily Operations Report. Excel MC252 001 ST00BP00 Sperry Rpt 035A (BP MDL2179VOL000001-007)
File- Halliburton Sperry Drilling Services/BP OCSG-32306 Macondo Prospect Daily Operations Report. Excel MC252 001 ST00BP00 Sperry Rpt 036 (BP MDL2179VOL000001-007)
File- Halliburton Sperry Drilling Services/BP OCSG-32306 Macondo Prospect Daily Operations Report. Excel MC252 001 ST00BP00 Sperry Rpt 036A (BP MDL2179VOL000001-007)
File- Halliburton Sperry Drilling Services/BP OCSG-32306 Macondo Prospect Daily Operations Report. Excel MC252 001 ST00BP00 Sperry Rpt 037 (BP MDL2179VOL000001-007)
File- Halliburton Sperry Drilling Services/BP OCSG-32306 Macondo Prospect Daily Operations Report. Excel MC252 001 ST00BP00 Sperry Rpt 037A (BP MDL2179VOL000001-007)
File- Halliburton Sperry Drilling Services/BP OCSG-32306 Macondo Prospect Daily Operations Report. Excel MC252 001 ST00BP00 Sperry Rpt 038 (BP MDL2179VOL000001-007)
File- Halliburton Sperry Drilling Services/BP OCSG-32306 Macondo Prospect Daily Operations Report. Excel MC252 001 ST00BP00 Sperry Rpt 038A (BP MDL2179VOL000001-007)
File- Halliburton Sperry Drilling Services/BP OCSG-32306 Macondo Prospect Daily Operations Report. Excel MC252 001 ST00BP00 Sperry Rpt 039 (BP MDL2179VOL000001-007)
File- Halliburton Sperry Drilling Services/BP OCSG-32306 Macondo Prospect Daily Operations Report. Excel MC252 001 ST00BP00 Sperry Rpt 039A (BP MDL2179VOL000001-007)
File- Halliburton Sperry Drilling Services/BP OCSG-32306 Macondo Prospect Daily Operations Report. Excel MC252 001 ST00BP00 Sperry Rpt 040 (BP MDL2179VOL000001-007)
File- Halliburton Sperry Drilling Services/BP OCSG-32306 Macondo Prospect Daily Operations Report. Excel MC252 001 ST00BP00 Sperry Rpt 040A (BP MDL2179VOL000001-007)
File- Halliburton Sperry Drilling Services/BP OCSG-32306 Macondo Prospect Daily Operations Report. Excel MC252 001 ST00BP00 Sperry Rpt 041 (BP MDL2179VOL000001-007)

File- Halliburton Sperry Drilling Services/BP OCSG-32306 Macondo Prospect Daily Operations Report. Excel MC252 001 ST00BP00 Sperry Rpt 041A (BP MDL2179VOL000001-007)
File- Halliburton Sperry Drilling Services/BP OCSG-32306 Macondo Prospect Daily Operations Report. Excel MC252 001 ST00BP00 Sperry Rpt 042 (BP MDL2179VOL000001-007)
File- Halliburton Sperry Drilling Services/BP OCSG-32306 Macondo Prospect Daily Operations Report. Excel MC252 001 ST00BP00 Sperry Rpt 042A (BP MDL2179VOL000001-007)
File- Halliburton Sperry Drilling Services/BP OCSG-32306 Macondo Prospect Daily Operations Report. Excel MC252 001 ST00BP00 Sperry Rpt 043 (BP MDL2179VOL000001-007)
File- Halliburton Sperry Drilling Services/BP OCSG-32306 Macondo Prospect Daily Operations Report. Excel MC252 001 ST00BP00 Sperry Rpt 043A (BP MDL2179VOL000001-007)
File- Halliburton Sperry Drilling Services, BP Exploration & Production Summary: OCS-G 32306 001 ST00BP00 & BP01 Mississippi Canyon Block 252 surface data logging and pore pressure prediction services. MS Word MC252_001_ST00BP01_EOWR (BP MDL2179VOL000001-007)
File- Sperry Drilling Services ZOI / Show Report for Well: OCS-G-32306 001 ST00BP01 Mississippi Canyon 252 No1 ST00BP01, Prepared By Josph Keith. Excel MC252_001_ST00BP00_ZOI_A (BP MDL2179VOL000001-007)
File- End-User License Agreement Supplied by Halliburton Under Rights of Sublicense from Larson Software Technology, Inc. pdf HalliburtonLogViewerPro9.50_EndUserLicense (BP MDL2179VOL000001-007)
Halliburton Log Viewer Pro V9.5.0 Release Notes and Installation / Operation Instructions.pdf HalliburtonLogViewerPro9.50_ReleaseNotes (BP MDL2179VOL000001-007)
Installation Link for Installing Halliburton Log Viewer Pro9.50. Install Wizard HalliburtonLogViewerPro950Install (BP MDL2179VOL000001-007)
Instructions for Installing Halliburton Log Viewer Pro9.50. pdf InstallingHalliburtonLogViewerPro9.50 (BP MDL2179VOL000001-007)
MC252_001_ST00BP00_1MD_COMBO_LOG (BP MDL2179VOL000001-007)
MC252_001_ST00BP00_1MD_ENGINEERING_LOG (BP MDL2179VOL000001-007)
MC252_001_ST00BP00_1TVD_PRESSURE_LOG (BP MDL2179VOL000001-007)
MC252_001_ST00BP00_5MD_COMBO_LOG (BP MDL2179VOL000001-007)
File- Sperry Drilling Services BP Macondo Mississippi Canyon 252 No.1 Daily Operations Report - AM.Excel MC252_001_ST00BP00_MudlogRpt_01_08Oct09 (BP MDL2179VOL000001-008)
File- Sperry Drilling Services BP Macondo Mississippi Canyon 252 No.1 Daily Operations Report - AM.Excel MC252_001_ST00BP00_MudlogRpt_02_09Oct09 (BP MDL2179VOL000001-008)
File- Sperry Drilling Services BP Macondo Mississippi Canyon 252 No.1 Daily Operations Report - AM.Excel MC252_001_ST00BP00_MudlogRpt_03_10Oct09 (BP MDL2179VOL000001-008)
File- Sperry Drilling Services BP Macondo Mississippi Canyon 252 No.1 Daily Operations Report - AM.Excel MC252_001_ST00BP00_MudlogRpt_04_11Oct09 (BP MDL2179VOL000001-008)
File- Sperry Drilling Services BP Macondo Mississippi Canyon 252 No.1 Daily Operations Report - AM.Excel MC252_001_ST00BP00_MudlogRpt_05_12Oct09 (BP MDL2179VOL000001-008)
File- Sperry Drilling Services BP Macondo Mississippi Canyon 252 No.1 Daily Operations Report - AM.Excel MC252_001_ST00BP00_MudlogRpt_06_13Oct09 (BP MDL2179VOL000001-008)
File- Sperry Drilling Services BP Macondo Mississippi Canyon 252 No.1 Daily Operations Report - AM.Excel MC252_001_ST00BP00_MudlogRpt_07_14Oct09 (BP MDL2179VOL000001-008)
File- Sperry Drilling Services BP Macondo Mississippi Canyon 252 No.1 Daily Operations Report - AM.Excel MC252_001_ST00BP00_MudlogRpt_08_15Oct09 (BP MDL2179VOL000001-008)
File- Sperry Drilling Services BP Macondo Mississippi Canyon 252 No.1 Daily Operations Report - AM.Excel MC252_001_ST00BP00_MudlogRpt_10_17Oct09 (BP MDL2179VOL000001-008)
File- Sperry Drilling Services BP Macondo Mississippi Canyon 252 No.1 Daily Operations Report - AM.Excel MC252_001_ST00BP00_MudlogRpt_11_18Oct09 (BP MDL2179VOL000001-008)
File- Sperry Drilling Services BP Macondo Mississippi Canyon 252 No.1 Daily Operations Report - AM.Excel MC252_001_ST00BP00_MudlogRpt_12_19Oct09 (BP MDL2179VOL000001-008)
File- Sperry Drilling Services BP Macondo Mississippi Canyon 252 No.1 Daily Operations Report - AM.Excel MC252_001_ST00BP00_MudlogRpt_13_20Oct09 (BP MDL2179VOL000001-008)
File- Sperry Drilling Services BP Macondo Mississippi Canyon 252 No.1 Daily Operations Report - AM.Excel MC252_001_ST00BP00_MudlogRpt_14_21Oct09 (BP MDL2179VOL000001-008)
File- Sperry Drilling Services BP Macondo Mississippi Canyon 252 No.1 Daily Operations Report - AM.Excel MC252_001_ST00BP00_MudlogRpt_15_22Oct09 (BP MDL2179VOL000001-008)
File- Sperry Drilling Services BP Macondo Mississippi Canyon 252 No.1 Daily Operations Report - AM.Excel MC252_001_ST00BP00_MudlogRpt_16_23Oct09 (BP MDL2179VOL000001-008)
File- Sperry Drilling Services BP Macondo Mississippi Canyon 252 No.1 Daily Operations Report - AM.Excel MC252_001_ST00BP00_MudlogRpt_17_24Oct09 (BP MDL2179VOL000001-008)
File- Sperry Drilling Services BP Macondo Mississippi Canyon 252 No.1 Daily Operations Report - AM.Excel MC252_001_ST00BP00_MudlogRpt_18_25Oct09 (BP MDL2179VOL000001-008)
File- Sperry Drilling Services BP Macondo Mississippi Canyon 252 No.1 Daily Operations Report - AM.Excel MC252_001_ST00BP00_MudlogRpt_19_26Oct09 (BP MDL2179VOL000001-008)
File- Sperry Drilling Services BP Macondo Mississippi Canyon 252 No.1 Daily Operations Report - AM.Excel MC252_001_ST00BP00_MudlogRpt_20_27Oct09 (BP MDL2179VOL000001-008)
File- Sperry Drilling Services BP Macondo Mississippi Canyon 252 No.1 Daily Operations Report - AM.Excel MC252_001_ST00BP00_MudlogRpt_21_28Oct09 (BP MDL2179VOL000001-008)
File- Sperry Drilling Services BP Macondo Mississippi Canyon 252 No.1 Daily Operations Report - AM.Excel MC252_001_ST00BP00_MudlogRpt_22_29Oct09 (BP MDL2179VOL000001-008)

APPENDIX F. FACTS AND DATA WE CONSIDERED IN FORMING OUR OPINIONS

File- Sperry Drilling Services BP Macondo Mississippi Canyon 252 No.1 Daily Operations Report - AM.Excel MC252_001_ST00BP00_MudlogRpt_23_30Oct09 (BP MDL2179VOL000001-008)
File- Sperry Drilling Services BP Macondo Mississippi Canyon 252 No.1 Daily Operations Report - AM.Excel MC252_001_ST00BP00_MudlogRpt_24_31Oct09 (BP MDL2179VOL000001-008)
File- Sperry Drilling Services BP Macondo Mississippi Canyon 252 No.1 Daily Operations Report - AM.Excel MC252_001_ST00BP00_MudlogRpt_25_01Nov09 (BP MDL2179VOL000001-008)
File- Halliburton Sperry Drilling Services/Surface Data Logging Systems, Well Summary BP Exploration & Production Inc. Macondo Prospect OCS-G 32306 001 ST00BP00 Mississippi Canyon Blk. 252 RIG: TRANSOCEAN MARIANAS. MS Word MC252_001_ST00BP00_END_OF_WELL_REPORT (BP MDL2179VOL000001-008)
File- End-User License Agreement Supplied by Halliburton Under Rights of Sublicense from Larson Software Technology, Inc. pdf HalliburtonLogViewerPro9.50_EndUserLicense (BP MDL2179VOL000001-008)
File- Halliburton Log Viewer Pro V9.5.0 Release Notes and Installation / Operation Instructions.pdf HalliburtonLogViewerPro9.50_ReleaseNotes (BP MDL2179VOL000001-008)
File- Installation Link for Installing Halliburton Log Viewer Pro9.50. Install Wizard HalliburtonLogViewerPro950Install (BP MDL2179VOL000001-008)
File- Instructions for Installing Halliburton Log Viewer Pro9.50. pdf InstallingHalliburtonLogViewerPro9.50 (BP MDL2179VOL000001-008)
MC252_001_ST00BP00_1MD_COMBO (BP MDL2179VOL000001-008)
MC252_001_ST00BP00_1MD_ENGINEERING (BP MDL2179VOL000001-008)
MC252_001_ST00BP00_1TVD_COMBO (BP MDL2179VOL000001-008)
MC252_001_ST00BP00_5MD_COMBO (BP MDL2179VOL000001-008)
MC252_001_ST00BP00_5TVD_COMBO (BP MDL2179VOL000001-008)
MC252_001_ST00BP00_TVD_PRESSURE (BP MDL2179VOL000001-008)
BP Shallow Hazard April 2010 Compared to Baseline from TGS 2000 3D Survey.pdf macondo_hr_april28_V3 (BP MDL2179VOL000001-009)
BP EXPLORATION Memorandum SUBJECT: MC 252 Post Blowout 2HR ReViewer of Relief Well Locations. MS Word MC252_HR2D_Memo1 (BP MDL2179VOL000001-009)
BP America Multibeam Backscatter Map; Site Specific Survey of Proposed A & B Wells Macondo Prospect Block 252 (OCS-G-32306) Mississippi Canyon Area. pdf 084083_WELL_SITE Backscatter (BP MDL2179VOL000001-009)
Color Shaded Bathymetry Map; Site Specific Survey of Proposed A & B Wells Macondo Prospect Block 252 (OCS-G-32306) Mississippi Canyon Area. pdf 084083_WELL_SITE Bathy (BP MDL2179VOL000001-009)
Gradient Map; Site Specific Survey of Proposed A & B Wells Macondo Prospect Block 252 (OCS-G-32306) Mississippi Canyon Area. pdf 084083_WELL_SITE Gradient (BP MDL2179VOL000001-009)
ARCHAEOLOGICAL & HAZARD MAP; Site Specific Survey of Proposed A & B Wells Macondo Prospect Block 252 (OCS-G-32306) Mississippi Canyon Area. pdf 084083_WELL_SITE Hazard (BP MDL2179VOL000001-009)
Isopach Map; Site Specific Survey of Proposed A & B Wells Macondo Prospect Block 252 (OCS-G-32306) Mississippi Canyon Area.pdf 084083_WELL_SITE Isopach (BP MDL2179VOL000001-009)
Side Scan Sonar Mosaic Map; Site Specific Survey of Proposed A & B Wells Macondo Prospect Block 252 (OCS-G-32306) Mississippi Canyon Area.pdf 084083_WELL_SITE Mosaic (BP MDL2179VOL000001-009)
Site Specific Archaeological and Hazard Study "Macondo Prospect" Blocks 252 (OCS-G-32306) and 253 (OCS-G-24062) Mississippi Canyon Area.pdf 084083-094742-BP_SiteSpec-Report_Final (BP MDL2179VOL000001-009)
BP Shallow Hazards Assessment Proposed Macondo Exploration Well MC 252 #1 Surface Location in Block 252 (OCS-G-32306) Mississippi Canyon Area Gulf of Mexico.pdf MacondoSHA_with_Plates (BP MDL2179VOL000001-009)
BP Site Clearance Narrative Proposed MC252 "A" Location Block 252, OCS-G-32306 Mississippi Canyon Area Gulf of Mexico.pdf MC252A-EP-Final-Feb2009_V1 (BP MDL2179VOL000001-009)
Fugro Geoservices Inc. Shallow Hazards Assessment Rigel Project Blocks 252, 296 and Vicinity OCS-G-18207 and OCS-G-21164 Mississippi Canyon Area Gulf of Mexico.pdf OSG-SHALLOW_ HAZARD_ SURVEY_ MC_ 252_296 (BP MDL2179VOL000001-009)
Structure Outline Archaeological Survey Folder.MS Word Structure Outline (BP MDL2179VOL000001-009)
Comprehensive Analysis Disclaimer for Index Subject to the Terms and Conditions Agreed Upon Between and the Company.pdf Disclaimer (BP MDL2179VOL000001-010)
Enclosed CD Data OverViewer, Field Final Report.pdf Field_Final_Report_CD_Data_OverViewer (BP MDL2179VOL000001-010)
Comprehensive Analysis Disclaimer Subject to the Terms and Conditions Agreed Upon Between and the Company.pdf Disclaimer (BP MDL2179VOL000001-010)
BP Exploration & Production, Inc. Well Name OCS-G 32306 001 ST00BP01 Field Name Mississippi Canyon 252; Modular Formation Dynamics Tester Complete Report.pdf Report Cover (BP MDL2179VOL000001-010)
Field Final Report Table of Contents.pdf Table Of Contents (BP MDL2179VOL000001-010)
Section 1 Written Comments Cover Page.pdf 1__Written_Comments (BP MDL2179VOL000001-010)
Written Comments Field Remarks.pdf Written_Comments (BP MDL2179VOL000001-010)
Optical Fluid Analysis Summary with Optical Analysis Table.pdf Written_Comments_DFA (BP MDL2179VOL000001-010)

Pretest Pressure Analysis Radial and/or Spherical Flow.pdf Written_Comments_Radial_Spherical_Flow (BP MDL2179VOL000001-010)
Zone Tops Table.pdf Zone Tops Table (BP MDL2179VOL000001-010)
Section 2 Fluid Gradients Cover Page.pdf 2__Fluid_Gradients (BP MDL2179VOL000001-010)
Pressure Gradients Chart, Well OCS-G 32306 001 ST00BP01.pdf Pressure Gradients.pdf (BP MDL2179VOL000001-010)
Section 3 Pressure Results Summary and Pretest Pressure Listing Cover Page.pdf 3__ Pressure_Results (BP MDL2179VOL000001-010)
Pretest Formation Pressure Quality Grading Description Table.pdf Formation_Pressure_Quality_Grading_Description (BP MDL2179VOL000001-010)
Pump Out Summary Table.pdf PO Summary Table (BP MDL2179VOL000001-010)
Test Point Summary Table.pdf Test Point Summary Table (BP MDL2179VOL000001-010)
Test Point Table.pdf Test Point Table (BP MDL2179VOL000001-010)
Section 4 Well/Job Data Cover Page.pdf 4__ Well_Job_Data (BP MDL2179VOL000001-010)
Field Print Header Modular Formation Dynamics Tester for Well OCS-G 32306 001 ST00BP01.pdf Field_Print_Header (BP MDL2179VOL000001-010)
Field Print Remarks Run Number 1 for Well OCS-G 32306 001 ST00BP01.pdf Field_Print_Remarks (BP MDL2179VOL000001-010)
Field Print Remarks Depth Summary Listing - Depth System Equipment for Well OCS-G 32306 001 ST00BP01.pdf Field_Print_Remarks_Depth (BP MDL2179VOL000001-010)
Sample Summary Point 1 for Well OCS-G 32306 001 ST00BP01.pdf Field_Print_Sample_Sum_1 (BP MDL2179VOL000001-010)
Sample Summary Point 2 for Well OCS-G 32306 001 ST00BP01.pdf Field_Print_Sample_Sum_2 (BP MDL2179VOL000001-010)
Sample Summary Point 3 for Well OCS-G 32306 001 ST00BP01.pdf Field_Print_Sample_Sum_3 (BP MDL2179VOL000001-010)
Field Print Tool Sketch Equipment Description for Well OCS-G 32306 001 ST00BP01.pdf Field_Print_Tool_Sketch (BP MDL2179VOL000001-010)
Inclinometry Tables, Source : Well Assumed Vertical for Well OCS-G 32306 001 ST00BP01.pdf Inclinometry Tables (BP MDL2179VOL000001-010)
Well Path Plots Graphs for Well OCS-G 32306 001 ST00BP01.pdf Well Path Plots (BP MDL2179VOL000001-010)
Section 5 Pressure vs. Depth Displays Cover Page.pdf 5__Pressure_vs_Depth_Displays (BP MDL2179VOL000001-010)
OverViewer Pressure Mobility Color by Quality Chart for Well OCS-G 32306 001 ST00BP01.pdf OverViewer__Pressure_Mobility_Color_by_Quality (BP MDL2179VOL000001-010)
OverViewer Hydrostatic Pressure Color by Descent Chart for Well OCS-G 32306 001 ST00BP01.pdf OverViewer_Hydrostatic_Pressure_Color_by_Descent (BP MDL2179VOL000001-010)
OverViewer Pressure Mobility Color by PO Chart for Well OCS-G 32306 001 ST00BP01.pdf for Well OCS-G 32306 001 ST00BP01.pdf OverViewer_Pressure_Mobility_Color_by_PO (BP MDL2179VOL000001-010)
Zone 1-3 Pressure Mobility Color by Quality Chart for Well OCS-G 32306 001 ST00BP01.pdf Zone_1-3_Pressure_Mobility_Color_by_Quality (BP MDL2179VOL000001-010)
Zone 4 Pressure Mobility Color by Quality Chart for Well OCS-G 32306 001 ST00BP01.pdf Zone_4_Pressure_Mobility_Color_by_Quality (BP MDL2179VOL000001-010)
Zone 5 Pressure Mobility Color by Quality Chart for Well OCS-G 32306 001 ST00BP01.pdf Zone_5_Pressure_Mobility_Color_by_Quality (BP MDL2179VOL000001-010)
Zone 5 Pressure Mobility Color by Quality Gradient Chart for Well OCS-G 32306 001 ST00BP01.pdf Zone_5_Pressure_Mobility_Color_by_Quality_Gradient (BP MDL2179VOL000001-010)
Section 6 Optical Fluid Analysis Cover Page.pdf 6__Optical_Fluid_Analysis (BP MDL2179VOL000001-010)
Comments Page about Optical Fluid Analysis Summary and Optical Density Evaluation.pdf Comments_DFA (BP MDL2179VOL000001-010)
Header Page Optical Density Displays File 143 - Test 13 18123.93 (md) - 18113 (tvd).pdf F143T13__Header (BP MDL2179VOL000001-010)
Dual LFA Analysis Plot File 143 Test 13 18123.93 ft (MD) 18113.00 ft (TVD) Graph and Event Table for Well OCS-G 32306 001 ST00BP01.pdf. F143T13__LFA__Display (BP MDL2179VOL000001-010)
Methane & Oil Channel Data - LFA Graph for Well OCS-G 32306 001 ST00BP01.pdf F143T13__LFA_Analysis (BP MDL2179VOL000001-010)
LFA Optical Density and GOR Plot for Well OCS-G 32306 001 ST00BP01.pdf F143T13_Field_Print_GOR_LFA (BP MDL2179VOL000001-010)
LFA2 Optical Density and GOR Plot for Well OCS-G 32306 001 ST00BP01.pdf F143T13_Field_Print_GOR_LFA2 (BP MDL2179VOL000001-010)
Header Page Optical Density Displays File 144 - Test 15 18085.97 (md) - 18075.04 (tvd).pdf F144T15__Header (BP MDL2179VOL000001-010)

APPENDIX F. FACTS AND DATA WE CONSIDERED IN FORMING OUR OPINIONS

Dual LFA Analysis Plot File 144 Test 15 18085.97 ft (MD) 18075.04 ft (TVD) Chart for Well OCS-G 32306 001 ST00BP01.pdf F144T15__LFA__Display (BP MDL2179VOL000001-010)
Methane & Oil Channel Data - LFA for Well OCS-G 32306 001 ST00BP01.pdf F144T15__LFA_Analysis (BP MDL2179VOL000001-010)
LFA Optical Density and GOR Plot for Well OCS-G 32306 001 ST00BP01.pdf F144T15_Field_Print_GOR_LFA (BP MDL2179VOL000001-010)
LFA2 Optical Density and GOR Plot for Well OCS-G 32306 001 ST00BP01.pdf F144T15_Field_Print_GOR_LFA2 (BP MDL2179VOL000001-010)
Header Page Optical Density Displays File 147 - Test 20 18142 (md) - 18131.07 (tvd) for Well OCS-G 32306 001 ST00BP01.pdf F147T20__Header (BP MDL2179VOL000001-010)
Dual LFA Analysis Plot File 147 Test 20 18142.00 ft (MD) 18131.07 ft (TVD)F147T20__LFA__Display for Well OCS-G 32306 001 ST00BP01.pdf F147T20__LFA__Display (BP MDL2179VOL000001-010)
Methane & Oil Channel Data - LFA for Well OCS-G 32306 001 ST00BP01.pdf F147T20__LFA_Analysis (BP MDL2179VOL000001-010)
LFA Optical Density and GOR Plot for Well OCS-G 32306 001 ST00BP01.pdf F147T20_Field_Print_GOR_LFA (BP MDL2179VOL000001-010)
LFA2 Optical Density and GOR Plot for Well OCS-G 32306 001 ST00BP01.pdf F147T20_Field_Print_GOR_LFA2 (BP MDL2179VOL000001-010)
Pump Out Summary Table for Well OCS-G 32306 001 ST00BP01.pdf PO Summary Table (BP MDL2179VOL000001-010)
Section 7 Reference Data Cover Page.pdf 7__Reference_Data (BP MDL2179VOL000001-010)
MDT Pretest Interpretation ReViewer Plot.pdf a__Pretest_Interpretation (BP MDL2179VOL000001-010)
Excess Pressure Definition and Flow Chart.pdf b__Excess_Pressure (BP MDL2179VOL000001-010)
DCS MDT Analysis Report Package.pdf c__Geosolution_Complete_Report (BP MDL2179VOL000001-010)
MDT Optical Fluid Density LFA Oil and Gas sample evaluation before lab results.pdf d__GeoSolution_LFA_Oil (BP MDL2179VOL000001-010)
MDT Optical Fluid Density LFA GAS Oil and Gas sample evaluation before lab results.pdf e__GeoSolution_LFA_GAS (BP MDL2179VOL000001-010)
MDT Optical Fluid Density Oil and Gas sample evaluation before lab results.pdf f__GeoSolution_OFA_Gas_Oil (BP MDL2179VOL000001-010)
Basic Data Channels Associated with the Tool: MDT, CHDT, & Dual-Packer Table.pdf g__Basic_Channel_Descriptions (BP MDL2179VOL000001-010)
More Basic Data Channels Associated with Tools: MDT, XPT Dual Probe, Horizontal & Gauge Temperature Channels Table.pdf h__Basic_Channel_Descriptions (BP MDL2179VOL000001-010)
Basic Data Channels Associated with the Tool: MDT, CHDT, & Dual-Packer Table.pdf i__Basic_Channel_Descriptions (BP MDL2179VOL000001-010)
More Basic Data Channels Associated with Tools: MDT, XPT Dual Probe, Horizontal & Gauge Temperature Channels table.pdf j__Basic_Channel_Descriptions (BP MDL2179VOL000001-010)
More Basic Data Channels Associated with Tools: MDT Pump Out, CFA Table.pdf k__Basic_Channel_Descriptions (BP MDL2179VOL000001-010)
Section 8 Notes Page.pdf 8__Notes (BP MDL2179VOL000001-010)
Complete Report: BP Exploration & Production, Inc. OCS-G 32306 001 ST00BP01 Mississippi Canyon 252 Modular Formation Dynamics Tester.pdf Comprehensive_Analysis_Report (BP MDL2179VOL000001-010)
MDT Complete Report DVD Cover.pdf DVD_Label (BP MDL2179VOL000001-010)
Cover of Complete Report: BP Exploration & Production, Inc. OCS-G 32306 001 ST00BP01 Mississippi Canyon 252 Modular Formation Dynamics Tester.Windows Photo Viewer Report Cover (BP MDL2179VOL000001-010)
Cover of Complete Report: BP Exploration & Production, Inc. OCS-G 32306 001 ST00BP01 Mississippi Canyon 252 Modular Formation Dynamics Tester.pdf Report Cover (BP MDL2179VOL000001-010)
Labels.pdf Side_label (BP MDL2179VOL000001-010)
Field Print Remarks Run Number 1 for Well OCS-G 32306 001 ST00BP01.pdf Field_Print_Remarks (BP MDL2179VOL000001-010)
Field Print Remarks Run Number 1 for Well OCS-G 32306 001 ST00BP01.Windows Photo Viewer Field_Print_Remarks (BP MDL2179VOL000001-010)
Field Print Remarks Depth Summary Listing - Depth System Equipment for Well OCS-G 32306 001 ST00BP01.pdf Field_Print_Remarks_Depth (BP MDL2179VOL000001-010)
Field Print Remarks Depth Summary Listing - Depth System Equipment for Well OCS-G 32306 001 ST00BP01.Windows Photo Viewer Field_Print_Remarks_Depth (BP MDL2179VOL000001-010)
Fluid Gradient Table.Excel Fluid_Gradient_table (BP MDL2179VOL000001-010)
Pressure Gradients Table.pdf Pressure Gradients (BP MDL2179VOL000001-010)

Pump Out Summary Table for Well OCS-G 32306 001 ST00BP01.pdf PO Summary Table (BP MDL2179VOL000001-010)
Test Point Summary Table for Well OCS-G 32306 001 ST00BP01.pdf Test Point Summary Table (BP MDL2179VOL000001-010)
Test Point Table for Well OCS-G 32306 001 ST00BP01.pdf Test Point Table (BP MDL2179VOL000001-010)
Test Point Table for Well OCS-G 32306 001 ST00BP01.Excel test_point_table (BP MDL2179VOL000001-010)
Field Print Header Modular Formation Dynamics Tester for Well OCS-G 32306 001 ST00BP01.pdf Field_Print_Header (BP MDL2179VOL000001-010)
Field Print Header Modular Formation Dynamics Tester for Well OCS-G 32306 001 ST00BP01.Windows Photo Viewer Field_Print_Header (BP MDL2179VOL000001-010)
Field Print Tool Sketch Equipment Description for Well OCS-G 32306 001 ST00BP01.pdf Field_Print_Tool_Sketch (BP MDL2179VOL000001-010)
Field Print Tool Sketch Equipment Description for Well OCS-G 32306 001 ST00BP01.Windows Photo Viewer Field_Print_Tool_Sketch (BP MDL2179VOL000001-010)
OverViewer Pressure Mobility Color by Quality Chart for Well OCS-G 32306 001 ST00BP01.pdf OverViewer__Pressure_Mobility_Color_by_Quality (BP MDL2179VOL000001-010)
OverViewer Hydrostatic Pressure Color by Descent Chart for Well OCS-G 32306 001 ST00BP01.pdf OverViewer_Hydrostatic_Pressure_Color_by_Descent (BP MDL2179VOL000001-010)
OverViewer Pressure Mobility Color by PO Chart for Well OCS-G 32306 001 ST00BP01.pdf for Well OCS-G 32306 001 ST00BP01.pdf OverViewer_Pressure_Mobility_Color_by_PO (BP MDL2179VOL000001-010)
Zone 1-3 Pressure Mobility Color by Quality Chart for Well OCS-G 32306 001 ST00BP01.pdf Zone_1-3_Pressure_Mobility_Color_by_Quality (BP MDL2179VOL000001-010)
Zone 4 Pressure Mobility Color by Quality Chart for Well OCS-G 32306 001 ST00BP01.pdf Zone_4_Pressure_Mobility_Color_by_Quality (BP MDL2179VOL000001-010)
Zone 5 Pressure Mobility Color by Quality Chart for Well OCS-G 32306 001 ST00BP01.pdf Zone_5_Pressure_Mobility_Color_by_Quality (BP MDL2179VOL000001-010)
Zone 5 Pressure Mobility Color by Quality Gradient Chart for Well OCS-G 32306 001 ST00BP01.pdf Zone_5_Pressure_Mobility_Color_by_Quality_Gradient (BP MDL2179VOL000001-010)
Sample Summary Point 1 for Well OCS-G 32306 001 ST00BP01.pdf Field_Print_Sample_Sum_1of3 (BP MDL2179VOL000001-010)
Sample Summary Point 1 for Well OCS-G 32306 001 ST00BP01.Windows Photo Viewer Field_Print_Sample_Sum_1of3 (BP MDL2179VOL000001-010)
Sample Summary Point 1 for Well OCS-G 32306 001 ST00BP01.Text Field_Print_Sample_Sum_1of3 (BP MDL2179VOL000001-010)
Sample Summary Point 2 for Well OCS-G 32306 001 ST00BP01.pdf Field_Print_Sample_Sum_2of3 (BP MDL2179VOL000001-010)
Sample Summary Point 2 for Well OCS-G 32306 001 ST00BP01.Windows Photo Viewer Field_Print_Sample_Sum_2of3 (BP MDL2179VOL000001-010)
Sample Summary Point 2 for Well OCS-G 32306 001 ST00BP01.Text Field_Print_Sample_Sum_2of3 (BP MDL2179VOL000001-010)
Sample Summary Point 3 for Well OCS-G 32306 001 ST00BP01.pdf Field_Print_Sample_Sum_3of3 (BP MDL2179VOL000001-010)
Sample Summary Point 3 for Well OCS-G 32306 001 ST00BP01.Windows Photo Viewer Field_Print_Sample_Sum_3of3 (BP MDL2179VOL000001-010)
Sample Summary Point 3 for Well OCS-G 32306 001 ST00BP01.Text Field_Print_Sample_Sum_3of3 (BP MDL2179VOL000001-010)
Field Print Test Point Graph.pdf Field_Print_Test_Point_Sum_1of2 (BP MDL2179VOL000001-010)
Field Print Test Point Graph.pdf Field_Print_Test_Point_Sum_2of2 (BP MDL2179VOL000001-010)
Comments Page about Optical Fluid Analysis Summary and Optical Density Evaluation.pdf Comments_DFA (BP MDL2179VOL000001-010)
Header Page Optical Density Displays File 143 - Test 13 18123.93 (md) - 18113 (tvd).pdf F143T13__Header (BP MDL2179VOL000001-010)
Dual LFA Analysis Plot File 143 Test 13 18123.93 ft (MD) 18113.00 ft (TVD) Graph and Event Table for Well OCS-G 32306 001 ST00BP01.pdf. F143T13__LFA__Display (BP MDL2179VOL000001-010)
Methane & Oil Channel Data - LFA Graph for Well OCS-G 32306 001 ST00BP01.pdf F143T13__LFA_Analysis (BP MDL2179VOL000001-010)
LFA Optical Density and GOR Plot for Well OCS-G 32306 001 ST00BP01.pdf F143T13_Field_Print_GOR_LFA (BP MDL2179VOL000001-010)
LFA2 Optical Density and GOR Plot for Well OCS-G 32306 001 ST00BP01.pdf F143T13_Field_Print_GOR_LFA2 (BP MDL2179VOL000001-010)
Header Page Optical Density Displays File 144 - Test 15 18085.97 (md) - 18075.04 (tvd).pdf F144T15__Header (BP MDL2179VOL000001-010)
Dual LFA Analysis Plot File 144 Test 15 18085.97 ft (MD) 18075.04 ft (TVD) Chart for Well OCS-G 32306 001 ST00BP01.pdf F144T15__LFA__Display (BP MDL2179VOL000001-010)
Methane & Oil Channel Data - LFA for Well OCS-G 32306 001 ST00BP01.pdf F144T15__LFA_Analysis (BP MDL2179VOL000001-010)

APPENDIX F. FACTS AND DATA WE CONSIDERED IN FORMING OUR OPINIONS

LFA Optical Density and GOR Plot for Well OCS-G 32306 001 ST00BP01.pdf F144T15_Field_Print_GOR_LFA (BP MDL2179VOL000001-010)
LFA2 Optical Density and GOR Plot for Well OCS-G 32306 001 ST00BP01.pdf F144T15_Field_Print_GOR_LFA2 (BP MDL2179VOL000001-010)
Header Page Optical Density Displays File 147 - Test 20 18142 (md) - 18131.07 (tvd) for Well OCS-G 32306 001 ST00BP01.pdf F147T20__Header (BP MDL2179VOL000001-010)
Dual LFA Analysis Plot File 147 Test 20 18142.00 ft (MD) 18131.07 ft (TVD)F147T20__LFA__Display for Well OCS-G 32306 001 ST00BP01.pdf F147T20__LFA__Display (BP MDL2179VOL000001-010)
Methane & Oil Channel Data - LFA for Well OCS-G 32306 001 ST00BP01.pdf F147T20__LFA_Analysis (BP MDL2179VOL000001-010)
LFA Optical Density and GOR Plot for Well OCS-G 32306 001 ST00BP01.pdf F147T20_Field_Print_GOR_LFA (BP MDL2179VOL000001-010)
LFA2 Optical Density and GOR Plot for Well OCS-G 32306 001 ST00BP01.pdf F147T20_Field_Print_GOR_LFA2 (BP MDL2179VOL000001-010)
Pump Out Summary Table.pdf PO Summary Table (BP MDL2179VOL000001-010)
Polaris Plots Results.Excel Polaris_Plots_Results (BP MDL2179VOL000001-010)
Pressure Vs Time Plot : File 136 Test 1 18120.90 ft (MD) 18109.97 ft (TVD) for Well OCS-G 32306 001 ST00BP01.pdf Pretest_F136T1_BRD1_1 (BP MDL2179VOL000001-010)
Flow Regime Identification Plot : File 136 Test 1 18120.90 ft (MD) 18109.97 ft (TVD) for Well OCS-G 32306 001 ST00BP01.pdf Pretest_F136T1_BRD1_2 (BP MDL2179VOL000001-010)
Pressure Vs Time Plot : File 137 Test 4 18122.97 ft (MD) 18112.05 ft (TVD) for Well OCS-G 32306 001 ST00BP01.pdf Pretest_F137T4_BRD1_1 (BP MDL2179VOL000001-010)
Pressure Vs Time Plot : File 137 Test 4 18122.97 ft (MD) 18112.05 ft (TVD) for Well OCS-G 32306 001 ST00BP01.pdf Pretest_F137T4_BRD1_2 (BP MDL2179VOL000001-010)
Flow Regime Identification Plot : File 137 Test 4 18122.97 ft (MD) 18112.05 ft (TVD)for Well OCS-G 32306 001 ST00BP01.pdf Pretest_F137T4_BRD1_3 (BP MDL2179VOL000001-010)
Pressure Vs Time Plot : File 138 Test 6 18123.88 ft (MD) 18112.95 ft (TVD) for Well OCS-G 32306 001 ST00BP01.pdf Pretest_F138T6_BRD1_1 (BP MDL2179VOL000001-010)
Pressure Vs Time Plot : File 138 Test 6 18123.88 ft (MD) 18112.95 ft (TVD) for Well OCS-G 32306 001 ST00BP01.pdf Pretest_F138T6_BRD1_2 (BP MDL2179VOL000001-010)
Flow Regime Identification Plot : File 138 Test 6 18123.88 ft (MD) 18112.95 ft (TVD) for Well OCS-G 32306 001 ST00BP01.pdf Pretest_F138T6_BRD1_3 (BP MDL2179VOL000001-010)
Pressure Vs Time Plot : File 139 Test 7 18126.01 ft (MD) 18115.08 ft (TVD) for Well OCS-G 32306 001 ST00BP01.pdf Pretest_F139T7_BRD1_1 (BP MDL2179VOL000001-010)
Flow Regime Identification Plot : File 139 Test 7 18126.01 ft (MD) 18115.08 ft (TVD) for Well OCS-G 32306 001 ST00BP01.pdf Pretest_F139T7_BRD1_2 (BP MDL2179VOL000001-010)
Pressure Vs Time Plot : File 140 Test 8 18132.97 ft (MD) 18122.04 ft (TVD) for Well OCS-G 32306 001 ST00BP01.pdf Pretest_F140T8_BRD1_1 (BP MDL2179VOL000001-010)
Flow Regime Identification Plot : File 140 Test 8 18132.97 ft (MD) 18122.04 ft (TVD) for Well OCS-G 32306 001 ST00BP01.pdf Pretest_F140T8_BRD1_2 (BP MDL2179VOL000001-010)
Pressure Vs Time Plot : File 141 Test 9 18129.90 ft (MD) 18118.97 ft (TVD) for Well OCS-G 32306 001 ST00BP01.pdf Pretest_F141T9_BRD1_1 (BP MDL2179VOL000001-010)
Flow Regime Identification Plot : File 141 Test 9 18129.90 ft (MD) 18118.97 ft (TVD) for Well OCS-G 32306 001 ST00BP01.pdf Pretest_F141T9_BRD1_2 (BP MDL2179VOL000001-010)
Pressure Vs Time Plot : File 143 Test 10 18123.93 ft (MD) 18113.00 ft (TVD) for Well OCS-G 32306 001 ST00BP01.pdf Pretest_F143T10_PQRD2_1 (BP MDL2179VOL000001-010)
Pressure Vs Time Plot : File 143 Test 10 18123.93 ft (MD) 18113.00 ft (TVD) for Well OCS-G 32306 001 ST00BP01.pdf Pretest_F143T10_PQRD2_2 (BP MDL2179VOL000001-010)
Flow Regime Identification Plot : File 143 Test 10 18123.93 ft (MD) 18113.00 ft (TVD)for Well OCS-G 32306 001 ST00BP01.pdf Pretest_F143T10_PQRD2_3 (BP MDL2179VOL000001-010)
Pressure Vs Time Plot : File 143 Test 13 18123.93 ft (MD) 18113.00 ft (TVD) for Well OCS-G 32306 001 ST00BP01.pdf Pretest_F143T13_PQRD2_1 (BP MDL2179VOL000001-010)
Pressure Vs Time Plot : File 143 Test 13 18123.93 ft (MD) 18113.00 ft (TVD) for Well OCS-G 32306 001 ST00BP01.pdf Pretest_F143T13_PQRD2_2 (BP MDL2179VOL000001-010)
Flow Regime Identification Plot : File 143 Test 13 18123.93 ft (MD) 18113.00 ft (TVD) for Well OCS-G 32306 001 ST00BP01.pdf Pretest_F143T13_PQRD2_3 (BP MDL2179VOL000001-010)
Pressure Vs Time Plot : File 143 Test 13 18123.93 ft (MD) 18113.00 ft (TVD) for Well OCS-G 32306 001 ST00BP01.pdf Pretest_F143T13po_PQRD2_1 (BP MDL2179VOL000001-010)
Pressure Vs Time Plot : File 143 Test 13 18123.93 ft (MD) 18113.00 ft (TVD) for Well OCS-G 32306 001 ST00BP01.pdf Pretest_F143T13po_PQRD2_2 (BP MDL2179VOL000001-010)
Flow Regime Identification Plot : File 143 Test 13 18123.93 ft (MD) 18113.00 ft (TVD) for Well OCS-G 32306 001 ST00BP01.pdf Pretest_F143T13po_PQRD2_3 (BP MDL2179VOL000001-010)
Pressure Vs Time Plot : File 144 Test 14 18085.97 ft (MD) 18075.04 ft (TVD) for Well OCS-G 32306 001 ST00BP01.pdf Pretest_F144T14_PQRD2_1 (BP MDL2179VOL000001-010)
Pressure Vs Time Plot : File 144 Test 14 18085.97 ft (MD) 18075.04 ft (TVD) for Well OCS-G 32306 001 ST00BP01.pdf Pretest_F144T14_PQRD2_2 (BP MDL2179VOL000001-010)
Flow Regime Identification Plot : File 144 Test 14 18085.97 ft (MD) 18075.04 ft (TVD) for Well OCS-G 32306 001 ST00BP01.pdf Pretest_F144T14_PQRD2_3 (BP MDL2179VOL000001-010)

Pressure Vs Time Plot : File 144 Test 15 18085.97 ft (MD) 18075.04 ft (TVD) for Well OCS-G 32306 001 ST00BP01.pdf Pretest_F144T15_PQRD2_1 (BP MDL2179VOL000001-010)
Pressure Vs Time Plot : File 144 Test 15 18085.97 ft (MD) 18075.04 ft (TVD) for Well OCS-G 32306 001 ST00BP01.pdf Pretest_F144T15_PQRD2_2
Flow Regime Identification Plot : File 144 Test 15 18085.97 ft (MD) 18075.04 ft (TVD) for Well OCS-G 32306 001 ST00BP01.pdf Pretest_F144T15_PQRD2_3
Pressure Vs Time Plot : File 144 Test 15 18085.97 ft (MD) 18075.04 ft (TVD) for Well OCS-G 32306 001 ST00BP01.pdf Pretest_F144T15po_PQRD2_1
Pressure Vs Time Plot : File 144 Test 15 18085.97 ft (MD) 18075.04 ft (TVD) for Well OCS-G 32306 001 ST00BP01.pdf Pretest_F144T15po_PQRD2_2 (BP MDL2179VOL000001-010)
Flow Regime Identification Plot : File 144 Test 15 18085.97 ft (MD) 18075.04 ft (TVD) for Well OCS-G 32306 001 ST00BP01.pdf Pretest_F144T15po_PQRD2_3 (BP MDL2179VOL000001-010)
Pressure Vs Time Plot : File 145 Test 16 18140.02 ft (MD) 18129.09 ft (TVD) for Well OCS-G 32306 001 ST00BP01.pdf Pretest_F145T16_PQRD2_1 (BP MDL2179VOL000001-010)
Flow Regime Identification Plot : File 145 Test 16 18140.02 ft (MD) 18129.09 ft (TVD) for Well OCS-G 32306 001 ST00BP01.pdf Pretest_F145T16_PQRD2_2 (BP MDL2179VOL000001-010)
Pressure Vs Time Plot : File 146 Test 17 18144.93 ft (MD) 18134.00 ft (TVD) for Well OCS-G 32306 001 ST00BP01.pdf Pretest_F146T17_PQRD2_1 (BP MDL2179VOL000001-010)
Flow Regime Identification Plot : File 146 Test 17 18144.93 ft (MD) 18134.00 ft (TVD) for Well OCS-G 32306 001 ST00BP01.pdf Pretest_F146T17_PQRD2_2 (BP MDL2179VOL000001-010)
Pressure Vs Time Plot : File 147 Test 18 18142.00 ft (MD) 18131.07 ft (TVD) for Well OCS-G 32306 001 ST00BP01.pdf Pretest_F147T18_PQRD2_1 (BP MDL2179VOL000001-010)
Pressure Vs Time Plot : File 147 Test 18 18142.00 ft (MD) 18131.07 ft (TVD) for Well OCS-G 32306 001 ST00BP01.pdf Pretest_F147T18_PQRD2_2 (BP MDL2179VOL000001-010)
Flow Regime Identification Plot : File 147 Test 18 18142.00 ft (MD) 18131.07 ft (TVD) for Well OCS-G 32306 001 ST00BP01.pdf Pretest_F147T18_PQRD2_3 (BP MDL2179VOL000001-010)
Pressure Vs Time Plot : File 147 Test 18 18142.00 ft (MD) 18131.07 ft (TVD) for Well OCS-G 32306 001 ST00BP01.pdf Pretest_F147T18po_PQRD2_1 (BP MDL2179VOL000001-010)
Pressure Vs Time Plot : File 147 Test 18 18142.00 ft (MD) 18131.07 ft (TVD) for Well OCS-G 32306 001 ST00BP01.pdf Pretest_F147T18po_PQRD2_2 (BP MDL2179VOL000001-010)
Flow Regime Identification Plot : File 147 Test 18 18142.00 ft (MD) 18131.07 ft (TVD) for Well OCS-G 32306 001 ST00BP01.pdf Pretest_F147T18po_PQRD2_3 (BP MDL2179VOL000001-010)
Pressure Vs Time Plot : File 147 Test 20 18142.00 ft (MD) 18131.07 ft (TVD)for Well OCS-G 32306 001 ST00BP01.pdf Pretest_F147T20_PQRD2_1 (BP MDL2179VOL000001-010)
Pressure Vs Time Plot : File 147 Test 20 18142.00 ft (MD) 18131.07 ft (TVD) for Well OCS-G 32306 001 ST00BP01.pdf Pretest_F147T20_PQRD2_2 (BP MDL2179VOL000001-010)
Flow Regime Identification Plot : File 147 Test 20 18142.00 ft (MD) 18131.07 ft (TVD) for Well OCS-G 32306 001 ST00BP01.pdf Pretest_F147T20_PQRD2_3 (BP MDL2179VOL000001-010)
Pressure Vs Time Plot : File 148 Test 21 18156.92 ft (MD) 18145.99 ft (TVD) for Well OCS-G 32306 001 ST00BP01.pdf Pretest_F148T21_BRD1_1 (BP MDL2179VOL000001-010)
Flow Regime Identification Plot : File 148 Test 21 18156.92 ft (MD) 18145.99 ft (TVD) for Well OCS-G 32306 001 ST00BP01.pdf Pretest_F148T21_BRD1_2 (BP MDL2179VOL000001-010)
Pressure Vs Time Plot : File 149 Test 22 18166.97 ft (MD) 18156.04 ft (TVD) for Well OCS-G 32306 001 ST00BP01.pdf Pretest_F149T22_BRD1_1 (BP MDL2179VOL000001-010)
Flow Regime Identification Plot : File 149 Test 22 18166.97 ft (MD) 18156.04 ft (TVD) for Well OCS-G 32306 001 ST00BP01.pdf Pretest_F149T22_BRD1_2 (BP MDL2179VOL000001-010)
Pressure Vs Time Plot : File 150 Test 23 18179.97 ft (MD) 18169.04 ft (TVD) for Well OCS-G 32306 001 ST00BP01.pdf Pretest_F150T23_BRD1_1 (BP MDL2179VOL000001-010)
Flow Regime Identification Plot : File 150 Test 23 18179.97 ft (MD) 18169.04 ft (TVD) for Well OCS-G 32306 001 ST00BP01.pdf Pretest_F150T23_BRD1_2 (BP MDL2179VOL000001-010)
Pressure Vs Time Plot : File 151 Test 25 18129.86 ft (MD) 18118.93 ft (TVD) for Well OCS-G 32306 001 ST00BP01.pdf Pretest_F151T25_BRD1_1 (BP MDL2179VOL000001-010)
Pressure Vs Time Plot : File 151 Test 25 18129.86 ft (MD) 18118.93 ft (TVD) for Well OCS-G 32306 001 ST00BP01.pdf Pretest_F151T25_BRD1_2 (BP MDL2179VOL000001-010)
Flow Regime Identification Plot : File 151 Test 25 18129.86 ft (MD) 18118.93 ft (TVD) for Well OCS-G 32306 001 ST00BP01.pdf Pretest_F151T25_BRD1_3 (BP MDL2179VOL000001-010)
Pressure Vs Time Plot : File 152 Test 28 18081.92 ft (MD) 18070.99 ft (TVD) for Well OCS-G 32306 001 ST00BP01.pdf Pretest_F152T28_BRD1_1 (BP MDL2179VOL000001-010)
Pressure Vs Time Plot : File 152 Test 28 18081.92 ft (MD) 18070.99 ft (TVD) for Well OCS-G 32306 001 ST00BP01.pdf Pretest_F152T28_BRD1_2 (BP MDL2179VOL000001-010)
Flow Regime Identification Plot : File 152 Test 28 18081.92 ft (MD) 18070.99 ft (TVD) for Well OCS-G 32306 001 ST00BP01.pdf Pretest_F152T28_BRD1_3 (BP MDL2179VOL000001-010)
Pressure Vs Time Plot : File 153 Test 31 18068.98 ft (MD) 18058.06 ft (TVD) for Well OCS-G 32306 001 ST00BP01.pdf Pretest_F153T31_BRD1_1 (BP MDL2179VOL000001-010)
Pressure Vs Time Plot : File 153 Test 31 18068.98 ft (MD) 18058.06 ft (TVD) for Well OCS-G 32306 001 ST00BP01.pdf Pretest_F153T31_BRD1_2 (BP MDL2179VOL000001-010)
Flow Regime Identification Plot : File 153 Test 31 18068.98 ft (MD) 18058.06 ft (TVD) for Well OCS-G 32306 001 ST00BP01.pdf Pretest_F153T31_BRD1_3 (BP MDL2179VOL000001-010)
Pressure Vs Time Plot : File 157 Test 1 18076.73 ft (MD) 18065.80 ft (TVD) for Well OCS-G 32306 001 ST00BP01.pdf Pretest_F157T1_PQRD2_1 (BP MDL2179VOL000001-010)

APPENDIX F. FACTS AND DATA WE CONSIDERED IN FORMING OUR OPINIONS

Flow Regime Identification Plot : File 157 Test 1 18076.73 ft (MD) 18065.80 ft (TVD) for Well OCS-G 32306 001 ST00BP01.pdf Pretest_F157T1_PQRD2_2 (BP MDL2179VOL000001-010)
Pressure Vs Time Plot : File 158 Test 2 17976.02 ft (MD) 17965.10 ft (TVD) for Well OCS-G 32306 001 ST00BP01.pdf Pretest_F158T2_PQRD2_1 (BP MDL2179VOL000001-010)
Flow Regime Identification Plot : File 158 Test 2 17976.02 ft (MD) 17965.10 ft (TVD) for Well OCS-G 32306 001 ST00BP01.pdf Pretest_F158T2_PQRD2_2 (BP MDL2179VOL000001-010)
Pressure Vs Time Plot : File 159 Test 3 17976.89 ft (MD) 17965.97 ft (TVD) for Well OCS-G 32306 001 ST00BP01.pdf Pretest_F159T3_PQRD2_1 (BP MDL2179VOL000001-010)
Flow Regime Identification Plot : File 159 Test 3 17976.89 ft (MD) 17965.97 ft (TVD) for Well OCS-G 32306 001 ST00BP01.pdf Pretest_F159T3_PQRD2_2 (BP MDL2179VOL000001-010)
Pressure Vs Time Plot : File 160 Test 4 17974.98 ft (MD) 17964.06 ft (TVD) for Well OCS-G 32306 001 ST00BP01.pdf Pretest_F160T4_PQRD2_1 (BP MDL2179VOL000001-010)
Flow Regime Identification Plot : File 160 Test 4 17974.98 ft (MD) 17964.06 ft (TVD) for Well OCS-G 32306 001 ST00BP01.pdf Pretest_F160T4_PQRD2_2 (BP MDL2179VOL000001-010)
Pressure Vs Time Plot : File 162 Test 5 17805.03 ft (MD) 17794.12 ft (TVD) for Well OCS-G 32306 001 ST00BP01.pdf Pretest_F162T5_PQRD2_1 (BP MDL2179VOL000001-010)
Flow Regime Identification Plot : File 162 Test 5 17805.03 ft (MD) 17794.12 ft (TVD) for Well OCS-G 32306 001 ST00BP01.pdf Pretest_F162T5_PQRD2_2 (BP MDL2179VOL000001-010)
Pressure Vs Time Plot : File 163 Test 6 17805.94 ft (MD) 17795.03 ft (TVD) for Well OCS-G 32306 001 ST00BP01.pdf Pretest_F163T6_PQRD2_1 (BP MDL2179VOL000001-010)
Flow Regime Identification Plot : File 163 Test 6 17805.94 ft (MD) 17795.03 ft (TVD) for Well OCS-G 32306 001 ST00BP01.pdf Pretest_F163T6_PQRD2_2 (BP MDL2179VOL000001-010)
Pressure Vs Time Plot : File 164 Test 8 17807.00 ft (MD) 17796.09 ft (TVD) for Well OCS-G 32306 001 ST00BP01.pdf Pretest_F164T8_PQRD2_1 (BP MDL2179VOL000001-010)
Pressure Vs Time Plot : File 164 Test 8 17807.00 ft (MD) 17796.09 ft (TVD) for Well OCS-G 32306 001 ST00BP01.pdf Pretest_F164T8_PQRD2_2 (BP MDL2179VOL000001-010)
Flow Regime Identification Plot : File 164 Test 8 17807.00 ft (MD) 17796.09 ft (TVD) for Well OCS-G 32306 001 ST00BP01.pdf Pretest_F164T8_PQRD2_3 (BP MDL2179VOL000001-010)
Pressure Vs Time Plot : File 165 Test 9 17703.00 ft (MD) 17692.09 ft (TVD) for Well OCS-G 32306 001 ST00BP01.pdf Pretest_F165T9_PQRD2_1 (BP MDL2179VOL000001-010)
Pressure Vs Time Plot : File 166 Test 10 17705.82 ft (MD) 17694.91 ft (TVD) for Well OCS-G 32306 001 ST00BP01.pdf Pretest_F166T10_PQRD2_1 (BP MDL2179VOL000001-010)
Pressure Vs Time Plot : File 167 Test 11 17701.03 ft (MD) 17690.12 ft (TVD) for Well OCS-G 32306 001 ST00BP01.pdf Pretest_F167T11_PQRD2_1 (BP MDL2179VOL000001-010)
Inclinometry Tables, Source : Well Assumed Vertical for Well OCS-G 32306 001 ST00BP01.pdf Inclinometry Tables (BP MDL2179VOL000001-010)
Well Path Plots Graphs for Well OCS-G 32306 001 ST00BP01.pdf Well Path Plots (BP MDL2179VOL000001-010)
Field Print Header Modular Formation Dynamics Tester for Well OCS-G 32306 001 ST00BP01.pdf Field_Print_Header (BP MDL2179VOL000001-010)
Field Print PDS Segments.Excel Field_Print_PDS_Segments (BP MDL2179VOL000001-010)
Field Print Remarks Run Number 1 for Well OCS-G 32306 001 ST00BP01.pdf Field_Print_Remarks (BP MDL2179VOL000001-010)
Field Print Remarks Depth Summary Listing - Depth System Equipment for Well OCS-G 32306 001 ST00BP01.pdf Field_Print_Remarks_Depth (BP MDL2179VOL000001-010)
Sample Summary Point 1 for Well OCS-G 32306 001 ST00BP01.pdf Field_Print_Sample_Sum_1 (BP MDL2179VOL000001-010)
Sample Summary Point 2 for Well OCS-G 32306 001 ST00BP01.pdf Field_Print_Sample_Sum_2 (BP MDL2179VOL000001-010)
Sample Summary Point 3 for Well OCS-G 32306 001 ST00BP01.pdf Field_Print_Sample_Sum_3 (BP MDL2179VOL000001-010)
Field Print Tool Sketch Equipment Description for Well OCS-G 32306 001 ST00BP01.pdf Field_Print_Tool_Sketch (BP MDL2179VOL000001-010)
Inclinometry Tables, Source : Well Assumed Vertical for Well OCS-G 32306 001 ST00BP01.pdf Inclinometry Tables (BP MDL2179VOL000001-010)
Comments Page about Optical Fluid Analysis Summary and Optical Density Evaluation.pdf Comments_DFA (BP MDL2179VOL000001-010)
Header Page Optical Density Displays File 143 - Test 13 18123.93 (md) - 18113 (tvd).pdf F143T13__Header (BP MDL2179VOL000001-010)
Dual LFA Analysis Plot File 143 Test 13 18123.93 ft (MD) 18113.00 ft (TVD) Graph and Event Table for Well OCS-G 32306 001 ST00BP01.pdf. F143T13__LFA__Display (BP MDL2179VOL000001-010)
Methane & Oil Channel Data - LFA Graph for Well OCS-G 32306 001 ST00BP01.pdf F143T13__LFA_Analysis (BP MDL2179VOL000001-010)
LFA Optical Density and GOR Plot for Well OCS-G 32306 001 ST00BP01.pdf F143T13_Field_Print_GOR_LFA (BP MDL2179VOL000001-010)
LFA2 Optical Density and GOR Plot for Well OCS-G 32306 001 ST00BP01.pdf F143T13_Field_Print_GOR_LFA2 (BP MDL2179VOL000001-010)
Header Page Optical Density Displays File 144 - Test 15 18085.97 (md) - 18075.04 (tvd).pdf F144T15__Header (BP MDL2179VOL000001-010)

APPENDIX F. FACTS AND DATA WE CONSIDERED IN FORMING OUR OPINIONS

Dual LFA Analysis Plot File 144 Test 15 18085.97 ft (MD) 18075.04 ft (TVD) Chart for Well OCS-G 32306 001 ST00BP01.pdf F144T15__LFA__Display (BP MDL2179VOL000001-010)
Methane & Oil Channel Data - LFA for Well OCS-G 32306 001 ST00BP01.pdf F144T15__LFA_Analysis (BP MDL2179VOL000001-010)
LFA Optical Density and GOR Plot for Well OCS-G 32306 001 ST00BP01.pdf F144T15_Field_Print_GOR_LFA (BP MDL2179VOL000001-010)
LFA2 Optical Density and GOR Plot for Well OCS-G 32306 001 ST00BP01.pdf F144T15_Field_Print_GOR_LFA2 (BP MDL2179VOL000001-010)
Header Page Optical Density Displays File 147 - Test 20 18142 (md) - 18131.07 (tvd) for Well OCS-G 32306 001 ST00BP01.pdf F147T20__Header (BP MDL2179VOL000001-010)
Dual LFA Analysis Plot File 147 Test 20 18142.00 ft (MD) 18131.07 ft (TVD)F147T20__LFA__Display for Well OCS-G 32306 001 ST00BP01.pdf F147T20__LFA__Display (BP MDL2179VOL000001-010)
Methane & Oil Channel Data - LFA for Well OCS-G 32306 001 ST00BP01.pdf F147T20__LFA_Analysis (BP MDL2179VOL000001-010)
LFA Optical Density and GOR Plot for Well OCS-G 32306 001 ST00BP01.pdf F147T20_Field_Print_GOR_LFA (BP MDL2179VOL000001-010)
LFA2 Optical Density and GOR Plot for Well OCS-G 32306 001 ST00BP01.pdf F147T20_Field_Print_GOR_LFA2 (BP MDL2179VOL000001-010)
Field Print Event Summary.Windows Photo Viewer Field_Print_Event_Sum_F143T191 (BP MDL2179VOL000001-010)
Field Print Event Summary. Text Field_Print_Event_Sum_F143T191 (BP MDL2179VOL000001-010)
Field Print Event Summary.Windows Photo Viewer Field_Print_Event_Sum_F144T193 (BP MDL2179VOL000001-010)
Field Print Event Summary.Text Field_Print_Event_Sum_F144T193 (BP MDL2179VOL000001-010)
Field Print Event Summary.Windows Photo Viewer Field_Print_Event_Sum_F147T199 (BP MDL2179VOL000001-010)
Field Print Event Summary.Text Field_Print_Event_Sum_F147T199 (BP MDL2179VOL000001-010)
Pump Out Summary Table.pdf PO Summary Table (BP MDL2179VOL000001-010)
Pressure Vs Time Plot : File 136 Test 1 18120.90 ft (MD) 18109.97 ft (TVD) for Well OCS-G 32306 001 ST00BP01.Windows Photo Viewer Pretest_F136T1_BRD1_1 (BP MDL2179VOL000001-010)
Flow Regime Identification Plot : File 136 Test 1 18120.90 ft (MD) 18109.97 ft (TVD) for Well OCS-G 32306 001 ST00BP01.Windows Photo Viewer Pretest_F136T1_BRD1_2 (BP MDL2179VOL000001-010)
Pressure Vs Time Plot : File 137 Test 4 18122.97 ft (MD) 18112.05 ft (TVD) for Well OCS-G 32306 001 ST00BP01.Windows Photo Viewer Pretest_F137T4_BRD1_1 (BP MDL2179VOL000001-010)
Pressure Vs Time Plot : File 137 Test 4 18122.97 ft (MD) 18112.05 ft (TVD) for Well OCS-G 32306 001 ST00BP01.Windows Photo Viewer Pretest_F137T4_BRD1_2 (BP MDL2179VOL000001-010)
Flow Regime Identification Plot : File 137 Test 4 18122.97 ft (MD) 18112.05 ft (TVD)for Well OCS-G 32306 001 ST00BP01.Windows Photo Viewer Pretest_F137T4_BRD1_3 (BP MDL2179VOL000001-010)
Pressure Vs Time Plot : File 138 Test 6 18123.88 ft (MD) 18112.95 ft (TVD) for Well OCS-G 32306 001 ST00BP01.Windows Photo Viewer Pretest_F138T6_BRD1_1 (BP MDL2179VOL000001-010)
Pressure Vs Time Plot : File 138 Test 6 18123.88 ft (MD) 18112.95 ft (TVD) for Well OCS-G 32306 001 ST00BP01.Windows Photo Viewer Pretest_F138T6_BRD1_2 (BP MDL2179VOL000001-010)
Flow Regime Identification Plot : File 138 Test 6 18123.88 ft (MD) 18112.95 ft (TVD) for Well OCS-G 32306 001 ST00BP01.Windows Photo Viewer Pretest_F138T6_BRD1_3 (BP MDL2179VOL000001-010)
Pressure Vs Time Plot : File 139 Test 7 18126.01 ft (MD) 18115.08 ft (TVD) for Well OCS-G 32306 001 ST00BP01.Windows Photo Viewer Pretest_F139T7_BRD1_1 (BP MDL2179VOL000001-010)
Flow Regime Identification Plot : File 139 Test 7 18126.01 ft (MD) 18115.08 ft (TVD) for Well OCS-G 32306 001 ST00BP01.Windows Photo Viewer Pretest_F139T7_BRD1_2 (BP MDL2179VOL000001-010)
Pressure Vs Time Plot : File 140 Test 8 18132.97 ft (MD) 18122.04 ft (TVD) for Well OCS-G 32306 001 ST00BP01.Windows Photo Viewer Pretest_F140T8_BRD1_1 (BP MDL2179VOL000001-010)
Flow Regime Identification Plot : File 140 Test 8 18132.97 ft (MD) 18122.04 ft (TVD) for Well OCS-G 32306 001 ST00BP01.Windows Photo Viewer Pretest_F140T8_BRD1_2 (BP MDL2179VOL000001-010)
Pressure Vs Time Plot : File 141 Test 9 18129.90 ft (MD) 18118.97 ft (TVD) for Well OCS-G 32306 001 ST00BP01.Windows Photo Viewer Pretest_F141T9_BRD1_1 (BP MDL2179VOL000001-010)
Flow Regime Identification Plot : File 141 Test 9 18129.90 ft (MD) 18118.97 ft (TVD) for Well OCS-G 32306 001 ST00BP01.Windows Photo Viewer Pretest_F141T9_BRD1_2 (BP MDL2179VOL000001-010)
Pressure Vs Time Plot : File 143 Test 10 18123.93 ft (MD) 18113.00 ft (TVD) for Well OCS-G 32306 001 ST00BP01.Windows Photo Viewer Pretest_F143T10_PQRD2_1 (BP MDL2179VOL000001-010)
Pressure Vs Time Plot : File 143 Test 10 18123.93 ft (MD) 18113.00 ft (TVD) for Well OCS-G 32306 001 ST00BP01.Windows Photo Viewer Pretest_F143T10_PQRD2_2 (BP MDL2179VOL000001-010)
Flow Regime Identification Plot : File 143 Test 10 18123.93 ft (MD) 18113.00 ft (TVD)for Well OCS-G 32306 001 ST00BP01.Windows Photo Viewer Pretest_F143T10_PQRD2_3 (BP MDL2179VOL000001-010)
Pressure Vs Time Plot : File 143 Test 13 18123.93 ft (MD) 18113.00 ft (TVD) for Well OCS-G 32306 001 ST00BP01.Windows Photo Viewer Pretest_F143T13_PQRD2_1 (BP MDL2179VOL000001-010)
Pressure Vs Time Plot : File 143 Test 13 18123.93 ft (MD) 18113.00 ft (TVD) for Well OCS-G 32306 001 ST00BP01.Windows Photo Viewer Pretest_F143T13_PQRD2_2 (BP MDL2179VOL000001-010)

Flow Regime Identification Plot : File 143 Test 13 18123.93 ft (MD) 18113.00 ft (TVD) for Well OCS-G 32306 001 ST00BP01.Windows Photo Viewer Pretest_F143T13_PQRD2_3 (BP MDL2179VOL000001-010)
Pressure Vs Time Plot : File 143 Test 13 18123.93 ft (MD) 18113.00 ft (TVD) for Well OCS-G 32306 001 ST00BP01.Windows Photo Viewer Pretest_F143T13po_PQRD2_1 (BP MDL2179VOL000001-010)
Pressure Vs Time Plot : File 143 Test 13 18123.93 ft (MD) 18113.00 ft (TVD) for Well OCS-G 32306 001 ST00BP01.Windows Photo Viewer Pretest_F143T13po_PQRD2_2 (BP MDL2179VOL000001-010)
Flow Regime Identification Plot : File 143 Test 13 18123.93 ft (MD) 18113.00 ft (TVD) for Well OCS-G 32306 001 ST00BP01.Windows Photo Viewer Pretest_F143T13po_PQRD2_3 (BP MDL2179VOL000001-010)
Pressure Vs Time Plot : File 144 Test 14 18085.97 ft (MD) 18075.04 ft (TVD) for Well OCS-G 32306 001 ST00BP01.Windows Photo Viewer Pretest_F144T14_PQRD2_1 (BP MDL2179VOL000001-010)
Pressure Vs Time Plot : File 144 Test 14 18085.97 ft (MD) 18075.04 ft (TVD) for Well OCS-G 32306 001 ST00BP01.Windows Photo Viewer Pretest_F144T14_PQRD2_2 (BP MDL2179VOL000001-010)
Flow Regime Identification Plot : File 144 Test 14 18085.97 ft (MD) 18075.04 ft (TVD) for Well OCS-G 32306 001 ST00BP01.Windows Photo Viewer Pretest_F144T14_PQRD2_3 (BP MDL2179VOL000001-010)
Pressure Vs Time Plot : File 144 Test 15 18085.97 ft (MD) 18075.04 ft (TVD) for Well OCS-G 32306 001 ST00BP01.Windows Photo Viewer Pretest_F144T15_PQRD2_1 (BP MDL2179VOL000001-010)
Pressure Vs Time Plot : File 144 Test 15 18085.97 ft (MD) 18075.04 ft (TVD) for Well OCS-G 32306 001 ST00BP01.Windows Photo Viewer Pretest_F144T15_PQRD2_2 (BP MDL2179VOL000001-010)
Flow Regime Identification Plot : File 144 Test 15 18085.97 ft (MD) 18075.04 ft (TVD) for Well OCS-G 32306 001 ST00BP01.Windows Photo Viewer Pretest_F144T15_PQRD2_3 (BP MDL2179VOL000001-010)
Pressure Vs Time Plot : File 144 Test 15 18085.97 ft (MD) 18075.04 ft (TVD) for Well OCS-G 32306 001 ST00BP01.Windows Photo Viewer Pretest_F144T15po_PQRD2_1 (BP MDL2179VOL000001-010)
Pressure Vs Time Plot : File 144 Test 15 18085.97 ft (MD) 18075.04 ft (TVD) for Well OCS-G 32306 001 ST00BP01.Windows Photo Viewer Pretest_F144T15po_PQRD2_2 (BP MDL2179VOL000001-010)
Flow Regime Identification Plot : File 144 Test 15 18085.97 ft (MD) 18075.04 ft (TVD) for Well OCS-G 32306 001 ST00BP01.Windows Photo Viewer Pretest_F144T15po_PQRD2_3 (BP MDL2179VOL000001-010)
Pressure Vs Time Plot : File 145 Test 16 18140.02 ft (MD) 18129.09 ft (TVD) for Well OCS-G 32306 001 ST00BP01.Windows Photo Viewer Pretest_F145T16_PQRD2_1 (BP MDL2179VOL000001-010)
Flow Regime Identification Plot : File 145 Test 16 18140.02 ft (MD) 18129.09 ft (TVD) for Well OCS-G 32306 001 ST00BP01.Windows Photo Viewer Pretest_F145T16_PQRD2_2 (BP MDL2179VOL000001-010)
Pressure Vs Time Plot : File 146 Test 17 18144.93 ft (MD) 18134.00 ft (TVD) for Well OCS-G 32306 001 ST00BP01.Windows Photo Viewer Pretest_F146T17_PQRD2_1 (BP MDL2179VOL000001-010)
Flow Regime Identification Plot : File 146 Test 17 18144.93 ft (MD) 18134.00 ft (TVD) for Well OCS-G 32306 001 ST00BP01.Windows Photo Viewer Pretest_F146T17_PQRD2_2 (BP MDL2179VOL000001-010)
Pressure Vs Time Plot : File 147 Test 18 18142.00 ft (MD) 18131.07 ft (TVD) for Well OCS-G 32306 001 ST00BP01.Windows Photo Viewer Pretest_F147T18_PQRD2_1 (BP MDL2179VOL000001-010)
Pressure Vs Time Plot : File 147 Test 18 18142.00 ft (MD) 18131.07 ft (TVD) for Well OCS-G 32306 001 ST00BP01.Windows Photo Viewer Pretest_F147T18_PQRD2_2 (BP MDL2179VOL000001-010)
Flow Regime Identification Plot : File 147 Test 18 18142.00 ft (MD) 18131.07 ft (TVD) for Well OCS-G 32306 001 ST00BP01.Windows Photo Viewer Pretest_F147T18_PQRD2_3 (BP MDL2179VOL000001-010)
Pressure Vs Time Plot : File 147 Test 18 18142.00 ft (MD) 18131.07 ft (TVD) for Well OCS-G 32306 001 ST00BP01.Windows Photo Viewer Pretest_F147T18po_PQRD2_1 (BP MDL2179VOL000001-010)
Pressure Vs Time Plot : File 147 Test 18 18142.00 ft (MD) 18131.07 ft (TVD) for Well OCS-G 32306 001 ST00BP01.Windows Photo Viewer Pretest_F147T18po_PQRD2_2 (BP MDL2179VOL000001-010)
Flow Regime Identification Plot : File 147 Test 18 18142.00 ft (MD) 18131.07 ft (TVD) for Well OCS-G 32306 001 ST00BP01.Windows Photo Viewer Pretest_F147T18po_PQRD2_3 (BP MDL2179VOL000001-010)
Pressure Vs Time Plot : File 147 Test 20 18142.00 ft (MD) 18131.07 ft (TVD) for Well OCS-G 32306 001 ST00BP01.Windows Photo Viewer Pretest_F147T20_PQRD2_1 (BP MDL2179VOL000001-010)
Pressure Vs Time Plot : File 147 Test 20 18142.00 ft (MD) 18131.07 ft (TVD) for Well OCS-G 32306 001 ST00BP01.Windows Photo Viewer Pretest_F147T20_PQRD2_2 (BP MDL2179VOL000001-010)
Flow Regime Identification Plot : File 147 Test 20 18142.00 ft (MD) 18131.07 ft (TVD) for Well OCS-G 32306 001 ST00BP01.Windows Photo Viewer Pretest_F147T20_PQRD2_3 (BP MDL2179VOL000001-010)
Pressure Vs Time Plot : File 148 Test 21 18156.92 ft (MD) 18145.99 ft (TVD) for Well OCS-G 32306 001 ST00BP01.Windows Photo Viewer Pretest_F148T21_BRD1_1 (BP MDL2179VOL000001-010)
Flow Regime Identification Plot : File 148 Test 21 18156.92 ft (MD) 18145.99 ft (TVD) for Well OCS-G 32306 001 ST00BP01.Windows Photo Viewer Pretest_F148T21_BRD1_2 (BP MDL2179VOL000001-010)
Pressure Vs Time Plot : File 149 Test 22 18166.97 ft (MD) 18156.04 ft (TVD) for Well OCS-G 32306 001 ST00BP01.Windows Photo Viewer Pretest_F149T22_BRD1_1 (BP MDL2179VOL000001-010)
Flow Regime Identification Plot : File 149 Test 22 18166.97 ft (MD) 18156.04 ft (TVD) for Well OCS-G 32306 001 ST00BP01.Windows Photo Viewer Pretest_F149T22_BRD1_2 (BP MDL2179VOL000001-010)
Pressure Vs Time Plot : File 150 Test 23 18179.97 ft (MD) 18169.04 ft (TVD) for Well OCS-G 32306 001 ST00BP01.Windows Photo Viewer Pretest_F150T23_BRD1_1 (BP MDL2179VOL000001-010)
Flow Regime Identification Plot : File 150 Test 23 18179.97 ft (MD) 18169.04 ft (TVD) for Well OCS-G 32306 001 ST00BP01.Windows Photo Viewer Pretest_F150T23_BRD1_2 (BP MDL2179VOL000001-010)
Pressure Vs Time Plot : File 151 Test 25 18129.86 ft (MD) 18118.93 ft (TVD) for Well OCS-G 32306 001 ST00BP01.Windows Photo Viewer Pretest_F151T25_BRD1_1 (BP MDL2179VOL000001-010)
Pressure Vs Time Plot : File 151 Test 25 18129.86 ft (MD) 18118.93 ft (TVD) for Well OCS-G 32306 001 ST00BP01.Windows Photo Viewer Pretest_F151T25_BRD1_2 (BP MDL2179VOL000001-010)
Flow Regime Identification Plot : File 151 Test 25 18129.86 ft (MD) 18118.93 ft (TVD) for Well OCS-G 32306 001 ST00BP01.Windows Photo Viewer Pretest_F151T25_BRD1_3 (BP MDL2179VOL000001-010)

APPENDIX F. FACTS AND DATA WE CONSIDERED IN FORMING OUR OPINIONS

Pressure Vs Time Plot : File 152 Test 28 18081.92 ft (MD) 18070.99 ft (TVD) for Well OCS-G 32306 001 ST00BP01.Windows Photo Viewer Pretest_F152T28_BRD1_1 (BP MDL2179VOL000001-010)
Pressure Vs Time Plot : File 152 Test 28 18081.92 ft (MD) 18070.99 ft (TVD) for Well OCS-G 32306 001 ST00BP01.Windows Photo Viewer Pretest_F152T28_BRD1_2 (BP MDL2179VOL000001-010)
Flow Regime Identification Plot : File 152 Test 28 18081.92 ft (MD) 18070.99 ft (TVD) for Well OCS-G 32306 001 ST00BP01.Windows Photo Viewer Pretest_F152T28_BRD1_3 (BP MDL2179VOL000001-010)
Pressure Vs Time Plot : File 153 Test 31 18068.98 ft (MD) 18058.06 ft (TVD) for Well OCS-G 32306 001 ST00BP01.Windows Photo Viewer Pretest_F153T31_BRD1_1 (BP MDL2179VOL000001-010)
Pressure Vs Time Plot : File 153 Test 31 18068.98 ft (MD) 18058.06 ft (TVD) for Well OCS-G 32306 001 ST00BP01.Windows Photo Viewer Pretest_F153T31_BRD1_2 (BP MDL2179VOL000001-010)
Flow Regime Identification Plot : File 153 Test 31 18068.98 ft (MD) 18058.06 ft (TVD) for Well OCS-G 32306 001 ST00BP01.Windows Photo Viewer Pretest_F153T31_BRD1_3 (BP MDL2179VOL000001-010)
Pressure Vs Time Plot : File 157 Test 1 18076.73 ft (MD) 18065.80 ft (TVD) for Well OCS-G 32306 001 ST00BP01.Windows Photo Viewer Pretest_F157T1_PQRD2_1 (BP MDL2179VOL000001-010)
Flow Regime Identification Plot : File 157 Test 1 18076.73 ft (MD) 18065.80 ft (TVD) for Well OCS-G 32306 001 ST00BP01.Windows Photo Viewer Pretest_F157T1_PQRD2_2 (BP MDL2179VOL000001-010)
Pressure Vs Time Plot : File 158 Test 2 17976.02 ft (MD) 17965.10 ft (TVD) for Well OCS-G 32306 001 ST00BP01.Windows Photo Viewer Pretest_F158T2_PQRD2_1 (BP MDL2179VOL000001-010)
Flow Regime Identification Plot : File 158 Test 2 17976.02 ft (MD) 17965.10 ft (TVD) for Well OCS-G 32306 001 ST00BP01.Windows Photo Viewer Pretest_F158T2_PQRD2_2 (BP MDL2179VOL000001-010)
Pressure Vs Time Plot : File 159 Test 3 17976.89 ft (MD) 17965.97 ft (TVD) for Well OCS-G 32306 001 ST00BP01.Windows Photo Viewer Pretest_F159T3_PQRD2_1 (BP MDL2179VOL000001-010)
Flow Regime Identification Plot : File 159 Test 3 17976.89 ft (MD) 17965.97 ft (TVD) for Well OCS-G 32306 001 ST00BP01.Windows Photo Viewer Pretest_F159T3_PQRD2_2 (BP MDL2179VOL000001-010)
Pressure Vs Time Plot : File 160 Test 4 17974.98 ft (MD) 17964.06 ft (TVD) for Well OCS-G 32306 001 ST00BP01.Windows Photo Viewer Pretest_F160T4_PQRD2_1 (BP MDL2179VOL000001-010)
Flow Regime Identification Plot : File 160 Test 4 17974.98 ft (MD) 17964.06 ft (TVD) for Well OCS-G 32306 001 ST00BP01.Windows Photo Viewer Pretest_F160T4_PQRD2_2 (BP MDL2179VOL000001-010)
Pressure Vs Time Plot : File 162 Test 5 17805.03 ft (MD) 17794.12 ft (TVD) for Well OCS-G 32306 001 ST00BP01.Windows Photo Viewer Pretest_F162T5_PQRD2_1 (BP MDL2179VOL000001-010)
Flow Regime Identification Plot : File 162 Test 5 17805.03 ft (MD) 17794.12 ft (TVD) for Well OCS-G 32306 001 ST00BP01.Windows Photo Viewer Pretest_F162T5_PQRD2_2 (BP MDL2179VOL000001-010)
Pressure Vs Time Plot : File 163 Test 6 17805.94 ft (MD) 17795.03 ft (TVD) for Well OCS-G 32306 001 ST00BP01.Windows Photo Viewer Pretest_F163T6_PQRD2_1 (BP MDL2179VOL000001-010)
Flow Regime Identification Plot : File 163 Test 6 17805.94 ft (MD) 17795.03 ft (TVD) for Well OCS-G 32306 001 ST00BP01.Windows Photo Viewer Pretest_F163T6_PQRD2_2 (BP MDL2179VOL000001-010)
Pressure Vs Time Plot : File 164 Test 8 17807.00 ft (MD) 17796.09 ft (TVD) for Well OCS-G 32306 001 ST00BP01.Windows Photo Viewer Pretest_F164T8_PQRD2_1 (BP MDL2179VOL000001-010)
Pressure Vs Time Plot : File 164 Test 8 17807.00 ft (MD) 17796.09 ft (TVD) for Well OCS-G 32306 001 ST00BP01.Windows Photo Viewer Pretest_F164T8_PQRD2_2 (BP MDL2179VOL000001-010)
Flow Regime Identification Plot : File 164 Test 8 17807.00 ft (MD) 17796.09 ft (TVD) for Well OCS-G 32306 001 ST00BP01.Windows Photo Viewer Pretest_F164T8_PQRD2_3 (BP MDL2179VOL000001-010)
Pressure Vs Time Plot : File 165 Test 9 17703.00 ft (MD) 17692.09 ft (TVD) for Well OCS-G 32306 001 ST00BP01.Windows Photo Viewer Pretest_F165T9_PQRD2_1 (BP MDL2179VOL000001-010)
Pressure Vs Time Plot : File 166 Test 10 17705.82 ft (MD) 17694.91 ft (TVD) for Well OCS-G 32306 001 ST00BP01.Windows Photo Viewer Pretest_F166T10_PQRD2_1 (BP MDL2179VOL000001-010)
Pressure Vs Time Plot : File 167 Test 11 17701.03 ft (MD) 17690.12 ft (TVD) for Well OCS-G 32306 001 ST00BP01.Windows Photo Viewer Pretest_F167T11_PQRD2_1 (BP MDL2179VOL000001-010)
Directional Spreadsheet.Excel directional (BP MDL2179VOL000001-010)
WFTI Inclinometry List Table Graph.Windows Photo Viewer WFTI_Inclinometry_Table (BP MDL2179VOL000001-010)
WFTI Inclinometry List Table Graph.Text WFTI_Inclinometry_Table (BP MDL2179VOL000001-010)
Pressure Test Readings for Well OCS-G 32306-001-ST00BP01.Excel BP_MC252_OCSG_32306_001_ST00BP01_R1D4_ Pressures (BP MDL2179VOL000001-011)
Check Shot Report for BP Exploration and Production; Well: OCS-G 32306 001 ST00BP01; Job Ref. No. B0FO-00037.pdf BP_MC252_OCSG_32306_001_ST00BP01_R1D7_Check Shot Report (BP MDL2179VOL000001-011)
Check Shot Report for BP Exploration and Production; Well: OCS-G 32306 001 ST00BP01; Job Ref. No. B0FO-00037.Text BP_MC252_OCSG_32306_001_ST00BP01_R1D7_Check Shot Report (BP MDL2179VOL000001-011)
Vertical Seismic Profile Composite Display; Well: OCS-G 32306 001 ST00BP01.MS Word BP_MC252_OCSG_32306_001_ST00BP01_R1D7_Composite (BP MDL2179VOL000001-011)
Vertical Seismic Profile Composite Display; Well: OCS-G 32306 001 ST00BP01.Windows Photo Viewer BP_MC252_OCSG_32306_001_ST00BP01_R1D7_Composite (BP MDL2179VOL000001-011)
Synthetic Scismogram Geogram Display; Well: OCS-G 32306 001 ST00BP01.MS Word BP_MC252_OCSG_32306_001_ST00BP01_R1D7_GEOGRAM (BP MDL2179VOL000001-011)
Synthetic Scismogram Geogram Display; Well: OCS-G 32306 001 ST00BP01.Windows Photo Viewer BP_MC252_OCSG_32306_001_ST00BP01_R1D7_GEOGRAM (BP MDL2179VOL000001-011)
Check Shot Survey Velocity Cross Plot; Well: OCS-G 32306 001 ST00BP01.MS Word BP_MC252_OCSG_32306_001_ST00BP01_R1D7_Velocity Cross Plot (BP MDL2179VOL000001-011)

APPENDIX F. FACTS AND DATA WE CONSIDERED IN FORMING OUR OPINIONS

Check Shot Survey Velocity Cross Plot; Well: OCS-G 32306 001 ST00BP01.Windows Photo Viewer MS WordBP_MC252_OCSG_32306_001_ST00BP01_R1D7_Velocity Cross Plot (BP MDL2179VOL000001-011)
Vertical Seismic Profile Z-Axis Processing Steps; Well: OCS-G 32306 001 ST00BP01.MS Word BP_MC252_OCSG_32306_001_ST00BP01_R1D7_VSP Processing Steps (BP MDL2179VOL000001-011)
Vertical Seismic Profile Z-Axis Processing Steps; Well: OCS-G 32306 001 ST00BP01.Windows Photo Viewer BP_MC252_OCSG_32306_001_ST00BP01_R1D7_VSP Processing Steps (BP MDL2179VOL000001-011)
Vertical Seismic Profile Z-Axis Waveshape and Corridors; Well: OCS-G 32306 001 ST00BP01.MS Word BP_MC252_OCSG_32306_001_ST00BP01_R1D7_Waveshape Decon Corridor Stack (BP MDL2179VOL000001-011)
Vertical Seismic Profile Z-Axis Waveshape and Corridors; Well: OCS-G 32306 001 ST00BP01.Windows Photo Viewer BP_MC252_OCSG_32306_001_ST00BP01_R1D7_Waveshape Decon Corridor Stack (BP MDL2179VOL000001-011)
Q-Borehole Survey Report; Survey Type: ZOVSP; BP Exploration & Production, Inc.; Well: OCS-G 32306 001 ST00BP01.pdf BP_MC252_OCSG_32306_001_ST00BP01_R1D7_ZOVSP Field Print (BP MDL2179VOL000001-011)
BP Deepwater Development Data Checklist.Excel BP-Macondo_32306_001_BP01_DVD_Inventory (BP MDL2179VOL000001-011)
LogDataToolbox21 (BP MDL2179VOL000001-012)
PDSView311_setup (BP MDL2179VOL000001-012)
MC252 001 ST00BP00 Final Surveys 0ft to 9090ft MD Proj. to TD Survey Report.Excel BP-G-32306-001-ST00BP00-MC252-DD-Surveys (BP MDL2179VOL000001-012)
End of Well Report for Well: OCS-G 32306 001 ST00BP00.MS Word OBP-G-32306-001-ST00BP00-MC252-EOWR (BP MDL2179VOL000001-012)
\MDL2179VOL000070-003\00000_Macondo.layout (Page 1 of 88) (BP-MDL2179VOL000070-003)
\MDL2179VOL000070-003\00000_Macondo_Chuck.layout (Page 1 of 55) (BP-MDL2179VOL000070-003)
\MDL2179VOL000070-003\00000_Macondo_Composite_MC.layout (Page 1 of 31) (BP-MDL2179VOL000070-003)
\MDL2179VOL000070-003\00000_Macondo_Composite_MC_small.layout (Page 1 of 11) (BP-MDL2179VOL000070-003)
\MDL2179VOL000070-003\00000_Macondo_Correlation.layout (Page 1 of 28) (BP-MDL2179VOL000070-003)
\MDL2179VOL000070-003\00000_Macondo_Correlation_OH.layout (Page 1 of 29) (BP-MDL2179VOL000070-003)
\MDL2179VOL000070-003\00000_Macondo_Dips.layout (Page 1 of 76) (BP-MDL2179VOL000070-003)
\MDL2179VOL000070-003\00000_Macondo_final.layout (Page 1 of 88) (BP-MDL2179VOL000070-003)
\MDL2179VOL000070-003\00000_Macondo_Intersept.layout (Page 1 of 44) (BP-MDL2179VOL000070-003)
\MDL2179VOL000070-003\00000_Macondo_losses.layout (Page 1 of 58) (BP-MDL2179VOL000070-003)
\MDL2179VOL000070-003\00000_Macondo_losses_TD.layout (Page 1 of 56) (BP-MDL2179VOL000070-003)
\MDL2179VOL000070-003\00000_Macondo_lwd.layout (Page 1 of 50) (BP-MDL2179VOL000070-003)
\MDL2179VOL000070-003\00000_Macondo_lwd_marianas.layout (Page 1 of 24) (BP-MDL2179VOL000070-003)
\MDL2179VOL000070-003\00000_Macondo_lwd_print.layout (Page 1 of 28) (BP-MDL2179VOL000070-003)
\MDL2179VOL000070-003\00000_Macondo_lwd_rt.layout (Page 1 of 51) (BP-MDL2179VOL000070-003)
\MDL2179VOL000070-003\00000_Macondo_lwd_RXD.layout (Page 1 of 53) (BP-MDL2179VOL000070-003)
\MDL2179VOL000070-003\00000_Macondo_OBMI_calipers.layout (Page 1 of 19) (BP-MDL2179VOL000070-003)
\MDL2179VOL000070-003\00000_Macondo_Pressure.layout (Page 1 of 18) (BP-MDL2179VOL000070-003)
\MDL2179VOL000070-003\00000_Macondo_RQ.layout (Page 1 of 68) (BP-MDL2179VOL000070-003)
\MDL2179VOL000070-003\00000_Macondo_RSWC.layout (Page 1 of 77) (BP-MDL2179VOL000070-003)
\MDL2179VOL000070-003\00000_Macondo_short.layout (Page 1 of 75) (BP-MDL2179VOL000070-003)
\MDL2179VOL000070-003\00000_Macondo_Sonic.layout (Page 1 of 73) (BP-MDL2179VOL000070-003)
\MDL2179VOL000070-003\00000_Macondo_temperature.layout (Page 1 of 31) (BP-MDL2179VOL000070-003)
\MDL2179VOL000070-003\00000_Macondo_w_OBMI.layout (Page 1 of 95) (BP-MDL2179VOL000070-003)
\MDL2179VOL000070-003\00000_Macondo_w_OBMI1.layout (Page 1 of 26) (BP-MDL2179VOL000070-003)
\MDL2179VOL000070-003\00000bw_Macondo_shaleRes.layout (Page 1 of 159) (BP-MDL2179VOL000070-003)
\MDL2179VOL000070-003\00000bw_Macondo_shlow_sand_count.layout (Page 1 of 37) (BP-MDL2179VOL000070-003)
\MDL2179VOL000070-003\00000bw_Macondo_shlow_sand_count_GS.layout (Page 1 of 14) (BP-MDL2179VOL000070-003)
\MDL2179VOL000070-003\00000bw_MacondoALL_shlow_sand_count.layout (Page 1 of 35) (BP-MDL2179VOL000070-003)
\MDL2179VOL000070-003\00000bw_sands_Macondo2.layout (Page 1 of 42) (BP-MDL2179VOL000070-003)
\MDL2179VOL000070-003\0000_Macondo_IMAGE_AND_DIP.layout (Page 1 of 67) (BP-MDL2179VOL000070-003)
\MDL2179VOL000070-003\00_density_correction.tp_evaluate (Page 1 of 1) (BP-MDL2179VOL000070-003)
\MDL2179VOL000070-003\00_gross_sand_macondo.tp_evaluate (Page 1 of 1) (BP-MDL2179VOL000070-003)
\MDL2179VOL000070-003\00_k_core_macondo.tp_evaluate (Page 1 of 1) (BP-MDL2179VOL000070-003)
\MDL2179VOL000070-003\00_K_Logs_Macondo.frequency (Page 1 of 2) (BP-MDL2179VOL000070-003)
\MDL2179VOL000070-003\00_K_NCS_Macondo.frequency (Page 1 of 2) (BP-MDL2179VOL000070-003)
\MDL2179VOL000070-003\00_macondo.well_list (Page 1 of 1) (BP-MDL2179VOL000070-003)
\MDL2179VOL000070-003\00_macondo_00042010_RT_samples.cgm (Page 1 of 1) (BP-MDL2179VOL000070-003)
00_macondo_00042010_RT_samples.cgm.meta (BP-MDL2179VOL000070-003)
\MDL2179VOL000070-003\00_macondo_01192010.cgm (Page 1 of 1) (BP-MDL2179VOL000070-003)
00_macondo_01192010.cgm.meta (BP-MDL2179VOL000070-003)
\MDL2179VOL000070-003\00_macondo_01192010.cgm.meta.prn (Page 1 of 1) (BP-MDL2179VOL000070-003)
\MDL2179VOL000070-003\00_macondo_02212010_losses1.cgm (Page 1 of 1) (BP-MDL2179VOL000070-003)
00_macondo_02212010_losses1.cgm.meta (BP-MDL2179VOL000070-003)
\MDL2179VOL000070-003\00_macondo_030110.cgm (Page 1 of 1) (BP-MDL2179VOL000070-003)
\MDL2179VOL000070-003\00_macondo_03012010.cgm (Page 1 of 1) (BP-MDL2179VOL000070-003)
00_macondo_03012010.cgm.meta (BP-MDL2179VOL000070-003)
\MDL2179VOL000070-003\00_macondo_03172010.cgm (Page 1 of 1) (BP-MDL2179VOL000070-003)
\MDL2179VOL000070-003\00_macondo_03312010.cgm (Page 1 of 1) (BP-MDL2179VOL000070-003)
\MDL2179VOL000070-003\00_macondo_04212010.cgm (Page 1 of 1) (BP-MDL2179VOL000070-003)

\MDL2179VOL000070-003\00_macondo_04212010_losses2.cgm (Page 1 of 1) (BP-MDL2179VOL000070-003)
\MDL2179VOL000070-003\00_macondo_04212010_losses3.cgm (Page 1 of 1) (BP-MDL2179VOL000070-003)
00_macondo_04212010_losses3.cgm.meta (BP-MDL2179VOL000070-003)
\MDL2179VOL000070-003\00_macondo_04262010.cgm (Page 1 of 1) (BP-MDL2179VOL000070-003)
\MDL2179VOL000070-003\00_macondo_04272010_Composite.cgm (Page 1 of 1) (BP-MDL2179VOL000070-003)
00_macondo_04272010_Composite.cgm.meta (BP-MDL2179VOL000070-003)
\MDL2179VOL000070-003\00_macondo_04272010_Composite.cgm.meta.prn (Page 1 of 1) (BP-MDL2179VOL000070-003)
\MDL2179VOL000070-003\00_macondo_04272010_Composite_Ross.cgm (Page 1 of 1) (BP-MDL2179VOL000070-003)
00_macondo_04272010_Composite_Ross.cgm.meta (BP-MDL2179VOL000070-003)
\MDL2179VOL000070-003\00_macondo_04272010_Composite_Ross.cgm.meta.prn (Page 1 of 1) (BP-MDL2179VOL000070-003)
\MDL2179VOL000070-003\00_macondo_04272010_Dips.cgm (Page 1 of 1) (BP-MDL2179VOL000070-003)
00_macondo_04272010_Dips.cgm.meta (BP-MDL2179VOL000070-003)
\MDL2179VOL000070-003\00_macondo_04272010_losses.cgm (Page 1 of 1) (BP-MDL2179VOL000070-003)
\MDL2179VOL000070-003\00_macondo_05052010.cgm (Page 1 of 1) (BP-MDL2179VOL000070-003)
\MDL2179VOL000070-003\00_macondo_05122010.cgm (Page 1 of 1) (BP-MDL2179VOL000070-003)
00_macondo_05122010.cgm.meta (BP-MDL2179VOL000070-003)
\MDL2179VOL000070-003\00_macondo_05122010.cgm.meta.prn (Page 1 of 1) (BP-MDL2179VOL000070-003)
\MDL2179VOL000070-003\00_macondo_05122010_final.cgm (Page 1 of 1) (BP-MDL2179VOL000070-003)
00_macondo_05122010_final.cgm.meta (BP-MDL2179VOL000070-003)
\MDL2179VOL000070-003\00_macondo_05192010_sands.cgm (Page 1 of 1) (BP-MDL2179VOL000070-003)
\MDL2179VOL000070-003\00_macondo_05242010_sands.cgm (Page 1 of 1) (BP-MDL2179VOL000070-003)
00_macondo_05242010_sands.cgm.meta (BP-MDL2179VOL000070-003)
\MDL2179VOL000070-003\00_macondo_05242010_sands.cgm.meta.prn (Page 1 of 1) (BP-MDL2179VOL000070-003)
\MDL2179VOL000070-003\00_macondo_06012010.cgm (Page 1 of 1) (BP-MDL2179VOL000070-003)
00_macondo_06012010.cgm.meta (BP-MDL2179VOL000070-003)
\MDL2179VOL000070-003\00_macondo_08042010_MEM_samples.cgm (Page 1 of 1) (BP-MDL2179VOL000070-003)
00_macondo_08042010_MEM_samples.cgm.meta (BP-MDL2179VOL000070-003)
\MDL2179VOL000070-003\00_macondo_08042010_MEM_samples.cgm.meta.prn (Page 1 of 1) (BP-MDL2179VOL000070-003)
\MDL2179VOL000070-003\00_macondo_09062010.cgm (Page 1 of 1) (BP-MDL2179VOL000070-003)
\MDL2179VOL000070-003\00_macondo_09152010_Intersept.cgm (Page 1 of 1) (BP-MDL2179VOL000070-003)
00_macondo_09152010_Intersept.cgm.meta (BP-MDL2179VOL000070-003)
\MDL2179VOL000070-003\00_macondo_09152010_Intersept_ZoomIn.cgm (Page 1 of 1) (BP-MDL2179VOL000070-003)
\MDL2179VOL000070-003\00_macondo_252-2_sands.cgm (Page 1 of 1) (BP-MDL2179VOL000070-003)
00_macondo_252-2_sands.cgm.meta (BP-MDL2179VOL000070-003)
\MDL2179VOL000070-003\00_Macondo_field_quicklook_triple-cmr_5inch.layout (Page 1 of 31) (BP-MDL2179VOL000070-003)
\MDL2179VOL000070-003\00_macondo_lgsa_vs_k_core.xplot (Page 1 of 3) (BP-MDL2179VOL000070-003)
\MDL2179VOL000070-003\00_Macondo_LWD_RT_sampling.layout (Page 1 of 18) (BP-MDL2179VOL000070-003)
\MDL2179VOL000070-003\00_macondo_MC252-2_sands.cgm (Page 1 of 1) (BP-MDL2179VOL000070-003)
00_macondo_MC252-2_sands.cgm.meta (BP-MDL2179VOL000070-003)
\MDL2179VOL000070-003\00_macondo_obmi_calipers.cgm (Page 1 of 1) (BP-MDL2179VOL000070-003)
00_macondo_obmi_calipers.cgm.meta (BP-MDL2179VOL000070-003)
\MDL2179VOL000070-003\00_macondo_obmi_calipers.cgm.meta.prn (Page 1 of 1) (BP-MDL2179VOL000070-003)
\MDL2179VOL000070-003\00_macondo_por_vs_k_core.xplot (Page 1 of 3) (BP-MDL2179VOL000070-003)
00_macondo_por_vs_por.xplot (BP-MDL2179VOL000070-003)
\MDL2179VOL000070-003\00_macondo_rhob_vs_phit_ncs.xplot (Page 1 of 3) (BP-MDL2179VOL000070-003)
\MDL2179VOL000070-003\00_macondo_rhog_vs_ecs.xplot (Page 1 of 3) (BP-MDL2179VOL000070-003)
\MDL2179VOL000070-003\00_macondo_RXD_07152010.cgm (Page 1 of 1) (BP-MDL2179VOL000070-003)
\MDL2179VOL000070-003\00_macondo_sands.cgm (Page 1 of 1) (BP-MDL2179VOL000070-003)
00_macondo_sands.cgm.meta (BP-MDL2179VOL000070-003)
\MDL2179VOL000070-003\00_macondo_sands.cgm.meta.prn (Page 1 of 1) (BP-MDL2179VOL000070-003)
\MDL2179VOL000070-003\00_macondo_section_05062010.cgm (Page 1 of 1) (BP-MDL2179VOL000070-003)
\MDL2179VOL000070-003\00_macondo_section_05112010.cgm (Page 1 of 1) (BP-MDL2179VOL000070-003)
00_macondo_section_05112010.cgm.meta (BP-MDL2179VOL000070-003)
\MDL2179VOL000070-003\00_macondo_section_05112010_final.cgm (Page 1 of 1) (BP-MDL2179VOL000070-003)
00_macondo_section_05112010_final.cgm.meta (BP-MDL2179VOL000070-003)
00_macondo_section_05112010_final.zip (BP-MDL2179VOL000070-003)
\MDL2179VOL000070-003\00_macondo_section_06142010.cgm (Page 1 of 1) (BP-MDL2179VOL000070-003)
\MDL2179VOL000070-003\00_macondo_TD_losses.cgm (Page 1 of 1) (BP-MDL2179VOL000070-003)
00_macondo_TD_losses.cgm.meta (BP-MDL2179VOL000070-003)
\MDL2179VOL000070-003\00_macondo_TD_petrophysics.cgm (Page 1 of 1) (BP-MDL2179VOL000070-003)
00_macondo_TD_petrophysics.cgm.meta (BP-MDL2179VOL000070-003)
\MDL2179VOL000070-003\00_net_sand_macondo.tp_evaluate (Page 1 of 1) (BP-MDL2179VOL000070-003)
\MDL2179VOL000070-003\00_pay_sand_macondo.tp_evaluate (Page 1 of 1) (BP-MDL2179VOL000070-003)
\MDL2179VOL000070-003\00_PEF_Macondo.frequency (Page 1 of 2) (BP-MDL2179VOL000070-003)
\MDL2179VOL000070-003\00_PHIT_D_Macondo.frequency (Page 1 of 2) (BP-MDL2179VOL000070-003)
\MDL2179VOL000070-003\00_phit_macondo.tp_evaluate (Page 1 of 1) (BP-MDL2179VOL000070-003)
\MDL2179VOL000070-003\00_PHIT_NCS_Macondo.frequency (Page 1 of 2) (BP-MDL2179VOL000070-003)
\MDL2179VOL000070-003\00_r0_macondo.tp_evaluate (Page 1 of 1) (BP-MDL2179VOL000070-003)
\MDL2179VOL000070-003\00_rhog_core.tp_evaluate (Page 1 of 1) (BP-MDL2179VOL000070-003)
\MDL2179VOL000070-003\00_RHOG_Macondo.frequency (Page 1 of 2) (BP-MDL2179VOL000070-003)

APPENDIX F. FACTS AND DATA WE CONSIDERED IN FORMING OUR OPINIONS

\MDL2179VOL000070-003\00_rw_macondo.tp_evaluate (Page 1 of 1) (BP-MDL2179VOL000070-003)
\MDL2179VOL000070-003\00_rwa_macondo.tp_evaluate (Page 1 of 1) (BP-MDL2179VOL000070-003)
\MDL2179VOL000070-003\00_Sw_Macondo.frequency (Page 1 of 2) (BP-MDL2179VOL000070-003)
\MDL2179VOL000070-003\00_sw_macondo.tp_evaluate (Page 1 of 1) (BP-MDL2179VOL000070-003)
\MDL2179VOL000070-003\BP_Macondo_OCSG_32306_001_ST00BP01_Main_Pass_MD_CMR_ECS_HNGS_097PUP.las (Page 1 of 449) (BP-MDL2179VOL000070-003)
BP_Macondo_OCSG_32306_001_ST00BP01_Main_Pass_MD_TCOM_033PUP.las (BP-MDL2179VOL000070-003)
BP_Macondo_OCSG_32306_001_ST00BP01_OBMI_DSI_Main_Pass_MD_125PUC.DLIS (BP-MDL2179VOL000070-003)
\MDL2179VOL000070-003\BP_Macondo_OCSG_32306_001_ST00BP01_OBMI_DSI_Main_Pass_MD_125PUP.las (Page 1 of 265) (BP-MDL2179VOL000070-003)
Copy of at0182_1st_cvx.well (BP-MDL2179VOL000070-003)
Copy of mc0252_1_bp2_tex.well (BP-MDL2179VOL000070-003)
Copy of mc0252_1_st01_bp.well (BP-MDL2179VOL000070-003)
Copy of mc0252_d.well (BP-MDL2179VOL000070-003)
\MDL2179VOL000070-003\k_macondo.macro (Page 1 of 1) (BP-MDL2179VOL000070-003)
macondo.dlis (BP-MDL2179VOL000070-003)
\MDL2179VOL000070-003\macondo.section (Page 1 of 3) (BP-MDL2179VOL000070-003)
\MDL2179VOL000070-003\macondo.well_list (Page 1 of 1) (BP-MDL2179VOL000070-003)
\MDL2179VOL000070-003\macondo_03022010_losses.cgm (Page 1 of 1) (BP-MDL2179VOL000070-003)
\MDL2179VOL000070-003\macondo_k_vs_por_core.macro (Page 1 of 1) (BP-MDL2179VOL000070-003)
\MDL2179VOL000070-003\macondo_pressure.csv (Page 1 of 5) (BP-MDL2179VOL000070-003)
\MDL2179VOL000070-003\macondo_rhge_vs_rhob.macro (Page 1 of 1) (BP-MDL2179VOL000070-003)
\MDL2179VOL000070-003\macondo_rhof_core.macro (Page 1 of 1) (BP-MDL2179VOL000070-003)
\MDL2179VOL000070-003\macondo_rhog_vs_rhge(ecs).macro (Page 1 of 1) (BP-MDL2179VOL000070-003)
\MDL2179VOL000070-003\macondo_rhog_vs_rhge.macro (Page 1 of 1) (BP-MDL2179VOL000070-003)
\MDL2179VOL000070-003\Macondo_sands.cgm (Page 1 of 1) (BP-MDL2179VOL000070-003)
Macondo_sands.cgm.meta (BP-MDL2179VOL000070-003)
\MDL2179VOL000070-003\macondo_smaller.section (Page 1 of 3) (BP-MDL2179VOL000070-003)
\MDL2179VOL000070-003\Macondo_Sonic.dat (Page 1 of 429) (BP-MDL2179VOL000070-003)
\MDL2179VOL000070-003\Macondo_TCMR.cgm (Page 1 of 1) (BP-MDL2179VOL000070-003)
\MDL2179VOL000070-003\Macondo_Tops_LWD_&_Wire.csv (Page 1 of 1) (BP-MDL2179VOL000070-003)
\MDL2179VOL000070-003\macondo_w_relief_wells.section (Page 1 of 3) (BP-MDL2179VOL000070-003)
\MDL2179VOL000070-003\macondo_w_RXD.section (Page 1 of 3) (BP-MDL2179VOL000070-003)
mc0252_1_bp.well (BP-MDL2179VOL000070-003)
mc0252_1_bp2_tex.well (BP-MDL2179VOL000070-003)
\MDL2179VOL000070-003\mc0252_1_bp_scmt.las (Page 1 of 326) (BP-MDL2179VOL000070-003)
mc0252_1_st01_bp.well (BP-MDL2179VOL000070-003)
\MDL2179VOL000070-003\mc0252_1_st01_bp_best.las (Page 1 of 736) (BP-MDL2179VOL000070-003)
\MDL2179VOL000070-003\mc0252_1_st01_bp_best_GrRes.las (Page 1 of 395) (BP-MDL2179VOL000070-003)
\MDL2179VOL000070-003\mc0252_1_st01_bp_directional.las (Page 1 of 3) (BP-MDL2179VOL000070-003)
\MDL2179VOL000070-003\mc0252_1_st01_bp_ds_lwdgr_2_wire.csv (Page 1 of 1) (BP-MDL2179VOL000070-003)
\MDL2179VOL000070-003\mc0252_1_st01_bp_ds_mwdsonic_2_chsonic.csv (Page 1 of 2) (BP-MDL2179VOL000070-003)
\MDL2179VOL000070-003\mc0252_1_st01_bp_lwd_run1400_tripout.las (Page 1 of 229) (BP-MDL2179VOL000070-003)
\MDL2179VOL000070-003\mc0252_1_st01_bp_mdt_pressure.csv (Page 1 of 1) (BP-MDL2179VOL000070-003)
\MDL2179VOL000070-003\mc0252_1_st01_bp_mwd.las (Page 1 of 363) (BP-MDL2179VOL000070-003)
\MDL2179VOL000070-003\mc0252_1_st01_bp_mwd_final.las (Page 1 of 4348) (BP-MDL2179VOL000070-003)
\MDL2179VOL000070-003\mc0252_1_st01_bp_r1d1_rtscanner.las (Page 1 of 202) (BP-MDL2179VOL000070-003)
\MDL2179VOL000070-003\mc0252_1_st01_bp_r1d3_obmi_calipers_shifted.las (Page 1 of 37) (BP-MDL2179VOL000070-003)
\MDL2179VOL000070-003\mc0252_1_st01_bp_rswc_all_samples.csv (Page 1 of 1) (BP-MDL2179VOL000070-003)
\MDL2179VOL000070-003\mc0252_1_st01_bp_sands_rp.csv (Page 1 of 2) (BP-MDL2179VOL000070-003)
\MDL2179VOL000070-003\mc0252_1_st01_bp_sands_rp.prn (Page 1 of 2) (BP-MDL2179VOL000070-003)
\MDL2179VOL000070-003\mc0252_1_st01_bp_tops_sand.csv (Page 1 of 1) (BP-MDL2179VOL000070-003)
\MDL2179VOL000070-003\mc0252_1_st01_bp_tops_sand_lwd.csv (Page 1 of 1) (BP-MDL2179VOL000070-003)
\MDL2179VOL000070-003\mc0252_1_st01_bp_tops_sand_m56d.csv (Page 1 of 1) (BP-MDL2179VOL000070-003)
\MDL2179VOL000070-003\mc0252_1_st01_bp_tops_sand_wire.csv (Page 1 of 1) (BP-MDL2179VOL000070-003)
\MDL2179VOL000070-003\mc0252_1_st01_bp_wire.las (Page 1 of 549) (BP-MDL2179VOL000070-003)
mc0252_3.well (BP-MDL2179VOL000070-003)
\MDL2179VOL000070-003\MC0252_DDII_Permeable_Intervals.cgm (Page 1 of 1) (BP-MDL2179VOL000070-003)
MC0252_DDII_Permeable_Intervals.cgm.meta (BP-MDL2179VOL000070-003)
mc0252_rxd.well (BP-MDL2179VOL000070-003)
\MDL2179VOL000070-003\mc0252_rxd_best.las (Page 1 of 479) (BP-MDL2179VOL000070-003)
\MDL2179VOL000070-003\mc0252_rxd_directional.las (Page 1 of 2) (BP-MDL2179VOL000070-003)
\MDL2179VOL000070-003\mc0252_rxd_mudlog.las (Page 1 of 1237) (BP-MDL2179VOL000070-003)
\MDL2179VOL000070-003\mc0252_rxd_mwd.las (Page 1 of 234) (BP-MDL2179VOL000070-003)
\MDL2179VOL000070-003\mc0252_rxd_wire.las (Page 1 of 197) (BP-MDL2179VOL000070-003)
\MDL2179VOL000070-003\MC252_001_ST00BP01_SURVEY.las (Page 1 of 4) (BP-MDL2179VOL000070-003)
\MDL2179VOL000070-003\MC252_002_BPX_COP_MEM_4989-9120.las (Page 1 of 905) (BP-MDL2179VOL000070-003)
\MDL2179VOL000070-003\MC252_002_BPX_MPR_MEM_5471-9120_50.las (Page 1 of 268) (BP-MDL2179VOL000070-003)
\MDL2179VOL000070-003\MC252_002_BPX_MPR_MEM_corrected-res-gam_5471-8650_50.las (Page 1 of 234) (BP-MDL2179VOL000070-003)
\MDL2179VOL000070-003\MC252_003_ST00BP00_BPX_LWD_PWDESD.xls (Page 1 of 1) (BP-MDL2179VOL000070-003)
\MDL2179VOL000070-003\MC252_003_ST00BP00_BPX_LWD_REC_1MD_CORR_6805.cgm (Page 1 of 1) (BP-MDL2179VOL000070-003)

APPENDIX F. FACTS AND DATA WE CONSIDERED IN FORMING OUR OPINIONS

MC252_003_ST00BP00_BPX_LWD_REC_1MD_CORR_6805.cgm.meta (BP-MDL2179VOL000070-003)
\MDL2179VOL000070-003\MC252_003_ST00BP00_BPX_LWD_REC_1MD_CORR_6805.pdf (Page 1 of 1) (BP-MDL2179VOL000070-003)
\MDL2179VOL000070-003\MC252_003_ST00BP00_BPX_LWD_REC_1MD_CORR_8788.cgm (Page 1 of 1) (BP-MDL2179VOL000070-003)
\MDL2179VOL000070-003\MC252_003_ST00BP00_BPX_LWD_REC_1MD_CORR_8788.pdf (Page 1 of 1) (BP-MDL2179VOL000070-003)
\MDL2179VOL000070-003\MC252_003_ST00BP00_BPX_LWD_REC_1MD_PWD_6805.cgm (Page 1 of 1) (BP-MDL2179VOL000070-003)
\MDL2179VOL000070-003\MC252_003_ST00BP00_BPX_LWD_REC_1MD_PWD_6805.pdf (Page 1 of 1) (BP-MDL2179VOL000070-003)
\MDL2179VOL000070-003\MC252_003_ST00BP00_BPX_LWD_REC_1MD_PWD_8788.cgm (Page 1 of 1) (BP-MDL2179VOL000070-003)
\MDL2179VOL000070-003\MC252_003_ST00BP00_BPX_LWD_REC_1MD_PWD_8788.pdf (Page 1 of 1) (BP-MDL2179VOL000070-003)
IGS076-000671- 0675
LAL134-003719
SNL144-000396
SNL043-000735
LNL075-008796- 8797
SNL087-001206- 5671
LNL075-013264- 13266
SNL144-012780-12805
BP-HZN-2179MDL07288560
BP-HZN-2179MDL06666023
LAL278-041293- 316
LAL169-000050 - 0083 SNL021-010802 - 0819 OSE140-008009 -8449 OSE141-000310 - 1373 SNL045-002301 - 2301 SNL021-019316 - 9350 IG683-003175 - 3176
SNL111-002678-SNL111-002755
SNL046-000421
SNL048-5360
SNL084-58529
BP-HZN-BLY00090901 - 90904
BP-HZN-2179MDL00412974
BP-HZN-2179MDL01942109
BP-HZN-2179MDL019421119
BP-HZN-2179MDL01942110
BP-HZN-2179MDL01942118
BP-HZN-2179MDL01942120
BP-HZN-BLY000297537 -297538
SNL048-055360
SNL045-001583
SNL046-082105
SNL046-082142
SNL021-007543
SNL042-002687
SDX009-0005287 - 5291
BP-HZN-2179MDL01672722
BP-HZN-2179MDL01627173 - 7196
BP-HZN-2179MDL01627171- 7172
BP-HZN-2179MDL-02175538
BP-HZN-2179MDL-02175525 - 5537
SNL046-070150
SNL084-058529
SNL046-000421
SNL046-071976
BP-HZN-2179MDL02114984
BP-HZN-2179MDL01627197 - 7210
SNL07528330
BP-HZN-2179MDL01951916
BP-HZN-2179MDL-02175510
BP-HZN-2179MDL-02175510

APPENDIX F. FACTS AND DATA WE CONSIDERED IN FORMING OUR OPINIONS

SNL110-017071
SNL110-012087
BP-HZN-2179MDL01627169 - 7170
BP-HZN-2179MDL02114982
Flow Report Data
M252 DataDump_071810.zip
SNL046-082640
BP-HZN-2179MDL01951970
BP-HZN-2179MDL01627211
SNL Flow Report Data Sources
SNL059-000136
SNL043-005207 -5232
SNL110-017070-7303
BP-HZN-2179MDL02114983
BP-HZN-2179MDL02114984
Collection Point 2 Location of Oil Collection Point Relative to BOP Restriction
Exhibit 7901
Exhibit 7902
Exhibit 7848
SNL087-001172- 1173
DOE-NNSA Flow Analysis Studies Associated with the Oil Release following the Deepwater Horizon Accident
HCG037-005979 - 5980
BP-HZN-219MDL01872218
BP-HZN-219MDL00063084
OSE114-003671
BCK-BP- NASA report.pdf
Choke Assembly and Gate Valve Inspection Report (Preliminary)
BP-HZN-2179MDL04480751
BP-HZN-2179MDL04480747 - 0748
BP-HZN-2179MDL04480749
BP-HZN-2179MDL04480752
BP-HZN-2179MDL04480750
BP-HZN-2179MDL04892862 - 2903
Exhibit 7918
BP-HZN-MBI00180472
BP-HZN-2179MDL04810383
BP-HZN-2179MDL04810383
BP-HZN-2179MDL02864019
Flow Data - Helix Producer 1
Choke Tubing Assembly & Tandem Gate Valve Inspection Summary
Breakout Torques - Choke Gate Valve and Kill Gate Valve
Notebooks - Book 1 - DNV Laboratory Notebook 490
Notebooks - Book 1 - DNV Laboratory Notebook 490
Notebooks - Book 1 - DNV Laboratory Notebook 490
Notebooks - Book 1 - DNV Laboratory Notebook 490
Notebooks - Book 1 - DNV Laboratory Notebook 490
Notebooks - Book 1 - DNV Laboratory Notebook 490
Notebooks - Book 1 - DNV Laboratory Notebook 490
Notebooks - Book 1 - DNV Laboratory Notebook 490
Notebooks - Book 1 - DNV Laboratory Notebook 490
Notebooks - Book 2 - DNV Laboratory Notebook 491
Notebooks - Book 2 - DNV Laboratory Notebook 491
Notebooks - Book 2 - DNV Laboratory Notebook 491
Notebooks - Book 2 - DNV Laboratory Notebook 491
Notebooks - Book 2 - DNV Laboratory Notebook 491
Notebooks - Book 2 - DNV Laboratory Notebook 491
Notebooks - Book 2 - DNV Laboratory Notebook 491
Notebooks - Book 2 - DNV Laboratory Notebook 491
Notebooks - Book 2 - DNV Laboratory Notebook 491
Physical Measurements - Collet Connector Measurements
Physical Measurements - Gate Valves and Seals Physical Measurements
Physical Measurements - Manual Valve Cage Physical Measurements (289-6)
Physical Measurements - Physical Measurements-refer to document from 20111115
Physical Measurements - Ram Cavity Physical Dimensions
Physical Measurements - Ram Cavity Physical Measurements
Physical Measurements - Results of Inspection at NASA Michoud Assembly Facility-measurements provided by Fastorq
Suface Profiles - Profile Descriptions - Description of Data
Suface Profiles - Surface Profiling
Surface Profiles - Item 287_Item 635 Profiles
Surface Profiles - Item 287-635 Profiles

Surface Profiles - Item 288_Profiles
Surface Profiles - Item 289A-6 Profiles
Surface Profiles - Item 289A-6 Profiles
Surface Profiles - Item 289B Profiles
Surface Profiles - Item 289C Profiles
Surface Profiles - Item 289G Profiles
Surface Profiles - Item 621A-1 Profiles
Surface Profiles - Item 621A-10 Profiles
Surface Profiles - Item 621A-11 Profiles
Surface Profiles - Item 621A-12 Profiles
Surface Profiles - Item 621A-2 Profiles
Surface Profiles - Item 621A-7 Profiles
Surface Profiles - Item 621A-8 Profiles
Surface Profiles - Item 621A-9 Profiles
Surface Profiles - Item 621B-1 Profiles
Surface Profiles - Item 621B-10 Profiles
Surface Profiles - Item 621B-11 Profiles
Surface Profiles - Item 621B-12 Profiles
Surface Profiles - Item 621B-2 Profiles
Surface Profiles - Item 621B-7 Profiles
Surface Profiles - Item 621B-8 Profiles
Surface Profiles - Item 621B-9 Profiles
Surface Profiles - Item 633_220 Profiles
Surface Profiles - Item 633_Item 220_Choke Profiles
Surface Profiles - Item 633_Item 220_Kill Profiles
Surface Profiles - Item 671 Profiles
Surface Profiles - Item 672 Profiles
Surface Profiles - Item 720 Profiles
Surface Profiles - Item289F Profiles
BP-HZN-2179MDL04884268
BP-HZN-2179MDL04884262
BP-HZN-2179MDL04884261 - 4268
BP-HZN-2179MDL04884263
BP-HZN 2179MDL04884264 - 4267
Numerical simulations of the Macondo well blowout reveal strong control of oil flow by reservoir permeability and exsolution of gas -- Oldenburg, et al., Numerical Simulations of the Macondo Well Blowout Reveal Strong Control of Oil Flow by Reservoir Permeability and Exsolution of Gas, PNAS (2011)
BP-HZN-2179MDL05297956
BP-HZN-BLY00116190
BP-HZN-2179MDL00648715
BP-HZN-2179MDL00667659
BP-HZN-2179MDL05646464
BP-HZN-2179MDL00676168
BP-HZN-2179MDL04480751
BP-HZN2179MDL00648725 -
BP-HZN-2179MDL0696319 - 6329
BP-HZN-2179MDL05646465
AE-HZN-2179MDL-00125801
BP-HZN-2179MDL07311974
BP-HZN-2179MDL04480747 - 0748
BP-HZN-2179MDL05297955
BP-HZN-2179MDL05646456 - 6463
BP-HZN-2179MDL05595964
BP-HZN-2179MDL00667653- BP-HZN-2179MDL00667658
BP-HZN-2179MDL00648713 - 8714
BP-HZN-BLY00116186 - 6190
BP-HZN-2179MDL00676164 - 6167
BP-HZN-BLY0016929
BP-HZN2179MDL00648722
AE-HZN-2179MDL-00127154
BP-HZN-2179MDL07311975 - 1986
BP-HZN-2179MDL00667660- 7673
BP-HZN-BLY00116192 - 6205
BP-HZN-2179MDL05602549
BP-HZN-2179MDL04729477
AE-HZN-2179MDL0123678
BP-HZN-2179MDL04480749
BP-HZN-2179MDL03838183
BP-HZN-2179MDL03838184
BP-HZN-2179MDL03838186
BP-HZN-2179MDL04480752

APPENDIX F. FACTS AND DATA WE CONSIDERED IN FORMING OUR OPINIONS

BP-HZN-BLY0116930- 6945
BP-HZN-2179MDL00648723 - 8725
AE-HZN-2179MDL0116288
AE-HZN-2179MDL0078658
BP-HZN-2179MDL00648716
BP-HZN-2179MDL00648717 - 8721
BP-HZN-2179MDL04480750
Ex. 7273
Ex. 9237
Ex. 8523
Ex. 4997
Ex. 4991
Ex. 4998
Ex. 8538
Ex. 5016
Ex. 9402
BP Witness Signature Letter and Errata Page of Mortsen Emilsen
Deposition of Bryan Ritchie and all exhibits and errata (Oct. 04-05, 2012)
Ex. 6124
Deposition of Graham Pinky Vinson and all exhibits and errata (Sep. 18-19, 2012)
Deposition of Matthew Lee Gochnour and all exhibits and errata (Sep. 13-14, 2012)
Deposition of Simon Bishop and all exhibits and errata (Sep. 28, 2011)
Deposition of Tom Knox and all exhibits and errata (Oct. 11, 2012)
Deposition Transcript for Paul Hsieh and all exhibits and errata (Sep. 11-12, 2012)
Deposition Transcript of Haug Emilsen (20110623)
Deposition Transcript of Haug Emilsen (20110624)
Deposition Transcript of Simon Bishop Final Transcript (20120927)
Ex. 9248
Ex. 5017
Ex. 9249
BP-HZN-2179MDL04883027- BP- HZN- 2179MDL04883031
HAL_1341690- HAL_1341692
HAL_1343759
HAL_0504124
AE-HZN-2179MDL00116749
HAL_07100195- HAL_07100199
ANA-MDL-000008010 - 8012
ANA-HEC1-000003355
HAL_0697229-HAL_0697234
BP-HZN-2179MDL00943274
APC-HEC1-000004652
APC-SHS2A-000001040 - APC-SHS2A-000001044
ANA-MDL-000003792
ANA-MDL-000039304
ANA-MDL-000034456 - ANA-MDL-000034458
AE- HZN-2179MDL00069648-9649
ANA-MDL-000020148
BP-HZN-2179MDL05335011
HDR011-001319-HDR011-001320
AE-HZN- 2179MDL00124410
AE-HZN-2179MDL00078052
BP-HZN-2179MDL01920214- BP-HZN-2179MDL01920223
ANA-MDL-000011652 -ANA-MDL-000011654
AE- HZN-2179MDL00117664
ANA-MDL-000004620 - ANA-MDL-000004621
ANA-MDL-000034816
ANA-MDL-000047991
ANA-MDL-000020195
ANA-MDL-000041749 - ANA-MDL-000041750
ANA-MDL-000013074 - ANA-MDL-000013075
ANA-MDL-000073345
ANA-MDL-000036761
ANA-MDL-000033885 - ANA-MDL-000033925
ANA-MDL-00261741-ANA-MDL-00261742
ANA-MDL-000016353 - ANA-MDL-000016355
HAL_0505402
HAL_0506499
HAL_0505402- HAL_0505408
HAL_0531285
HAL_0531335-HAL_0531340

APPENDIX F. FACTS AND DATA WE CONSIDERED IN FORMING OUR OPINIONS

HAL_1124000- HAL_1124001
AE-HZN-2179MDL00067353
AE-HZN-2179MDL00086330- 6331
AE-HZN-2179MDL00056033- AE-HZN-2179MDL00056034
AE-HZN-2179MDL00060126-AE-HZN- 2179MDL00060181
BP-HZN-2179MDL07237722
BP-HZN-2179MDL04887037- BP-HZN-2179MDL04887059
AE- HZN-2179MDL00084558- AE-HZN-2179MDL00084583
AE-HZN- 2179MDL00050712
BP-HZN-2179MDL04927015, BP-HZN-2179MDL04927017
BP- HZN-2179MDL05684398- BP-HZN-2179MDL05684399
BP-HZN-2179MDL04729492-BPD343-033451
BP- HZN-2179MDL04894453- BP-HZN-2179MDL04894455
BP-HZN-2179MDL04902309, BP-HZN-2179MDL04902311 - BP-HZN-2179MDL04902320
BP-HZN-2179MDL04902309-BP-HZN-2179MDL04902320
AE-HZN-2179MDL00050119
AE-HZN- 2179MDL00068186- AE-HZN-2179MDL00068191
AE-HZN-2179MDL00098912, AE-HZN-2179MDL00098914 - AE-HZN-2179MDL00098923
AE-HZN-2179MDL00127297- AE- HZN-2179MDL00082866
AE-HZN-2179MDL00097614-AE-HZN- 2179MDL00097615
ANA-MDL-0000038825 - ANA-MDL-0000038826
APC-HEC1-000003865
HAL_1342241- HAL_1342242
BP- HZN-2179MDL04855177
HAL_0505230
BP-HZN-2179MDL1793905- BP-HZN-2179MDL01793929
HAL_0507877- HAL_0507904
HAL_0507253
ANA-MDL2-000122779- ANA-MDL2-000122786
ANA-MDL-000017225 - ANA-MDL-000017226
BP-HZN-2179MDL05789875- BP-HZN- 2179MDL05789876
AE- HZN-2179MDL00086332
AE-HZN-2179MDL00091615
BP-HZN-2179MDL00660136- BP-HZN-2179MDL00660145
BP-HZN-2179MDL00638488
BP-HZN-2179MDL00572828 - BP-HZN-2179MDL00572846
HAL_0506020- HAL_0506031
Halliburton BP Macondo Top and Static Kill Operations
HAL_0511369
Halliburton Web Article Overview: Well Control
ANA-MDL-000277580
Letter From Minnie Adame to J. Robert Warren re: Deposition of Richard Frank Vargo
Lillehammer, Macondo- Well Control Effort
AE- HZN-2179MDL00148868 - 8882
BP-HZN-2179MDL00572771 - 2785
ANA-MDL-00277651
APC-HEC1-000004687
HAL_0504107 - 4111
BP-HZN-2179MDL00536425
AE- HZN-2179MDL00114487 - 4496
BP-HZN-2179MDL04825892 - 5893
AE-HZN-2179MDL00127297 - AE-HZN-2179MDL00127299
National Commission on the BP Deepwater Horizon Oil Spill and Offshore Drilling Stopping the Spill: The Five Month Effort To Kill The Macondo Well Staff Working Paper no.6
Ole Rygg Final Deposition Transcript, Word Index
BP- HZN-2179MDL05710203
HAL_0710197-HAL_0710199
Report Summary and Conclusions Deepwater Horizon Incident
Report Summary and Conclusions Deepwater Horizon Incident
BP-HZN-2179MDL01601482
Today's complex drilling operations demand sophisticated well-control modeling tools
Top 3 Risks by Procedure from HAZIDS of Top Kill Activities
HAL_0114609
BP-HZN-2179MDL05816610- BP-HZN-2179MDL05816636
Warren Letter- Deposition of Morsten H. Emilsen
ANA-MDL-000039354
BP-HZN-2179MDL04896195
BP-HZN-2179MDL04896196
BP-HZN-2179MDL07031517- BP-HZN-2179MDL0703151724
BP-HZN-2179MDL04920968

BP-HZN-2179MDL04869884
BP-HZN-2179MDL04920969
BP-HZN-2179MDL04869885
BP-HZN-2179MDL05237977
BP-HZN-2179MDL04929637
BP-HZN-2179MDL05333515
BP-HZN-2179MDL05333535
BP spreadsheet (252455819)
Agreed 30(b)(6) Deposition Notice of the United States
Assessment of Flow Rate Estimates for the Deepwater Horizon/Macondo Well Oil Spill
Assessment of Flow Rate Estimates for the Deepwater Horizon/Macondo Well Oil Spill
BP-HZN-BLY00140873-BP- HZN-BLY00140910
BP-HZN-2179MDL02200713-BP-HZN-2179MDL02200719
BP-HZN-BLY00125334- BP-HZN-BLY00125381
BP-HZN-2179MDL04815271
BP-HZN-2179MDL04834293 - BP-HZN-2179MDL04834294
BP-HZN-2179MDL05100565
BP-HZN-2179MDL04932738
BP-HZN-2179MDL04809667
Email From: CMolderburg@lbl.gov To: Guthrie, Georgie Subject: Are you cking email?
BP-HZN-2179MDL04884261
BP-HZN-2179MDL04912531-BP-HZN-2179MDL04912542
BP-HZN-2179MDL04912566-BP-HZN-2179MDL04912568
BP-HZN-2179MDL06520758- BP-HZN-2179MDL06520789
Email From: mcnutt@usgs.gov to hunsaker61@comcast.net Subject: Re: tom hunter feedback on new data
BP-HZN-2179MDL06144176-BP-HZN-2179MDL06144184
DW 0007239- DW 0007261
BP-HZN-2179MDL08412947 - BP-HZN2179MDL08412956
BP-HZN-2179MDL07587543
OSE111-000110
Current Fluid Property Models for Gulf Oil Spill
BP-HZN-2179MDL07588600- BP-HZN-2179MDL07588601
Deposition of Adam Lee Ballard (20121016)
Deposition of Adam Lee Ballard (20121017)
Deposition of Don Maclay (20121031)
Deposition of Galina Skripnikova (20110707)
Deposition of Galina Skripnikova (20110708)
Deposition of George Guthrie (20101115)
Deposition of George Guthrie (20101116)
Deposition of Jaime Loos (20120920)
Deposition of Jay Thorseth (20110920)
Deposition of Robert Merrill (20130115)
Deposition of Robert Merrill (20130116)
Deposition of Simon Bishop (20120927)
Deposition of Simon Bishop (20110928)
Deposition of Timothy Lockett (20121218)
Deposition of Timothy Lockett (20121219)
Deposition of Tony Liao (20130110)
Deposition of Tony Liao (20130111)
Deposition of Trevor Hill (20130114)
Deposition of Trevor Hill (20130115)
BP-HZN-BLY00125334- BP-HZN-BLY00125381
BP-HZN-2179MDL07443174
BP-HZN-2179MDL05749068-BP-HZN-2179MDL05749072
BP-HZN-2179MDL04809667
SDX005-0025766
BP-HZN-2179MDL02175510-
BP-HZN-2179MDL04874628
BP-HZN-2179MDL04934344 - BP-HZN-2179MDL04934345
BP-HZN-2179MDL04912566
BP-HZN-2179MDL02180263
BP-HZN-2179MDL04799584 - BP-HZN-2179MDL04799589
BP-HZN-2179MDL06062154
BP-HZN-2179MDL06304787- BP- HZN- 2179MDL06304792
BP-HZN-2179MDL04800285- BP-HZN-2179MDL04800289
BP-HZN-2179MDL06100234-BP-HZN-2179MDL06100238
BP-HZN-MDL04920338
BP-HZN-2179MDL04884944 - BP-HZN-2179MDL04884946
BP-HZN-2179MDL07038710 - BP-HZN-2179MDL07038712
BP-HZN-2179MDL07441681- BP-HZN-2179MDL07441683

BP-HZN-2179MDL06523495 - BP-HZN-2179MDL06523495
BP-HZN-2179MDL04874261
BP-HZN-2179MDL07094328
BP-HZN-2179MDL0418079
BP-HZN-2179MDL04820690- BP-HZN- 2179MDL04820722
BP-HZN-2179MDL05733433 - BP-HZN-2179MDL05733436
STC-MDL-0033324
BP-HZN-2179MDL07024984 - BP-HZN-2179MDL07024988
BP-HZN-2179MDL04896270
BP-HZN-2179MDL05700441 - BP-HZN-2179MDL05700443
Email from pnas@nas.edu To: Guthrie, George SubjectPNAS MS#2011-11099 Decision Notification Attachments: 2_reviewer_attachment_ 1 _1311956231_convrt.pdf
BP-HZN-2179MDL04877350
BP-HZN-2179MDL07445511
BP-HZN-2179MDL07256061
BP-HZN-2179MDL07444864
BP-HZN-2179MDL07444283- BP-HZN-217907444283
BP-HZN-2179MDL04896171 - BP-HZN-2179MDL04896179
BP-HZN-2179MDL05795380
HAL_0679913
BP-HZN-2179MDL04799584 - BP-HZN-2179MDL04799589
BP-HZN-2179MDL06537640
BP-HZN-2179MDL04908186-BP-HZN-2179MDL04908189
BP-HZN-2179MDL07265826
BP-HZN-2179MDL07266154
BP-HZN-2179MDL07266192
BP-HZN-2179MDL266255
BP-HZN-2179MDL06520758 - BP-HZN-2179MDL06520789
BP-HZN-2179MDL07133782- BP-HZN-2179MDL07133782
BP-HZN-2179MDL04908288 - BP-HZN-2179MDL04908507
BP-HZN-2179MDL04884261 - BP-HZN-2179MDL04884268
BP-HZN-217904909161
BP-HZN-2179MDL04802233 - BP-HZN-2179MDL04802235
BP-HZN-2179MDL07037064
BP-HZN-2179MDL04912531 - BP-HZN-2179MDL04912542
BP-HZN-2179MDL04854382
ETL080-002879
ETL078- 005091
ETL080-001026
BP-HZN-2179MDL05744945-BP-HZN-2179MDL05744946
ETL080-003525
LBN003- 267163
ETL080-009831
FML003- 024434
LBN003-270122
LBN003- 269986
BP-HZN-2179MDL04898308-BP-HZN-2179MDL04898316
BP-HZN-2179MDL04680345
BP-HZN-2179MDL03675260- BP-HZN-2179MDL03675264
BP-HZN-2179MDL04897017
BP-HZN-2179MDL07082923- BP-HZN-2179MDL07082924
BP-HZN-2179MDL02211574-BP-HZN-2179MDL02211576
BP-HZN-2179MDL07023887-BP-HZN-2179MDL07023888
BP-HZN-2179MDL04806436
BP-HZN-2179MDL04825799-BP-HZN-2179MDL048255812
BP-HZN-2179MDL00951054
BP-HZN-2179MDL06445201-BP-HZN-2179MDL06445202
BP-HZN-2179MDL07246568
BP-HZN-2179MDL04938354- BP-HZN-2179MDL04938355
BP-HZN-2179MDL01458005
BP-HZN-2179MDL04819263-BP-HZN-2179MDL04819267
BP- HZN-2179MDL04808637-8650
IMV435-017041
BP-HZN-2179MDL01920214- BP-HZN-2179MDL01920223
LBN003-001959
LBN003-270119
LAL037-009303 - 9322
BP-HZN-2179MDL07229353- BP-HZN-2179MDL07229354
AE-HZN-2179MDL00060126-AE-HZN- 2179MDL00060181
BP-HZN-2179MDL04902309-BP-HZN-2179MDL04902320

APPENDIX F. FACTS AND DATA WE CONSIDERED IN FORMING OUR OPINIONS

BP-HZN-2179MDL04927015
AE-HZN-2179MDL00098912-AE- HZN-2179MDL00098923
HCG266-012219-HCG266-012222
HAL_0507877- HAL_0507904
ETL080- 008574
BP-HZN-2179MDL06092293- BP-HZN-2179MDL06092303
BP-HZN-2179MDL02174876
BP-HZN-2179MDL07554744
BP-HZN-2179MDL05777677- BP-HZN-2179MDL05777680
BP-HZN-2179MDL04864491-4492
Ex. 6342
Ex. 6343
Ex. 6345
Ex. 6346
Ex. 6348
Ex. 6351
Ex. 6353
Ex. 6354
Ex. 6357
Ex. 8785
Ex. 8786
Ex. 8787
Ex. 8788
Ex. 8789
Ex. 8790
Ex. 8791
Ex. 8792
Ex. 8793
Ex. 8794
Ex. 8795
Ex. 8796
Ex. 8796
Ex. 8797
Ex. 8798
Ex. 8799
Ex. 9051
Ex. 9052
Ex. 9053
Ex. 9054
Ex. 9055
Ex. 9056
Ex. 9057
Ex. 9058
Ex. 9059
Ex. 9060
Ex. 9061
Ex. 9062
Ex. 9063
Ex. 9064
Ex. 9065
Ex. 9066
Ex. 9066
Ex. 9067
Ex. 9067
Ex. 9068
Ex. 9068
Ex. 9069
Ex. 9070
Ex. 9071
Ex. 9072
Ex. 9073
Ex. 9074
Ex. 9075
BP-HZN-2179MDL05073287 - BP-HZN-2179MDL05073304
LDX007-0000990-LDX007-0 001006
Galina Skripnikova Exhibit Nos. 3367-3399, 3483-3499, 3512-3550
BP-HZN-2179MDL07585569
Ex. 9490
BP-HZN-2179MDL07395849
Letter from Robert Gasaway to Judge Sally Shushan Re: MDL No. 2179- Phase 2 rule 30(b)(6) Deposition Scheduling

APPENDIX F. FACTS AND DATA WE CONSIDERED IN FORMING OUR OPINIONS

Linked In Page for Dustin Staiger
BP-HZN-2179MDL03801452-BP-HZN-2179MDL03801480
BP-HZN-2179MDL04440533-BP-HZN-2179MDL04440556
Macondo The Gulf Oil Disaster Chief Counsel's Report 2011
BP-HZN-2179MDL07300593 - BP-HZN-2179MDL07300597
BP-HZN-217907265901
ETL093-000592
BP-HZN-2179MDL04931703
BP-HZN-2179MDL04865116
ETL093-000116
LNL036007350-LNL03- 007353
BP- HZN-2179MDL05710203
BP- HZN-2179MDL05710203
HCG183-003405 - 3405
BP-HZN-2179MDL0253677 - 3688
Ex 9254
Ex 9050
Ex 9051
Ex 9052
Ex 9053
Ex 9054
Ex 9055
Ex 9056
Ex 9057
Ex 9058
Ex 9059
Ex 9060
Ex 9061
Ex 9062
Ex 9063
Ex 9064
Ex 9065
Ex 9066
Ex 9067
Ex 9068
Ex 9069
Ex 9070
Ex 9071
Ex 9072
Ex 9073
Ex 9074
Ex 9075
Ex 8785
Ex 8786
Ex 8787
Ex 8788
Ex 8789
Ex 8790
Ex 8791
Ex 8792
Ex 8793
Ex 8794
Ex 8795
Ex 8796
Ex 8797
Ex 8798
Ex 8799
Ex 3218
Ex 3221
Ex 3225
Ex 5063
Ex 6196
Ex 2198
Ex 7270
Ex 8811
Ex 9127
Ex 9132
Ex 9155
Ex 9160
Ex 92651

APPENDIX F. FACTS AND DATA WE CONSIDERED IN FORMING OUR OPINIONS

Ex 9439
Ex 9445
Ex 9446
Ex 9450
Ex 9459
Ex 9474
Ex 9489
Ex 10334
Ex 10337
Ex 10622
Ex 11132
Ex 11133
Ex 11134
Ex 11135
Ex 11136
Ex 11137
Ex 11138
Ex 11139
Ex 11140
Ex 11141
Ex 11142
Ex 11143
Ex 11144
Ex 11145
Ex 11146
Ex 11147
Ex 11148
Ex 11149
Ex 11150
Ex 11151
Ex 11152
Ex 11153
Ex 11154
Ex 11155
Ex 11156
Ex 11157
Ex 11158
Ex 11159
Ex 11160
Ex 11161
Ex 11162
Ex 11163
Ex 11164
Ex 11165
Ex 11166
Ex 3220
Ex 9156
Ex 9455
Ex 10635
Ex 10636
Ex 10637
Ex 10638
Ex 10639
Ex 10640
Ex 10641
Ex 10642
Ex 10643
Ex 10644
Ex 10645
Ex 10646
Ex 10647
Ex 10648
Ex 10649
Ex 10650
Ex 10651
Ex 10652
Ex 10653
Ex 10654
Ex 10655
Ex 10656

Ex 10657
Ex 10658
Ex 10659
Ex 10660
Ex 10661
Ex 10662
Ex 10663
Ex 10664
Ex 10665
Ex 10666
Ex 10667
Ex 10668
Ex 10669
Ex 10670
Ex 10671
Ex 3218
Ex 9121
Ex 9132
Ex 9155
Ex 9156
Ex 9159
Ex 9446
Ex 9452
Ex 9488
Ex 10132
Ex 10649
Ex 10651
Ex 9840
Ex 9841
Ex 9842
Ex 9843
Ex 9844
Ex 9845
Ex 9846
Ex 9847
Ex 9848
Ex 9849
Ex 9850
Ex 9851
Ex 9852
Ex 9853
Ex 9854
Ex 9855
Ex 9856
Ex 9857
Ex 9858
Ex 9859
Ex 9860
Ex 9861
Ex 9862
Ex 9863
Ex 9864
Ex 9865
Ex 9866
Ex 9867
Ex 9868
Ex 9869
Ex 9870
Ex 9871
Ex 9872
Ex 9873
Ex 3375
Ex 9734
Ex 9840
Ex 9841
Ex 9846
Ex 9850
Ex 10822
Ex 10823
Ex 10824

Ex 10825
Ex 10826
Ex 10827
Ex 10828
Ex 10829
Ex 10830
Ex 10831
Ex 10832
Ex 10833
Ex 10834
Ex 10835
Ex 10836
Ex 10837
Ex 10838
Ex 10839
Ex 10840
Ex 10841
Ex 10842
Ex 10843
Ex 10844
Ex 10845
Ex 10846
Ex 10847
Ex 10848
Ex 10849
Ex 10850
Ex 10851
Ex 10852
Ex 10853
Ex 10854
Ex 10855
Ex 10856
Ex 10857
Ex 10858
Ex 10859
Ex 10860
Ex 6200
Ex 10825
Ex 10826
Ex 10839
Ex 10841
Ex 10845
Ex 11134
Ex 3375
Ex 9734
Ex 9840
Ex 9841
Ex 9846
Ex 9850
BP-HZN-2179MDL05744785
BP-HZN-2179MDL06144176
BP-HZN-2179MDL05750104 - BP-HZN-2179MDL05750105
BP-HZN-2179MDL06532111
BP-HZN-2179MDL07038962
BP-HZN-2179MDL07135840 - BP-HZN-2179MDL07135841
AE-HZN-2179MDL00116749-AE- HZN-2179MDL00116751
BP-HZN-2179MDL07607981 - BP-HZN-2179MDL07608100
BP-HZN-2179MDL07122150 - BP-HZN-2179MDL07122152
Annual Report and Form 20-F 2011
BP Modified Cofferdam Installation Procedure with Helix Q4000 Vessel
BP-HZN-2179MDL07430235
BP-HP2179MDL04799584
Deposition of Farah Saidi Volume (20100208)
Deposition of Stephen Paul Carmichael (20121218)
Deposition of Stephen Paul Carmichael (20121219)
BP-HZN-2179MDL04801842
BP-HZN-2179MDL07381837 - BP-HZN2179MDL07381950
BP-HZN-2179MDL06447604- BP-HZN-2179MDL06447605
BP-HZN-2179-MDL07134957
BP-HZN-2179MDL06540691 - BP-HZN-2179MDL06540695

BP-HZN-2179MDL07122539
BP-HZN-2179MDL06541542
BP-HZN-2179MDL06447604- BP-HZN-2179MDL06447605
BP-HZN-2179MDL07134895 - BP-HZN-2179MDL07134895
BP-HZN-2179MDL06414071
BP-HZN-2179MDL06005330 - BP-HZN-2179MDL06005332
BP-HZN-2179MDL06566061 - 6062
BP-HZN-2179MDL06841747
BP-2179MDL06532286 - 2288
BP-HZN-2179MDL07138054
BP-HZN_2179MDL07443173 - 3179
BP-HZN-2179MDL03812714 - 2718
BP-HZN-2179MDL07024984
BP-HZN-2179MDL07271346 - 1347
BP-HZN-2179MDL06543674 - 3674
BP-HZN-2179MDL07256061
BP-HZN-2179MDL07559833 - 9835
BP- HZN-2179MDL04874261 - 4269
BP-HZN-2179MDL4866122 - 6124
BP-2179MDL04904681 - 4681
BP-HZN-2179MDL06149366
BP-HZN-2179MDL04898802
BP-HZN-2179MDL07254138 - 4169
BP- HZN-2179MDL07252719
BP-HZN-2179MDL06445201
BP-HZN-2179MDL06006522
BP-HZN-2179MDL06546258 - 6259
BP-HZN-2179MDL04845466 - 5507
BP-HZN-2179MDL06424831
BP-HZN-2179MDL04819783 - 9785
BP-HZN-2179MDL07129522 - 9523
BP-HZN-2179MDL07037064
BP-HZN-2179MDL04840184
BP-HZN-2179MDL04884944 - 4946
BP- HZN-2179MDL07024985 - 4988
BP-HZN- 2179MDL07559833 - 9835
BP-HZN-2179MDL01958480- 8482
BP- HZN-2179MDL06006522
BP-HZN-2179MDL07037064
BP-HZN-2179MDL04874261 - 4269
BP-HZN-2179MDL06545710-5712
BP-HZN-2179MDL04799584 - 9589
BP-HZN-2179MDL06540691- 0695
BP-HZN-2179MDL07138695- 8699
BP-HZN-2179MDL07135372- BP-HZN-2179ML07135375
BP-HZN-2179MDL06546754
BP-HZN-2179MDL07256615
BP-HZN-2179MDL07130658
BP-HZN-2179MDL04842359
BP-HZN-2179MDL07135372
BP- HZN- 2179MDL06565200 - BP-HZN-2179MDL06565205
BP-HZN-2179MDL06007479 - 7480
BP-HZN-2179MDL04864371 - 4372
BP-HZN-2179MDL07137861 - 7893
BP-HZN-2179MDL06546754
BP-HZN-2179MDL072166193
BP-HZN-2179MDL07266256
BP-HZN-2179MDL07266155
BP-HZN-2179MDL07265827
BP-HZN-2179MDL07435920 - BP-HZN-2179MDL07436172
BP-HZN-2179MDL07394740 - BP-HZN-2179MDL07394859
BP-HZN-2179MDL07436123- BP-HZN-2179MDL07436172
BP-HZN-2179MDL07418761
BP-HZN-2179MDL06533501
BP-HZN-2179MDL07425516
BP-HZN-2179MDL07425614
BP-HZN-2179MDL06413609
BP-HZN-2179MDL06533501
BP-HZN-2179MDL07426446

APPENDIX F. FACTS AND DATA WE CONSIDERED IN FORMING OUR OPINIONS

BP-HZN-2179MDL07427214
BP-HZN-2179MDL07431726
BP-HZN-2179MDL07431788
BP-HZN-2179MDL07421670
BP-HZN-2179MDL07424159
BP-HZN-2179MDL07426016
BP-HZN-2179MDL07426039
BP-HZN-2179MDL07183986
BP-HZN-2179MDL07190192
BP-HZN-2179MDL07190352
BP-HZN-2179MDL07190486
BP-HZN-2179MDL07191431
BP-HZN-2179MDL07198189
BP-HZN-2179MDL07208791
BP-HZN-2179MDL07212473
BP-HZN-2179MDL07223749
BP-HZN-2179MDL07241080
BP-HZN-2179MDL07273029
BP-HZN-2179MDL07273074
BP-HZN-2179MDL07277020
BP-HZN-2179MDL07277174
BP-HZN-2179MDL07159860
BP-HZN-2179MDL07160631
BP-HZN-2179MDL07163363
BP-HZN-2179MDL07163442
BP-HZN-2179MDL07164373
BP-HZN-2179MDL07172615
BP-HZN-2179MDL07431727
BP-HZN-2179MDL07420915
BP-HZN-2179MDL07421693
BP-HZN-2179MDL07421706
BP-HZN-2179MDL07421724
BP-HZN-2179MDL07424619
BP-HZN-2179MDL07425047
BP-HZN-2179MDL07425517
BP-HZN-2179MDL07425576
BP-HZN-2179MDL07427837
BP-HZN-2179MDL07428597
BP-HZN-2179MDL07428641
BP-HZN-2179MDL07431714
Macondo Black-Oil Lookup Tables, Aaron Zick, Zick Technologies (Jan. 29, 2013)
BP-HZN-2179MDL07381837 - 1950
Error Bands & Resistor Inaccuracy 0.01 mA Tables & Diagrams (Copy of 297204385)
SDX009-0001859
SNL516-001860
SDX009-0001862
BP-HZN-MBI0061593
BP-HZN-MBI00180472
Deposition of Michael Levitan (20130130)
Deposition of Michael Levitan (20130131)
Ex. 10917
Ex. 10918
Ex. 10919
Ex. 10920
Ex. 10921
Ex. 10922
Ex. 10923
Ex. 10924
Ex. 10925
Ex. 10926
Ex. 10927
Ex. 10928
Ex. 10929
Ex. 10930
Ex. 10931
Ex. 10932
Ex. 10933
Ex. 10934
Ex. 10935
Ex. 10936

APPENDIX F. FACTS AND DATA WE CONSIDERED IN FORMING OUR OPINIONS

Ex. 10937
Ex. 10938
Ex. 10939
Ex. 10940
Ex. 10941
Ex. 10942
Ex. 10943
Ex. 10944
Ex. 10945
Ex. 10946
Ex. 10947
Ex. 10948
Ex. 10949
Ex. 10100
Ex. 10772
Ex. 10777
Ex. 10825
Ex. 10839
Ex. 10850
Ex. 11145
Ex. 6199
Ex. 8463
Ex. 8771
Ex. 9453
Deposition Transcrip of Yun Wang (20121024)
Deposition Transcrip of Yun Wang (20121025)
BP-HZN-2179MDL06548051
BP-HZN-2179MDL04729496
BP-HZN-2179MDL06548054
BP-HZN-2179MDL04729495
BP-HZN-BLY00116192-BP-HZN-BLY00116205
BP-HZN-2179MDL000648713
BP-HZN-2179MDL000648715
BP-HZN-2179MDL00648716
BP-HZN-2179MDL00648722
BP-HZN-2179MDL00648723 - 8725
BP-HZN-2179MDL00648726 - 8733
BP-HZN-2179MDL00648717 - 8721
BP-HZN-2179MDL03838183
BP-HZN-2179MDL03838184
BP-HZN-2179MDL03838186
BP-HZN2179MDL04480749
BP-HZN2179MDL04480750
BP-HZN2179MDL04480751
BP-HZN2179MDL04480752
BP-HZN-2179MDL07576971 - 6972
BP-HZN-2179MDL07576974- 6978
BP-HZN-2179MDL06933836-3837
BP-HZN-BLY00133839
BP-HZN-BLY00133837-3838
BP-HZN-2179MDL06907946
BP-HZN-2179MDL05368302
BP-HZN-2179MDL04788584, BP-HZN-2179MDL04799585
AE-HZN-2179MDL69798-AE-HZN-2179MDL69803,
AE-HZN-2179MDL81990-AE-HZN-2179MDL81991,
AE-HZN-2179MDL00064585
BP-HZN-2179MDL06009210 - 9212
LNL067-006068- LNL067-006081
LNL067-006082
LNL067-006083
LNL067-006084
DSC-5606 Photo
DSC-5608 Photo
DSC-5611 Photo
BP-HZN-2179MDL00264803
BP-HZN-2179MDL06105310
BP-HZN-2179MDL06509350
BP-HZN-2179MDL06509351
BP-HZN-2179MDL00264804 - 4813

APPENDIX F. FACTS AND DATA WE CONSIDERED IN FORMING OUR OPINIONS

BP-HZN-2179MDL06105311
BP-HZN-2179MDL06105313
BP-HZN-2179MDL-04869503
Email Chain From: McMullen, Norm To: Lockett, Tim et al Subject: Re: Request water Entrainment Analysis
Relied-Upon Modeling Runs
Macondo EOS Fluid Characterization, Aaron Zick, Zick Technologies (Sept. 4, 2012)
Kelkar, M.: Natural Gas Production Engineering, PennWell Publications, Chapter 5 (2008).
Mead, H.N., A Practical Approach to Transient Pressure Behavior paper SPE 9901-MS presented at the SPE California Regional Meeting, March 25-27, Bakersfield, California (1981).
Haugland, T., Larsen, L., and Skjæveland, S.M., Analyzing Pressure Buildup Data by the Rectangular Hyperbola Approach," paper SPE 13079-MS presented at the SPE Annual Technical Conference and Exhibition, September 16-19, Houston, Texas, (1984).
Muskat, M.: "Use of Data on the Build-Up of Bottom-Hole Pressures," Trans. AIME 123 44-48 (1937).
Larson, V. C., Understanding the Muskat Method of Analyzing Pressure Build-Up Curves, J. Can. Pet. Tech. (3), 136-141 (1963).
Kuchuk, F. J., A New Method for Determination of Reservoir Pressure, Paper SPE 56418-MS presented at the SPE Annual Technical Conference and Exhibition, October 3-6, 1999, Houston, Texas.
Dake, L.P.: Fundamentals of Reservoir Engineering, El Sevier (1978) chapter 3.
Brown, K.E.: Artificial Lift Methods – Volume 4, PennWell Publications (1983)
Fiber Glass Pipe Design, American Water Works Association (2005)
Sarplast Iniziative Industriali Engineering Guide (2008)
www.c-a-m.com: Control Choke Catalog (2009).
Cameron Willis: Flow Curve for CC40 Plug and Cage Choke, Cameron Willis, Longford, Ireland.
Surbey, D.W.: "An Investigation of Two Phase Flow through Willis MOV Wellhead Chokes," MS Thesis, The University of Tulsa (1985).
Sookprasong, P.: "Two Phase Flow in Piping Components," MS Thesis, The University of Tulsa (1980).